Title
STUDIES ON THE SECONDARY STRUCTURE OF RIBONUCLEIC ACIDS INVOLVED IN PROTEIN SYNTHESIS

Author
Wickstrom, Eric.

Publication Date
1972-12-01

LBL-1545

STUDIES ON THE SECONDARY STRUCTURE OF RIBONUCLEIC ACIDS INVOLVED IN PROTEIN SYNTHESIS

Eric Wickstrom

(Ph. D. Thesis)

December 21, 1972

Prepared for the U. S. Atomic Energy Commission under Contract W-7405-ENG-48

LBL-1545

DISCLAIMER

This thesis is dedicated to my lover, Lois, and my terribly fierce daughters, Erica and Eileen, who are more important than clear solutions.

Acknowledgements

I would like to acknowledge first of all the contribution of my research director, Ignacio Tinoco, Jr., in allowing me, and aiding me, to fulfill the goals which I set for myself before coming to Berkeley: to expand my understanding of the physical interactions of biological macromolecules, and to study the interactions of tRNA, mRNA, and initiation factors in protein synthesis. He has tolerated my failures, dry spells, and periods of woe, allowing me to stick to my chosen course, which has finally been carried through to a successful conclusion; no one else in this department than he would have acted similarly.

I must also acknowledge the aid and inspiration given me by Dr. Olke Uhlenbeck, who provided me with many of the techniques used in this work, and with extremely helpful discussions and criticisms, as well.

Professors John Hearst and James Wang, and their many colleagues, gave generously of time and talent in discussing portions of my work, and helped particularly in the use of the analytical ultracentrifuge.

I have benefited greatly from association with the postdocs who have been in this laboratory: Drs. Werner Hug, Fritz Allen, Kashy Javaherian, and especially Don Gray, who initiated me in the high art of circular dichroism. My other colleagues, past and present, have been an enormous help in picking out the kernels of

meaning from my morass of results: Drs. Phil Borer, Arlene Blum, Dana Carroll, Lily Sun, and Carl Formoso; Carol Cech, Cemal Kemal, David Tang, and Mark Levine.

It has been a pleasure to draw on the valuable experience of Barbara Dengler, David Koh, and Mei Chou. I must express great appreciation for the excellent technical assistance of Ernest Foxman, who learned several complicated procedures and data reduction techniques in a short time, and performed them superbly, needing only the accompaniment of KSFX. I also appreciated the earlier assistance of Bahram Khaviari.

Sharon McConnell has my deepest gratitude for typing this thesis, bit by bit, as it was created. She was most patient and helpful, and in addition prepared many of the figures. Tanya Kmit and Nancy Monroe also have my deep appreciation for preparing the rest of the many figures in this thesis.

Lastly, I must thank the National Institutes of Health, whose grant No. GM 10840 supported this work, the Atomic Energy Commission, which paid for some of the computer time used in data analysis through its support of the Laboratory of Chemical Biodynamics, and the National Science Foundation, which supported me with a graduate fellowship for three years until including me in the 43% of continuing fellows to be cut off in 1971.

LIST OF ABBREVIATIONS

A	adenosine
C	cytidine
U	uridine
G	guanosine
T	ribothymidine
ψ	pseudouridine
X,Y,Z	any ribonucleoside
XMP, Xp	a ribonucleoside 3'-phosphate
XDP	a ribonucleoside 5'-diphosphate
XTP	a ribonucleoside 3'-triphosphate
Xp>	a ribonucleoside 3'-5' cyclic phosphate
XpYpZ	the oligoribonucleotide X 3'-phosphate-5' Y 3'-phosphate-5' Z
$X_nY_mZ_k$	the oligoribonucleotide $(Xp)_{n-1}Xp(Yp)_{m-1}Yp(Zp)_{k-1}Z$
poly(X,Y,Z)	the polymer containing a random sequence of the ribonucleoside X, Y, and Z, linked by 3'-phosphate-5' bonds.
dX	any deoxyribonucleotide
DNA	deoxyribonucleic acid
RNA	ribonucleic acid
mRNA	messenger RNA
tRNA	transfer RNA
$tRNA^{aa}$	a specific tRNA coding only for the amino acid, aa
CD	circular dichroism

UV	ultraviolet
A_{260}	absorbance of light with the wavelength 260 nm
met	methionine
fmet	formylmethionine
BSA	bovine serum albumin
DEAE	diethyl aminoethyl
PPO	2,5-diphenyloxazole
POPOP	1,4-bis(2-(5-phenyloxazolyl)) benzene
TCA	trichloroacetic acid
Tris-HCl	tris(hydroxyl)aminomethane, adjusted to desired pH with HCl
X mM Na^+ buffer	10 mM NaH_2PO_4, 0.1 mM EDTA, adjusted to pH 7.00 with NaOH, plus NaCl to desired Na^+ concentration
A_{260} unit	the ultraviolet absorbing material in 1 ml of a solution with an optical density of 1 at 260 nm.

STUDIES ON THE SECONDARY STRUCTURE OF RIBONUCLEIC ACIDS INVOLVED IN PROTEIN SYNTHESIS

Abstract

Eric Wickstrom

Two types of studies are reported here. Changes in the conformation of purified $tRNA_f^{met}$ from E. coli among the three species -$tRNA_f^{met}$, met-$tRNA_f^{met}$, and fmet-$tRNA_f^{met}$ were searched for using circular dichroism, but none could be found. The behavior of hairpin loops containing AUG was studied by equilibrium sedimentation, optical absorbance, optical circular dichroism, and binding to protein synthesis initiation factor f_3 from E. coli.

The kinetics of deacylation at 37°C of met-$tRNA_f^{met}$ in 10 mM Tris-HCl, 10 mM $MgCl_2$, 60 mM NH_4Cl and in 100 mM NaCacodylate, 10 mM $MgCl_2$ were measured as a function of pH, as were the deacylation kinetics of met-$tRNA_f^{met}$ in 100 mM NaCacodylate, 10 mM $MgCl_2$. At pH 5.5 for met-$tRNA_f^{met}$ and pH 6.5 for fmet-$tRNA_f^{met}$, circular dichroism spectra were taken repeatedly over 12-24 hr as deacylation occurred. The experiments were designed to observe a single sample solution at a fixed concentration undergoing changes in circular dichroism which could be unambiguously assigned to conformational changes due to deacylation. The circular dichroism spectra remained constant in each case over the course

of the experiment, and were identical in the case of met-$tRNA_f^{met}$ and fmet-$tRNA_f^{met}$. It was concluded that no detectable conformational changes occurred due to either formylation or acylation.

Oligonucleotides were synthesized with the sequence A_nUGU_m, where n = 7,8,9 and m = 1 - 12. When m = 5 - 10, the oligomers were found to form hairpin loops in 21 mM Na^+ and 101 mM Na^+, and double strand dimers in 1 M Na^+ and 21 mM Na^+, 10 mM Mg^{+2}, based on A_{260} vs. temperature profiles at different concentrations.

Equilibrium sedimentation studies supported the absence of dimer formation in 21 mM Na^+.

The A_{260} vs. temperature results showed all of the A_nUGU_m hairpin loops studied had higher T_m's than $A_6C_8U_6$ in the same solvent, and the measured value of $dT_m/d \log[Na^+] = 4.5 \pm 1.1°C$ indicates that $A_6C_{4,5,6}U_6$ would all be less stable than any of the A_nUGU_m in 21 mM Na^+.

This result is attributed to the presence of a uridine residue in each of the unbasepaired loop regions, specifically in the sequence AUG. The AUG trimer shows little stacking, and it is concluded that it acts as a universal joint in hairpin loop formation.

Using an enthalpy of base pairing, $\Delta H^* = -7.5$ kcal/mole, and assuming likely numbers of base pairs in each hairpin loop, the process of hairpin loop initiation was studied separately from the formation of subsequent base pairs. It was concluded that in an unbasepaired

loop with a given number of bases, A's are more stabilizing than U's, provided the loop contains an AUG joint, and that the most stable loop size is 6 for A_nUGU_m hairpin loops. However, the number for the most stable loop size depends directly on the number of base pairs assumed for the molecules.

The circular dichroism of A_7UGU_{6-8}, A_8UGU_{6-8}, and A_9UGU_6 was studied in 21 mM Na^+ and difference spectra were calculated between their CD spectra and the CD spectra of A_6U_6 in 1 M Na^+. Various weighting factors were used to represent different numbers of base pairs in each molecule, and the resulting difference spectra were presumed to represent the CD spectrum per base for each of the unbasepaired loops possible in an A_nUGU_m molecule with a given number of base pairs. In each case, the difference spectrum was compared with a model CD spectrum for the loop calculated from the measured CD spectra of ApA, ApUpGp, A, and U. The closest agreement between difference spectra and model spectra was found for hairpin loop models with 5 base pairs and 5-8 unbasepaired bases in the loop.

The affinity of E. coli initiation factor f_3 for AUG, single strands containing AUG, hairpin loops containing AUG, a single strand and a hairpin loop without AUG, poly(A,U,G), and f2 viral RNA was measured using a nitrocellulose filter assay. f_3 showed no affinity for oligomers lacking AUG, a weak binding to oligomers

containing AUG, and a strong binding to polymers containing AUG. It was concluded that f_3 has a specific affinity for AUG which is not enhanced when the AUG exists in the loop of a small hairpin loop molecule, but that some more complicated structural requirement exists to account for the strong binding of AUG-containing polymers to f_3. Initiation factor f_1 was found to have no affinity for AUG trimer, but inhibited AUG binding by f_3.

Table of Contents

Page

CHAPTER 1

INTRODUCTION

In 1944, Avery and MacLeod[1] identified DNA as the genetic material of bacteria, and launched the field of molecular biology and biophysical chemistry. In 1953, Watson and Crick[2] made a new great advance when they elucidated the double helical, base paired structure of DNA.

Tissieres and Watson[3] culminated the early work on microsomes and ribonucleoprotein in 1958 when they characterized E. coli ribosomes, and initiated the current broad field of protein synthesis. At the same time, tRNA was shown to be an intermediate in translating the mRNA code into polypeptide by Zamecnik and his colleagues.[4]

Following closely, the separate existence of mRNA was proven by Hall and Spiegelman,[5] the genetic code was worked out,[6] and then, significantly for this work, the first nucleotide sequence of a tRNA was elucidated by Holley and his colleagues in 1965.[7] Holley was able to predict three different secondary structures from the base pairing allowed by the primary sequence, and the most stable structure was the cloverleaf which is currently considered the true secondary structure.[8] This structure was notable for having three hairpin loops (the three leaves of the cloverleaf) and a helical stem composed from the free 5' and 3' ends. It is the physical behavior of this complex molecule which concerns us in Chapter 2 of this work, and the study of synthetic hairpin loops in Chapters 3-6.

Initiation of protein synthesis was found to depend, in 1966, on two new things. A particular codon was found, either AUG or GUG, which codes for formylmethionine as the original first amino acid in bacterial polypeptides, along with a specific initiation tRNA, $tRMA_f^{met}$.[9] Initiation factors were discovered which were found to be proteins removable from ribosomes in high salt, and essential for protein synthesis depending on AUG or natural mRNA and fmet-$tRNA_f^{met}$.[10,11] Subsequent work demonstrated different functions for the three initiation factors,[12] and sequencing studies by Steitz on R17 RNA[13] demonstrated the presence <u>in vivo</u> of AUG as an initiation codon.

The work of Steitz, of Fiers and his colleagues on MS2 RNA,[14] and of others, showed the likelihood of a multitude of hairpin loops in natural messengers. The characteristics of hairpin loops and the prediction of secondary structure from sequence now became doubly important.

A great deal of work has been done on the theory of helix-coil transitions in polynucleotides,[15] and attempts have been made to predict the secondary structure of various types of loops,[16,17] but dependable thermodynamic parameters to use in these equations are few in number. Studies have been made on hairpin loops formed by alternating $(dTA)_N$ oligonucleotides[18,19], fragments of tRNA's,[20,21] and synthetic hairpin loops with the structures $A_6C_mU_6$, m = 4,5,6,8,[22] $A_5GC_5U_5$,[22] and $A_4GC_mU_4$, m = 4,5,6.[23] These studies have yielded varying results;

some have assumed that the enthalpy of loop intiation, ΔH_i°, is zero,[18,19,23] while others[22] start from the assumption of a given value for the enthalpy of adding an additional base pair to a previously formed helix, ΔH_b°, and find a large positive ΔH_i°. Not the least of the problems of the experimenters is the difference from laboratory to laboratory in conditions, techniques of measurement, and analysis of data, even to the extent of differing definitions of the temperature where equal numbers of oligonucleotide strands are single-stranded or either hairpin loops of double strands, T_m.

Work is described in Chapters 3-5 on a class of hairpin loops with A-U base pairs and an AUG in the loop. The relative number of A's and U's in each molecule has been varied in order to give some information on the sequence dependence of loop stability, as well as the effect of the codon AUG on loop stability.

Included in this work is an examination of the binding specificity of initiation factor f_3, one of the protein synthesis initiation factors described above, and the one apparently responsible for recognition of natural mRNA's.[12] In Chapter 6 the binding specificity of f_3 is studied for hairpin loops containing AUG, single strands containing AUG, AUG trimer, poly (A,U,G), f2 RNA, and a hairpin loop, $A_5GC_5U_5$, and single strand, A_8U, without AUG.

REFERENCES

1. Avery, O. T., MacLeod, C. M., and McCarty, M., J. Exptl. Med. 79 (1944) 137.
2. Watson, J. D. and Crick, F. H. C., Nature 171 (1953) 737.
3. Tissieres, A. and Watson, J. D., Nature 182 (1958) 778.
4. Hoagland, M. B., Stephenson, M. L., Scott, J. F., Hecht, L. I., and Zamecnik, P. C., J. Biol. Chem. 231 (1958) 241.
5. Hall, B. D. and Spiegelman, S., Proc. Natl. Acad. Sci. U.S. 47 (1961) 137.
6. Crick, F. H. C., Barnett, L., Brenner, S., and Watts-Tobin, R. J., Nature 192 (1962) 1227.
7. Holley, R. W., Apgar, J., Everett, G. A., Madison, J. T., Marquisee, M., Merrill, S. H., Penswick, J. R., and Zamir, A., Science 147 (1965) 1462.
8. Cramer, F., Progress in Nucleic Acid Research and Molecular Biology 11 (1971) 391.
9. Adams, J. M. and Capecchi, M. R., Proc. Natl. Acad. Sci. U.S. 55 (1966) 147.
10. Stanley, W., Salas, M., Wahban, A. J., and Ochoa, S., Proc. Natl. Acad. Sci. U.S. 56 (1966) 290.
11. Brawerman, G. and Eisenstadt, J., Biochemistry 5 (1966) 2777.
12. Wahba, A. J., Iwasaki, K., Miller, M. J., Sabol, S., Sillero, M. A. G., and Vasquez, C., Cold Spring

Harbor Symp. Quant. Biol. 34 (1969) 291.

13. Steitz, J. A., Nature 224 (1969) 957.

14. Min Jou, W., Haegeman, G., Ysebaert, M., and Fiers, W., Nature 237 (1972) 82.

15. Poland, D. and Scheraga, H. A., Theory of Helix-Coil Transitions in Biopolymers, Academic Press, New York (1970).

16. Tinoco, I., Jr., Uhlenbeck, O. C., and Levine, M. D., Nature 230 (1971) 362.

17. DeLisi, C. and Crothers, D. M., Proc. Natl. Acad. Sci. U.S. 68 (1971) 2682.

18. Scheffler, I. E., Elson, E. L., and Baldwin, R. L., J. Mol. Biol. 48 (1970) 145.

19. Elson, E. L., Scheffler, I. E., and Baldwin, R. L., J. Mol. Biol. 54 (1970) 401.

20. Romer, R., Riesner, P., Maass, G., Wintermeyer, W., Thiebe, R., and Zachau, H. G., FEBS Letters 5 (1969) 15.

21. Coutts, S. M. Biochim. Biophys. Acta 232 (1971) 94.

22. Uhlenbeck, O. C., Borer, P. N., Dengler, B., and Tinoco, I., Jr., J. Mol. Biol., in press.

CHAPTER 2

CIRCULAR DICHROISM DURING DEACYLATION OF METHIONYL-$tRNA_f^{met}$ AND FORMYLMETHIONYL-$tRNA_f^{met}$ FROM *E. COLI*

SUMMARY

Circular dichroism spectra were taken of [^{14}C]-$tRNA_f^{met}$ and [^{14}C]fmet-$tRNA_f^{met}$ from E. coli at 37°C in 100 mM NaCacodylate, 10 mM $MgCl_2$, pH 5.5 and 6.5, respectively, conditions in which deacylation proceeded at similar rates. Any difference between the two sets of spectra, which would have converged toward the spectrum of unacylated $tRNA_f$, could have been interpreted as differences occurring between aminoacyl- and peptidyl-tRNA molecules in the A and P sites of ribosomes, as proposed by Woese. No differences could be detected; however, this result does not rule out the Woese model.

INTRODUCTION

Students of protein synthesis have searched for several years for structural differences between aminoacylated and unacylated tRNA* without a consistent pattern of results.[1-6] In addition, the special characteristics of the bacterial initiator, $tRNA_f^{met}$, have led to the suggestion of structural changes in met-$tRNA_f^{met}$ upon formylation.[7,8] The reciprocating ratchet model proposed by Woese[9] suggests that the anticodon loop of met-$tRNA_f^{met}$ is rearranged from a "Hodgson-Fuller" (5'-3' chain extended) structure to a "Fuller-Hodgson" (3'-5' chain extended) structure[10] when the methionine N-terminus is blocked by a formyl group.

Circular dichroism is sensitive to composition, structure, and sequence of polynucleotides, and should be able to detect gain or loss of 2-3 base pairs in a tRNA molecule.[11] However, when using optical methods to detect small changes in the state of a large molecule, important errors in concentration, and therefore in magnitude, can arise from trying to compare different solutions. In addition to dilution errors, changes may occur in molar extinction coefficients due to the very structural change one is studying, or due to preparation procedures.

*Abbreviations used in this paper: tRNA, transfer ribonucleic acid; met, methionine; fmet formylmethionine; ATP, adenosine triphosphate; CD, circular dichroism; UV, ultraviolet.

To avoid such problems in this experiment, successive CD spectra were taken of samples of [^{14}C]met-tRNA$_f^{met}$ and [^{14}C]fmet-tRNA$_f^{met}$ in the course of their deacylation. In this manner the CD spectra of the two species could be directly compared with one another and with deacylated tRNA$_f^{met}$ without manipulating the samples. No differences were found between the spectra of met-tRNA$_f^{met}$, fmet-tRNA$_f^{met}$, and tRNA$_f^{met}$. This result implies that any conformational differences among the three species are quite small or nonexistent.

MATERIALS AND METHODS

Aminoacylation and formylation were carried out similar to the method of Hershey and Thach.[12] A 1 ml reaction mixture contained 180 µg tRNA$_f^{met}$ (the gift of Dr. A. D. Kelmers,[13] Oak Ridge National Laboratory), 100 mM Tris-HCl, pH 7.4, 10 mM $MgCl_2$, 1 mM dithiothreitol, 2 mM ATP, 0.6 mM folinic acid (Lederle Laboratories) 100 λ S-100, and 0.1 mM [^{14}C]met, 51 Ci/mole (Schwarz). For [^{14}C]met-tRNA$_f^{met}$, the folinic acid was omitted.

Appropriate enzyme concentration was determined in 20 λ test reactions incubated for 10 minutes at 37°C under the conditions above, except that the amount of S-100 was varied, and assayed for TCA-precipitable [^{14}C]met as described below (Fig. 2-1). Appropriate incubation time was determined in a 100 λ test reaction

incubated at 37°C under the conditions described above, except that 20 λ aliquots were withdrawn at various times and assayed for TCA-precipitable [^{14}C]met (Fig. 2-2).

Incubation occurred at 37°C for 10 min.; the reaction was stopped by the addition of 0.2 volume of saturated KOAc, pH 5.3 and 1 volume of phenol saturated with 100 mM NaCacodylate, pH 4.5, 10 mM $MgCl_2$, extracted with vigorous shaking, and the aqueous layer removed. tRNA was precipitated from the aqueous layer by adding 4 volumes of ethanol, and freezing for 2 hr at -10°C. The ethanol precipitate was washed again with 95% ethanol, dissolved in a small amount of 100 mM NaCacodylate, pH 4.5, 10 $MgCl_2$, applied to a 0.6 × 25 cm column of Sephadex G-25 and eluted with the same buffer (Figure 2-3). In the case of [^{14}C]fmet-$tRNA_f^{met}$, the loading reaction was stopped by the addition of 0.0025 volume glacial acetic acid (17.4 M) and 0.25 volume 5 M NaCl, followed by phenol, rather than with saturated KOAc, pH 5.3. Furthermore, separation of tRNA from ATP was done on Sephadex G-50 rather than G-25 (Fig. 2-4). All of the above manipulations were done on ice or at 4°C. The large ATP peak in the column profile of [^{14}C]fmet-$tRNA_f^{met}$ implies greater precipitation of ATP under the salt and pH conditions used in the latter case.

Methionylation was 75-90% complete in the reac-

tion mixture, dropping to nearly 50% after purification, based on TCA-precipitable [^{14}C]met activity and optical density. Formylation of [^{14}C]met-tRNA$_f^{met}$ was 80-90% complete, based on a descending paper chromatography assay using a 90:10:25 n-butanol:glacial acetic acid: H_2O solvent. After elution for 10 cm, the paper was dried and cut into 1 cm strips, which were counted as below. A histogram of one assay with the positions of met and fmet is shown in Figure 2-5.

[^{14}C]met activity was measured by adding an aliquot of solution to 2 ml cold 10% TCA, followed by filtration on Millipore HAWP 25 filters, with four 1 ml washes of cold 5% TCA. Filters were dried under an infrared lamp and placed in scintillation vials with 10 ml of 4.0% (v/v) Fluor Concentrate II (Research Supplies Laboratory) in toluene, then counted in a Beckman LS-250 liquid scintillation counter with 74% efficiency.

UV absorption measurements were made on a Cary 15 recording spectrophotometer, and CD measurements were made on a Cary 60 recording spectropolarimeter with a Cary 6001 CD attachment. Spectra were digitized and smoothed by a Digital Equipment Corp. PDP8/S computer interfaced to the Cary 60.[14]

For CD spectra, fractions of [^{14}C]met-tRNA$_f^{met}$ or [^{14}C]fmet-tRNA$_f^{met}$ from the above step were diluted to about $A_{260\ nm} = 1$; dead volume fractions to be used as blanks were treated similarly.

1 ml of tRNA solution was adjusted to desired pH; 0.6 ml of this solution was added to a 0.6 ml, 1 cm path cylindrical cell and 0.4 ml was saved for assays. A UV absorption spectrum was taken at 20°C of the tRNA solution in the cell, which was then placed in the sample-holder of the Cary 6001, maintained at 37°C, at the same time the parallel solution was placed in a 37°C water bath. During spectrum-taking, 20 λ aliquots of the parallel solution were removed periodically and assayed for [^{14}C]met activity in order to monitor deacylation occurring in the CD cell. 9-12 CD spectra were taken of the tRNA solution in the cell over the course of 12-24 hr., after which another UV absorption spectrum was taken at 20°C. A blank UV absorption spectrum at 20°C and a CD base-line spectrum at 37°C were taken before and after the tRNA runs.

This procedure yielded a series of CD spectra of a tRNA, either [^{14}C]met-tRNA$_f^{met}$ or [^{14}C]fmet-tRNA$_f^{met}$, at identical concentrations over a broad range of aminoacylation levels. Any observed changes between such CD spectra would have been unambiguously due to changes in the molecule, since uncertainty over concentration, composition, and optical differences between two cells were eliminated.

RESULTS AND DISCUSSION

a. Deacylation kinetics. Deacylation kinetics at various pH's for [^{14}C]met-tRNA$_f^{met}$ in 10 mM Tris-HCl, 60 mM NH_4Cl, and 10 mM $MgCl_2$ appear in a semi-logarithmic plot in Figure 2-6. A similar plot for deacylation in 100 mM NaCacodylate, 10 mM $MgCl_2$ at various pH's appears in Figure 2-7, and a different plot of these data as half-life of acylated [^{14}C]met-tRNA$_f^{met}$ vs. pH is shown in Figure 2-8. Figure 2-9 shows the deacylation kinetics of [^{14}C]fmet-tRNA$_f^{met}$ in 100 mM NaCacodylate, 10 mM $MgCl_2$ at various pH's. Deacylation which proceeded quickly enough to do the spectral series with little evaporation, yet slowly enough that each 10 min spectrum could reasonably be said to represent a constant level of aminoacylation, determined the choice of pH's of the solutions in the two sets of spectra.

At pH 5.5 for [^{14}C]met-tRNA$_f^{met}$, and pH 6.5 for [^{14}C]fmet-tRNA$_f^{met}$, the first 10% of deacylation spread out over about 45 min, while 50% deacylation occurred in about five hr., and 80% in about 12 hr. Solutions used for CD spectra were adjusted to these two pH's for [^{14}C]met-tRNA$_f^{met}$ and [^{14}C]fmet-tRNA$_f^{met}$, respectively.

This work made clear that aminoacylated tRNA remains loaded only a very short time in common assay conditions. The deacylation kinetics of [^{14}C]met-tRNA in mixed tRNA at 37°C in 10 mM Tris HCl, pH 7.4, 60 mM

NH_4Cl, 10 mM $MgCl_2$ (Figure 2-6) are virtually the same as in cacodylate buffer, pH 6.5 (Figure 2-7). This should be kept firmly in mind when doing binding and incorporation assays with aminoacylated tRNA, where one may be tempted to regard the tRNA as remaining fully loaded.

b. Circular dichroism spectra. Figure 2-10 shows the circular dichroism spectrum of [^{14}C] met-$tRNA_f^{met}$ in 100 mM NaCacodylate, 10 mM $MgCl_2$, pH 5.5. The spectrum for [^{14}C]fmet-$tRNA_f^{met}$ is shown in Figure 2-11. For both [^{14}C]met-$tRNA_f^{met}$ and [^{14}C]fmet-$tRNA_f^{met}$, 9 successive spectra were averaged every 2.5 nm, or 0.5 nm in the region of the 265 nm peak and plotted. For wavelengths greater than 200 nm, the time-averaged circular dichroism, $\varepsilon_L - \varepsilon_R$, had an error ($2\sigma$) or less than or equal to 0.05 $M^{-1}cm^{-1}$ in each case or less than 1/2% in the region of the 265 nm peak. The two time-averaged CD spectra of [^{14}C]met-$tRNA_f^{met}$ and [^{14}C]fmet-$tRNA_f^{met}$ agreed with each other to the extent that no differences could be shown between fmet-$tRNA_f^{met}$, met-$tRNA_f^{met}$, or -$tRNA_f^{met}$.

However, this result should not be interpreted as absolute proof that there are no configurational differences among these three species. Rather, one may say that any differences which do exist are limited by instrument error to one or two base pairs, and one or two stacking interactions. For example, the exchange

of stacking interactions in the anticodon loop of a tRNA proposed by Woese[9] is not ruled out by this result, though a more drastic rearrangement would be. It should be pointed out for comparison that melting or denaturing of a tRNA substantially alters the shape and magnitude of its circular dichroism spectrum.[15,16]

REFERENCES

1. Sarin, P. S. and P. C. Zamecnik, Biochem. Biophys. Res. Commun., 20 (1965) 400.
2. Littauer, U. Z. and R. Stern, in Structure and Function of Transfer RNA and 5S-RNA, Academic Press, New York, 1967, p. 93.
3. Hashizume, H. and K. Imahori, J. Biochem. Tokyo, 61 (1967) 738.
4. Gantt, R. R., S. W. Englander, and M. V. Simpson, Biochemistry 8 (1969) 475.
5. Adler, A. J. and G. D. Fasman, Biochem. Biophys. Acta 204 (1970) 183.
6. Chatterjee, S. K. and H. Kaji, Biochem. Biophys. Acta 224 (1970) 88.
7. Henes, C., M. Krauskopf, and J. Ofengand, Biochemistry 8 (1969) 3024.
8. Schofield, P., Biochemistry 9 (1970) 1694.
9. Woese, C., Nature 226 (1970) 817.
10. Fuller, W. and A. Hodgson, Nature 215 (1967) 817.
11. Cantor, C. R., S. R. Jaskunas, and I. Tinoco, Jr., J. Mol. Biol., 20 (1966) 39.
12. Hershey, J. W. B. and R. E. Thach, Proc. Natl. Acad. Sci. U.S., 57 (1967) 759.
13. Weiss, J. F., R. L. Pearson, and A. D. Kelmers, Biochemistry 7 (1968) 3479.
14. Tomlinson, B. L., Ph.D. Thesis, University of California (1968) 102.

15. Brahms, J. and W. F. H. M. Mommaerts, J. Mol. Biol. 10 (1964) 73.

16. Adams, A., T. Lindahl, and J. R. Fresco, Proc. Natl. Acad. Sci. U.S. 57 (1967) 1684.

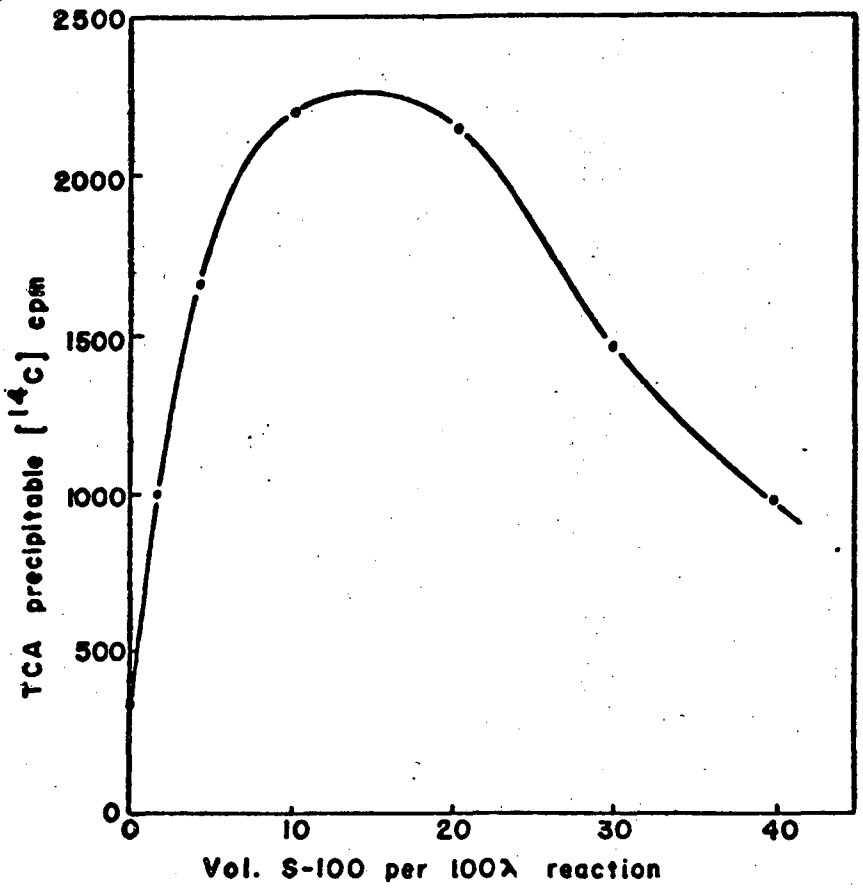

Figure 2-1. S-100 concentration dependence of the aminoacylation reaction. Points represent TCA-precipitable cpm per 20 λ reaction mixture at the indicated S-100 concentrations.

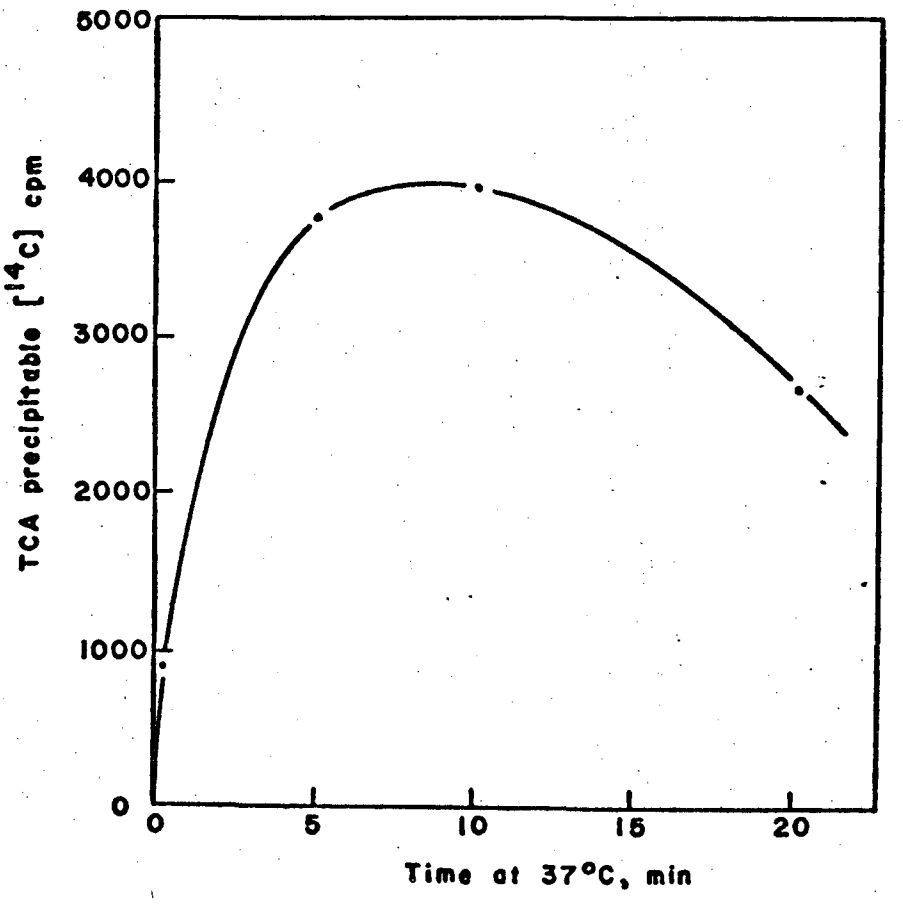

Figure 2-2. Aminoacylation kinetics at 10 λ S-100/100 reaction mixture. Points represent TCA-precipitable cpm per 20 λ aliquot at the times indicated.

Figures 2-3 and 2-4. Elution profiles of [^{14}C]met-tRNA$_f^{met}$ on Sephadex G-25, and [^{14}C]fmet-tRNA$_f^{met}$ on Sephadex G-50, respectively, eluted with 100 mM NaCacodylate, pH 4.5, 10 mM $MgCl_2$. Solid line: A_{260} of 1 ml column fractions. Dashed line: [^{14}C] cpm of 5 λ aliquots of each fraction, dissolved in 10 ml of scintillation fluid (see text) containing 2.5% Biosolve BBS-3 (Beckman).

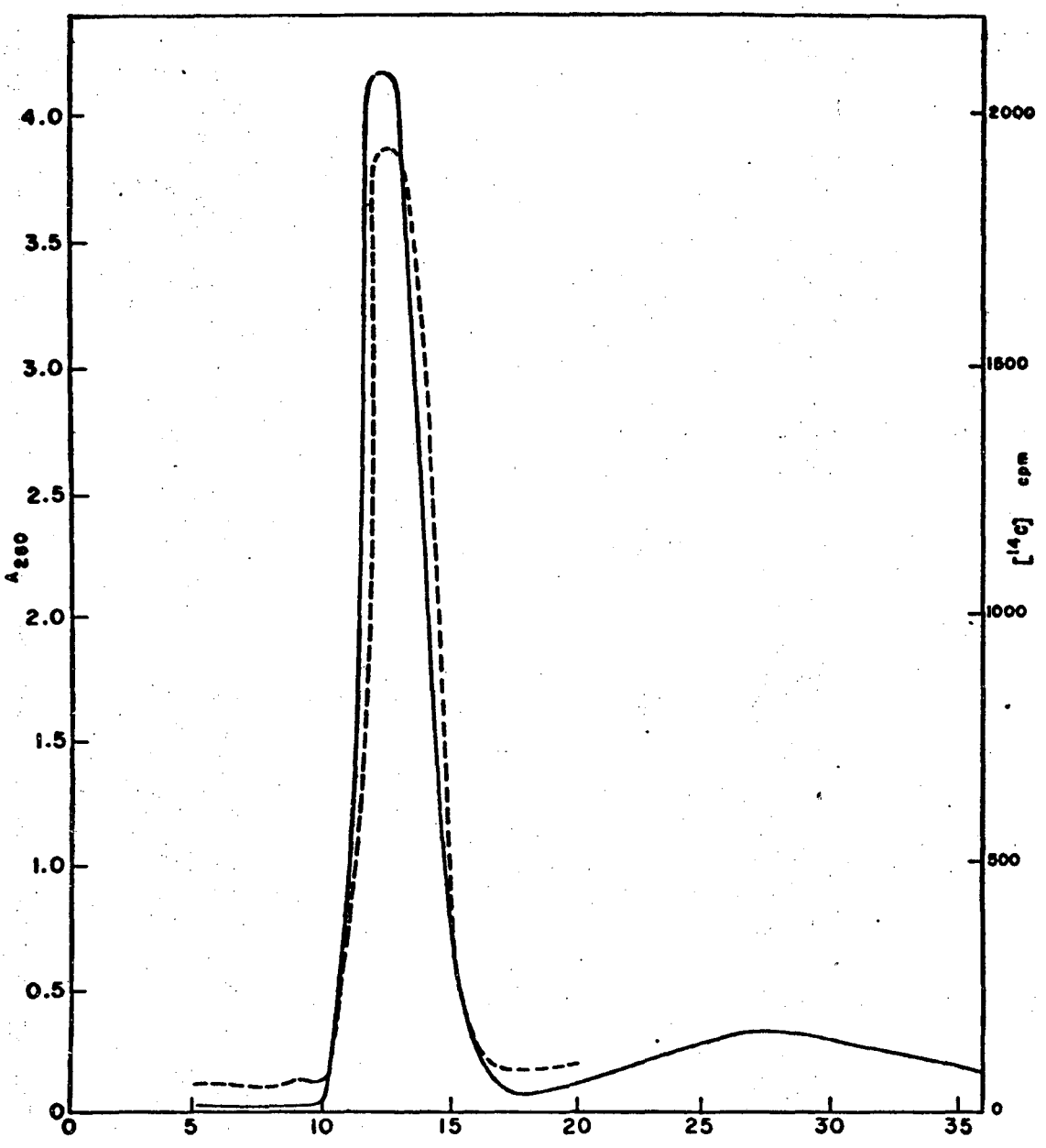
4.0
3.5
3.0
2.5
2.0
1.5
1.0
0.5
0
A_{280}
2000
1500
1000
500
0
[^{14}C] cpm
0
5
10
15
20
25
30
35

Figure 2-3

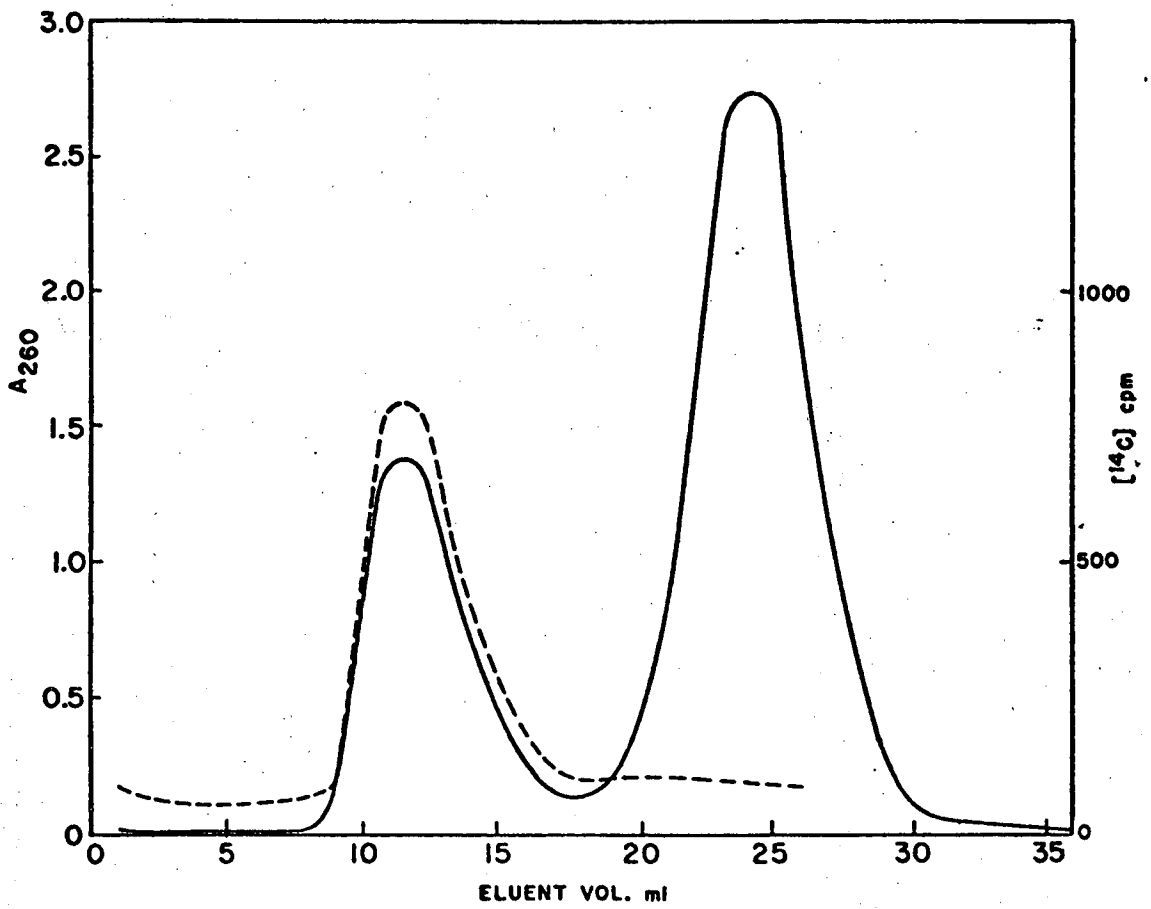
3.0
2.5
2.0
1.5
1.0
0.5
0
A260
0
5
10
15
20
25
30
35
ELUENT VOL. ml
1000
500
0
[14C] cpm

Figure 2-4.

Figure 2-5. Histogram of a paper chromatographic assay for formylation of [^{14}C]met-tRNA$_f^{met}$. Bar heights represent [^{14}C] cpm per 1 cm paper strip. Marker positions were determined by doing assays on tRNA$_f^{met}$ aminoacylated in the presence and absence of formyl donor.

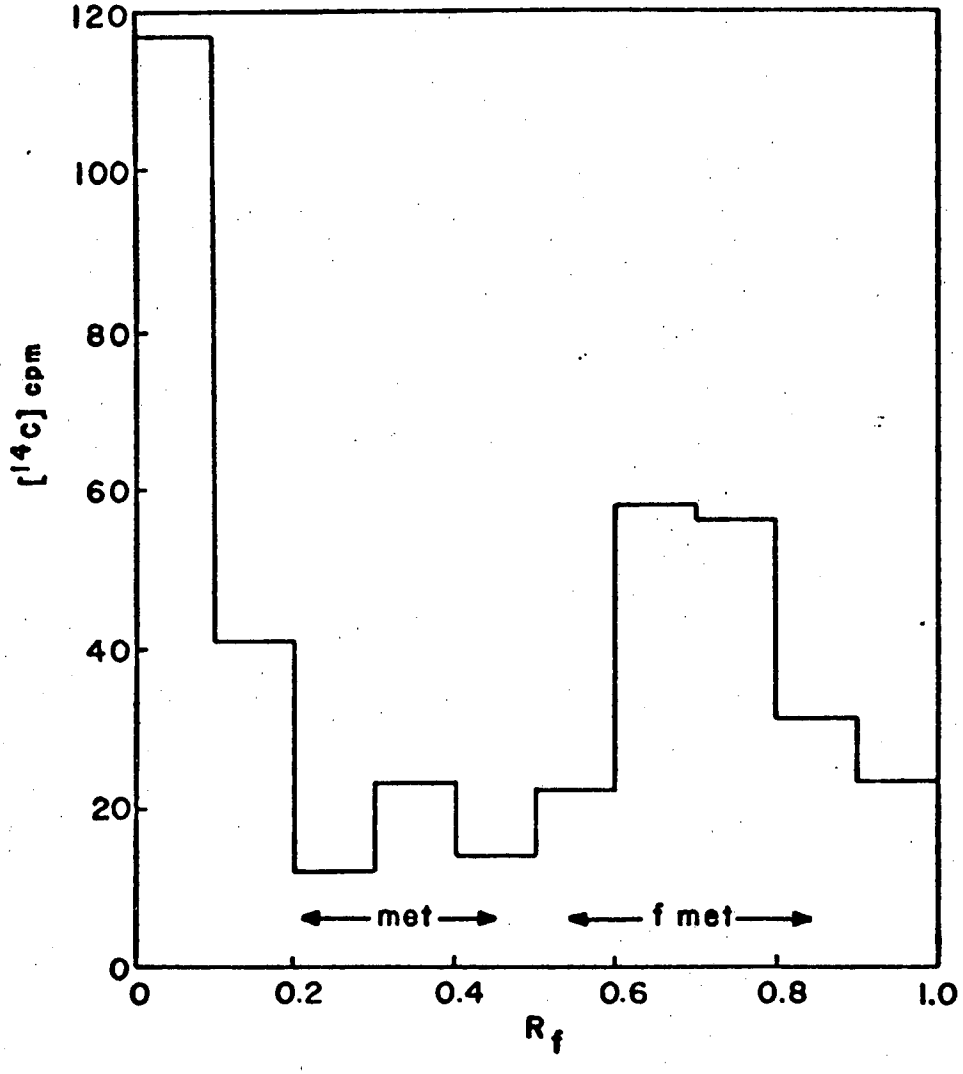

Figure 2-5.

Figure 2-6. Deacylation kinetics of [^{14}C]met-tRNA$_f^{met}$ in 10 mM Tris-HCl, 60 mM NH_4Cl, 10 mM $MgCl_2$ at 37°C. (■), pH 4.9. (●), pH 7.4. (▲), pH 8.2. (○), pH 9.0.

Figure 2-7. Deacylation kinetics of [^{14}C]met-tRNA$_f^{met}$ in 100 mM NaCacodylate, 10 mM $MgCl_2$ at 37°C. (■), pH 4.5. (●), pH 5.5. (▲), pH 6.0. (○), pH 6.5.

Figure 2-8. Half-life of acylated [^{14}C]met-tRNA$_f^{met}$ in 100 mM NaCacodylate, 10 mM $MgCl_2$ as a function of pH. Points represent time for 50% deacylation at 37°C.

Figure 2-9. Deacylation kinetics of [^{14}C]fmet-tRNA$_f^{met}$ in 100 mM NaCacodylate, 10 mM $MgCl_2$ at 37°C. (■), pH 5.0. (●), pH 6.5. (▲), pH 7.0. (○), pH 9.0.

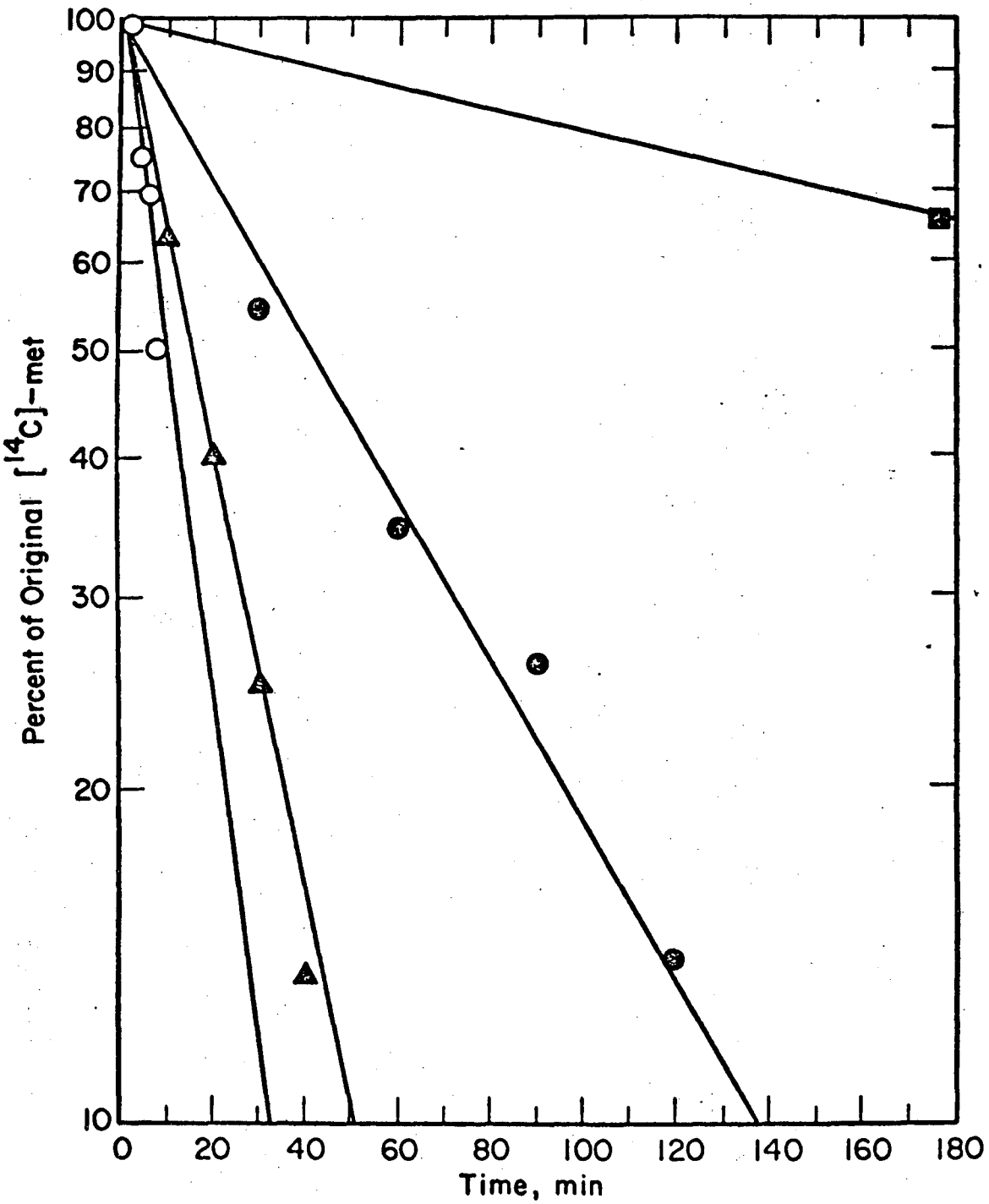
Percent of Original [14C]-met
100
90
80
70
60
50
40
30
20
10
0
20
40
60
80
100
120
140
160
180
Time, min

Figure 2-6.

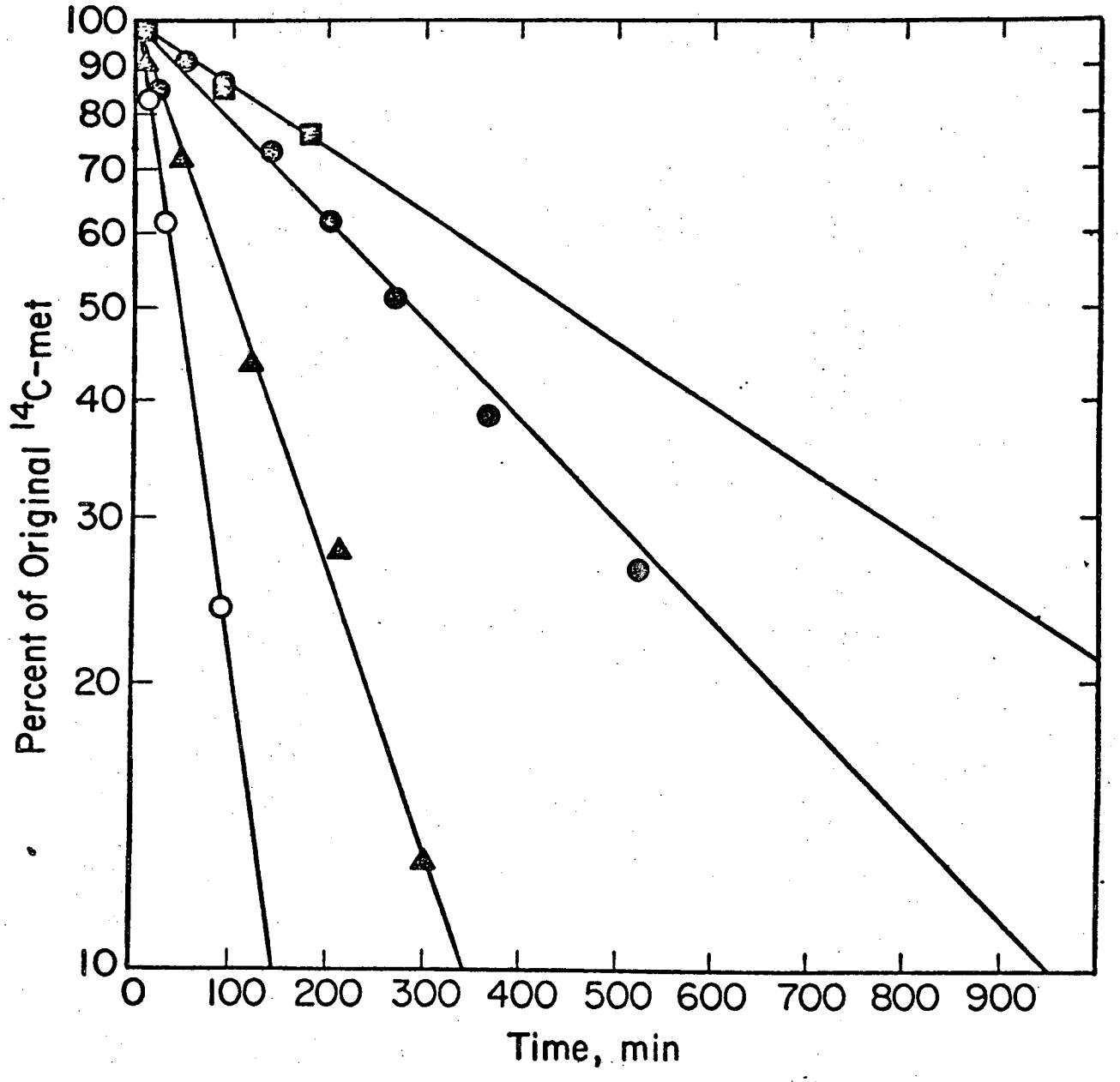
100
90
80
70
60
50
40
30
20
10
Percent of Original ^{14}C-met
0
100
200
300
400
500
600
700
800
900
Time, min

Figure 2-7.

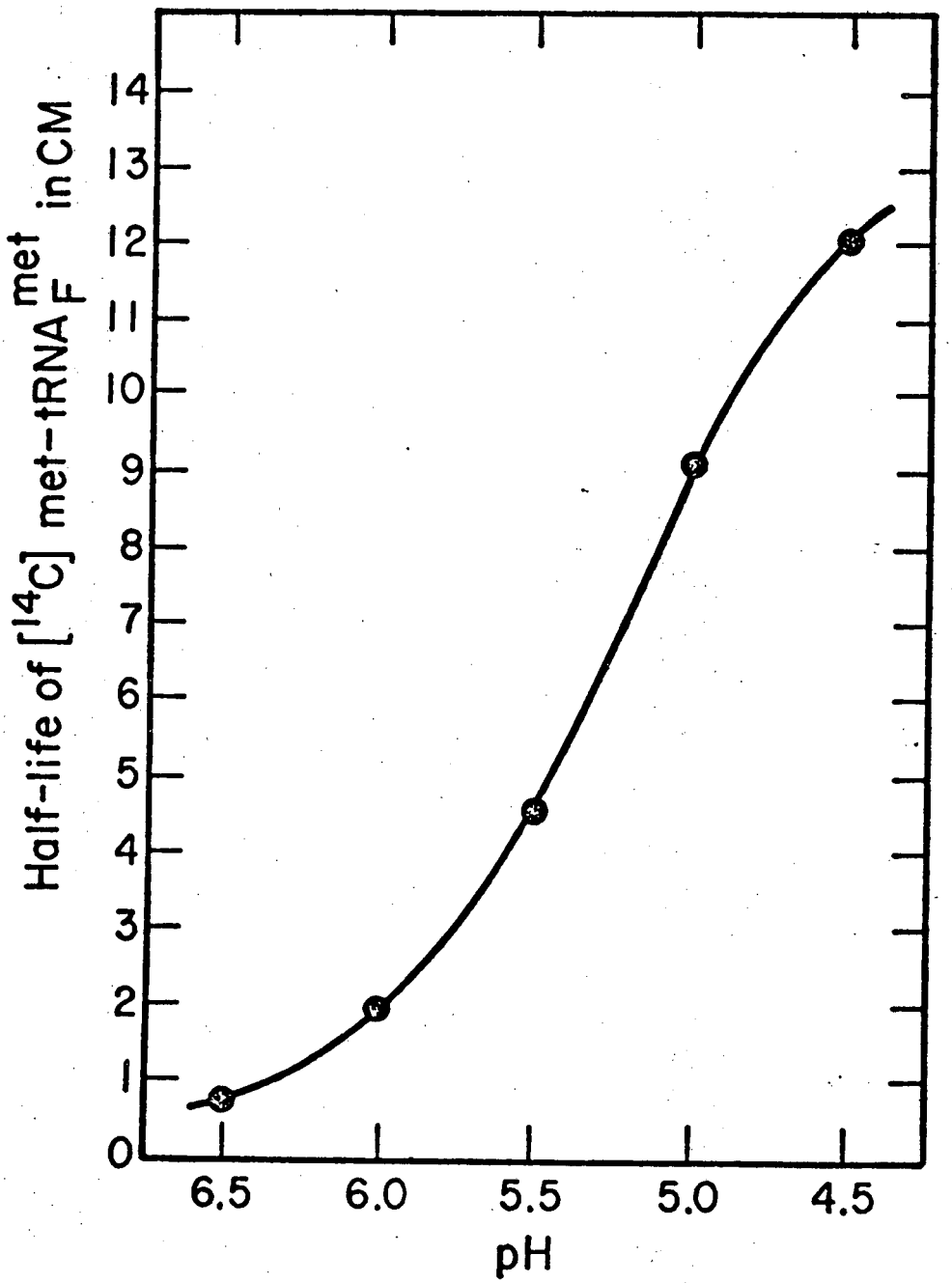
Half-life of [14C] met-tRNA$_F^{met}$ in CM
0
1
2
3
4
5
6
7
8
9
10
11
12
13
14
6.5
6.0
5.5
5.0
4.5
pH

Figure 2-8.

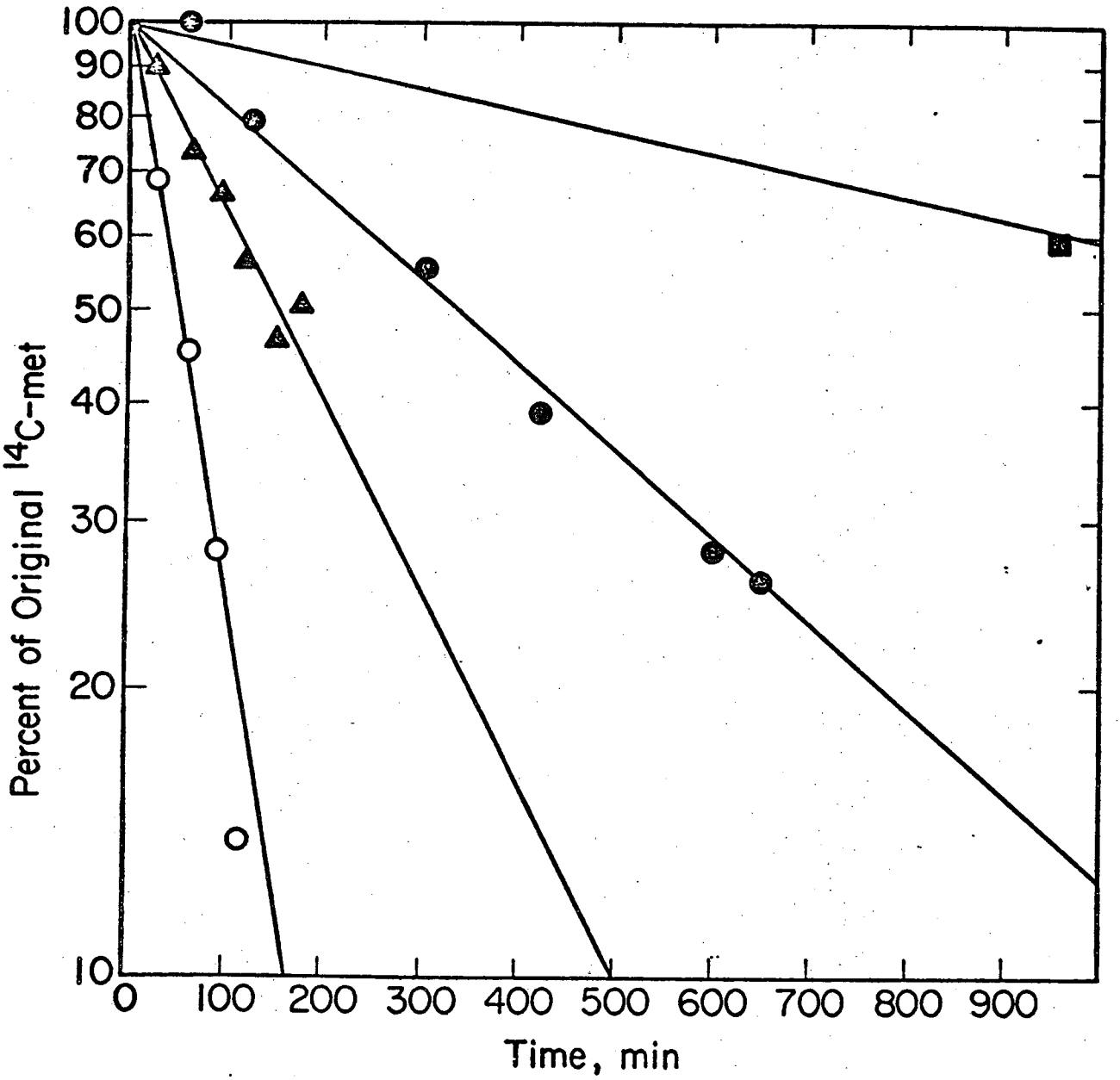
100
90
80
70
60
50
40
30
20
10
Percent of Original ^{14}C-met
0
100
200
300
400
500
600
700
800
900
Time, min

Figure 2-9.

Figures 2-10 and 2-11. Circular dichroism spectra of [^{14}C]met-tRNA$_f^{met}$ in 100 mM NaCacodylate, 10 mM $MgCl_2$, pH 5.5, and [^{14}C]fmet-tRNA$_f^{met}$ in 100 mM NaCacodylate, 10 mM $MgCl_2$, pH 6.5, respectively, at 37°C. Average of 9 spectra over 12 hr. Width of line equals random error to two standard deviations, except as indicated by error bars.

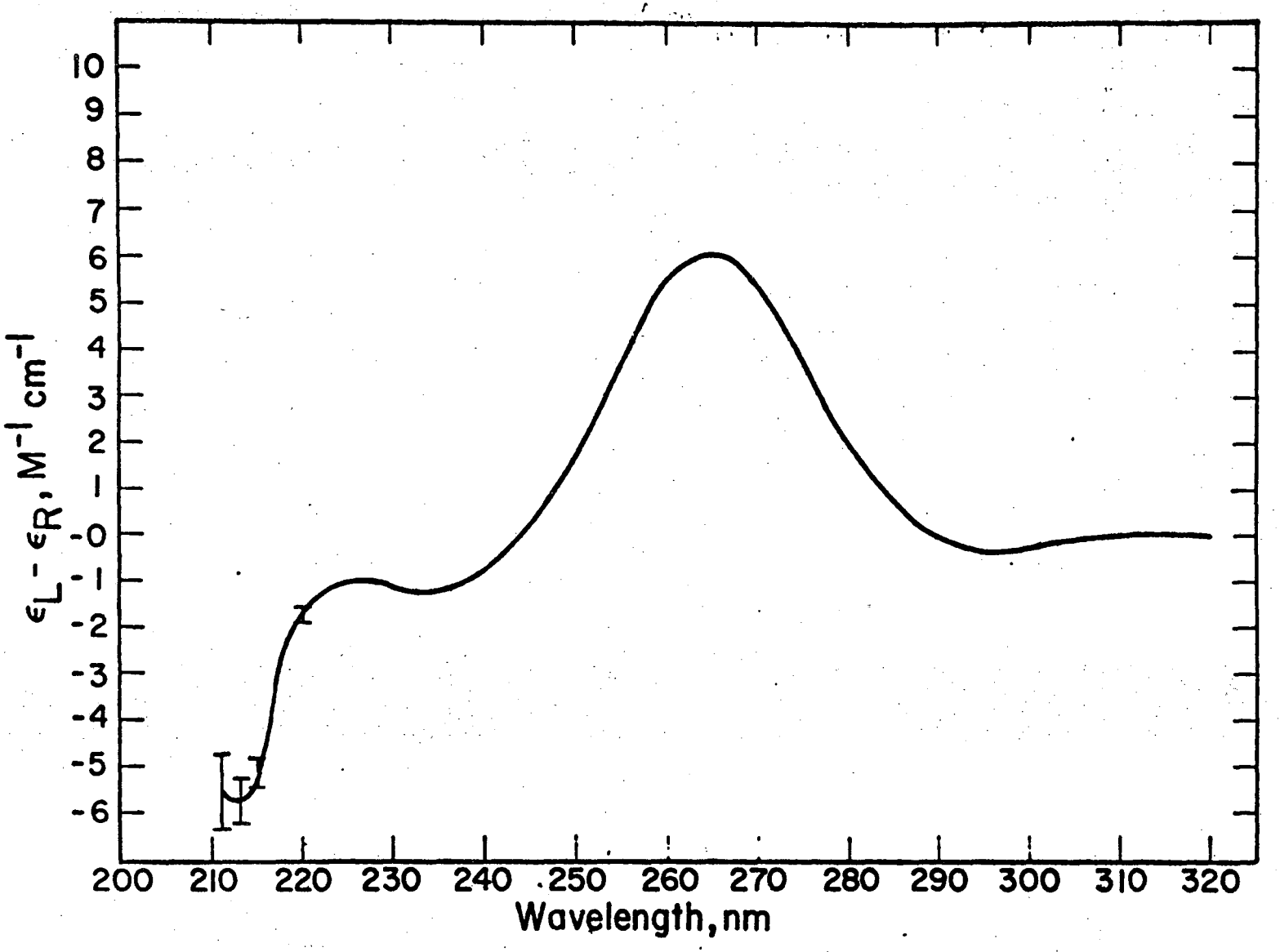
10
9
8
7
6
5
4
3
2
1
0
-1
-2
-3
-4
-5
-6
$\epsilon_L - \epsilon_R$, $M^{-1}\,cm^{-1}$
200
210
220
230
240
250
260
270
280
290
300
310
320
Wavelength, nm

Figure 2-10.

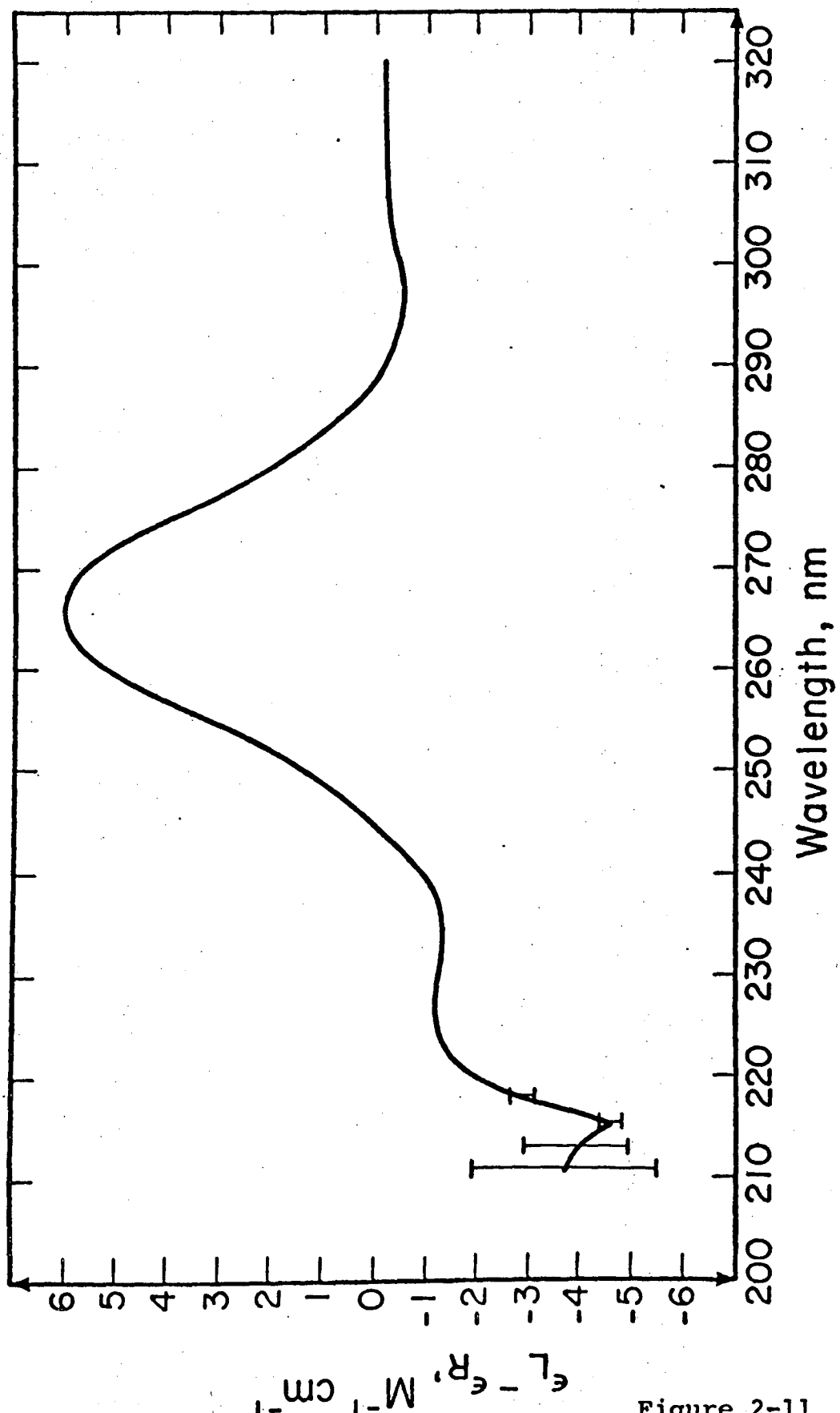
200
210
220
230
240
250
260
270
280
290
300
310
320
Wavelength, nm
6
5
4
3
2
1
0
-1
-2
-3
-4
-5
-6
$\epsilon_L - \epsilon_R$, M^{-1} cm^{-1}

Figure 2-11

CHAPTER 3

SYNTHESIS OF THE OLIGONUCLEOTIDES A_nUGU_m AND POLY(A,U,G)

SUMMARY

The oligonucleotides A_nUGU_m, where n = 7-9 and m = 1-12, and poly(A,U,G) were synthesized from nucleoside diphosphates using primer dependent and primer independent polynucleotide phosphorylase, and purified by ion-exchange column chromatography on DEAE cellulose, using a sodium chloride gradient in 7 M urea. Where m = 5-10, the oligomers were expected to form hairpin loops.

INTRODUCTION

RNA hairpin loops have attracted great interest ever since Holley and his co-workers[1] elucidated the nucleotide sequence of yeast $tRNA^{ala}$, and suggested that the most stable secondary structure was a cloverleaf with one helical stem including the 5' and 3' ends, and three hairpin loops, the dihydrouracil loop, the anticodon loop, and the TψC loop. A nonadecanucleotide including the anticodon loop E. coli $tRNA_f^{met}$ has been shown to bind to the 30S ribosomal subunit in the presence of AUG trimer in a manner analogous to that of the whole molecule.[2] These results and others imply that much may be learned about tRNA behavior from the study of hairpin loops.

The work of Steitz[3] on the sequences of initiation regions of R17 RNA suggests that the observed specificity of protein synthesis initiation for correct starting points, and the preferred translation of certain messengers in mixed RNA systems,[4-6] are both due to the secondary structure of the mRNA. The hypothesis is that initiation factors recognize particular hairpin loops in the messenger, where the initiator codon AUG is in the single-stranded loop region.

It seemed desirable, then, to attempt to imitate the hairpin loop possible in the initiator region of the R17 and MS2[7] coat protein cistrons in the form of a hairpin loop with an A-U base-paired stem and an AUG

in the loop. The hairpin loops $A_6C_mU_6$ were being successfully synthesized in this laboratory at the same time, so the techniques were readily at hand to synthesize the family of loops A_nUGU_m, for n = 7-9, m = 5-10.

MATERIALS AND METHODS

ADP, UDP, and GDP, trilithium nucleoside 5'-diphosphates were purchased from Plenum Biochemicals, and used without further purification. [^{3}H]-ADP (18.2 Ci/mmol), [^{3}H]-UDP (10.8 Ci/mmol), [^{3}H]-GDP (7 Ci/mmol), were purchased from Schwarz Bioresearch and [^{14}C]-UDP (51 Ci/mole), was purchased from Amersham/Searle. Primer-dependent and primer-independent polynucleotide phosphorylase (M. lysodeikticus) were purchased from P-L Biochemicals. Ultraviolet absorption spectra were taken using a Cary 15 spectrophotometer.

Oligonucleotides were synthesized by the methods of Uhlenbeck, Martin, and Doty.[8,9] Poly (A,U) synthesis was done at an A:U ratio of 5 in order to maximize A_6U through A_9U regions. The 150 ml reaction mixture contained 200 mM glycine, pH 9.3, 10 mM $MgCl_2$, 56 mM ADP, 14 mM UDP, 0.05 mM ApA, and 0.67 mg/ml primer-independent polynucleotide phosphorylase. The mixture was incubated 6 hrs at 37°C; polymerization was terminated by placing the reaction beaker in a boiling water bath for 2 min.

Another 150 ml of water was added to dilute the mixture, which was then dialyzed at 4°C against two

changes of 1 M NaCl, 0.01 M Tris-HCl, pH 8.1 to remove unpolymerized nucleotide diphosphates. The resulting white gel was dissolved in an additional 500 ml of water, brought up to 1 M NaCl with 5 M NaCl, and to pH 5 with 0.15 ml glacial acetic acid. 2 l of 95% ethanol were added to the solution, which was allowed to precipitate overnight at -10°C in a freezer.

The precipitated poly (A,U) was collected by sedimentation at 13,000g for 15 min at -10°C, dried, and dissolved in 250 ml of 100 mM Tris-HCl, pH 8.2, 10 mM $MgCl_2$. To this was added ribonuclease A (Worthington) to 20 µg/ml and bacterial alkaline phosphatase (Worthington) to 40 µg/ml. Digestion proceeded for 12 hrs at 37°C.

For chromatographic separation of the different A_nU's, solid urea was added to the solution in the ratio 62 g urea per 100 ml solution to yield a 7 M urea solution of A_nU, which was applied to a 4 × 75 cm column of DEAE cellulose (Bio-Rad) equilibrated with 7 M urea, 10 mM Tris-HCl pH 8.2. The oligonucleotides were eluted with a three part NaCl gradient in 7 M urea, 10 mM Tris-HCl pH 8.2, consisting of 4 l 0 to 0.12 M NaCl, 6 l 0.12 to 0.20 M NaCl, and 2 l 0.20 to 0.28 M NaCl, followed by 1 l of 1 M NaCl to remove any larger polymers.

Each desired peak of several hundred ml was pooled and diluted with 3 volumes of water, then passed through a 2 × 6 cm column of Sephadex A-25 equilibriated with 10 mM Tris-HCl pH 8.2. Several column volumes of 10 mM Tris-HCl pH 8.2 were then passed through the column.

Oligonucleotides adhered to the column material, allowing the complete removal of urea. Oligonucleotides were eluted from the column with 1 M NaCl, 10 mM Tris-HCl pH 8.2, and the A_{260} of the effluent was monitored with a Beckman DB spectrophotometer equipped with a flow cell and strip chart. The resulting 50-60 ml pools of oligonucleotides were then desalted by being passed through a 2.5 × 45 cm column of polyacrylamide gel beads, 200-400 mesh (Bio-Rad) equilbrated with water containing 3 drops conc. NH_4OH/l, and eluted with the latter, monitoring the effluent A_{260} as before. The resulting 50-100 ml pools were frozen and lyophilized, then desalted again.

Identity of the A_nU peaks was established by comparing unknown samples with A_2U, A_3U, A_4U, A_7U, A_8U, and A_9U from an earlier preparation in descending paper chromatography on Whatman 3 MM paper, using a 70:30 mixture of 95% ethanol: 1 M NH_4OAc, pH 7 as a solvent. The identity of A_2U and A_3U had previously been established by alkaline hydrolysis, paper chromatography, and the molar ratio of AMP and U in the spots, determined from A_{260}.

To remove any traces of ribonuclease A from A_nU samples, bentonite (washed free of UV absorbing contaminants) was added to a concentration of 1 mg/ml, the sample was stirred on a vortex mixer, and then sedimented at 1000 g for 10 min at 0°C. The supernatant was removed, and treated once more with bentonite. The final

supernatant was used as the stock solution for A_nUG synthesis.

A_nUG's were produced by using primer-dependent polynucleotide phosphorylase to add GDP to A_nU, while simultaneously removing all polymerized G's but one with ribonuclease T1. The 3-5 ml reaction mixtures contained 200 mM Tris-HCl pH 8.2, 10 mM $MgCl_2$, 400 mM NaCl, 1.0 mM A_7U, A_8U, or A_9U, 35 mM [^{3}H] GDP, 0.5 Ci/mole, 2 unit/ml primer-dependent polynucleotide phosphorylase, and 250 unit/ml ribonuclease T1 (Sankyo). The mixtures were incubated 24 hr at 37°C, then placed in a boiling water bath for 2 min. The pH of the solutions was adjusted to 2 with 12 M HCl, and they were incubated 2 hr at 37°C to decyclize 2'-3' cyclic phosphates remaining after ribonuclease T1 hydrolysis of polymers to A_nUGp.

Each mixture was then diluted tenfold with 7 M urea, 10 mM Tris-HCl pH 8.2, and applied to a 1.1 × 50 cm column of DEAE cellulose equilibrated with the latter solution, and eluted with 1 l gradient of 0.1 - 0.3 M NaCl in the same urea solution. The effluent A_{260} was monitored, and desired peaks were pooled and desalted as above.

Terminal phosphates of the resulting A_nUGp's were removed with bacterial alkaline phosphatase in a reaction mixture containing 100 mM Tris-HCl pH 8.2, 10 mM $MgCl_2$, about 2 mM A_nUGp, and 40 µg/ml phosphatase. Each mixture was incubated 4 hr at 37°C; the reaction

was stopped by the addition of one volume of phenol saturated with 1 M NaCl, adjusted to pH 4.5 with glacial acetic acid. After vigorous extraction, the aqueous layer was removed, brought to pH 4.5, added to 4 volumes of cold 100% ethanol, and allowed to precipitate overnight.

The precipitate was collected by sedimenting the solution at 10,000 g for 10 min at -10°C and then removing the supernatant; the precipitate was washed with 2 ml cold 95% ethanol and sedimented again. The final precipitate was dried, dissolved in water, and treated with bentonite as above.

Identity of A_7UG, A_8UG, and A_9UG was confirmed by the presence and specific activity of the [^{3}H]G.

UDP addition to A_nUG involved primer-dependent polynucleotide phosphorylase to yield A_nUGU_m's. Each 1-3 ml reaction mixture contained 200 mM glycine, pH 9.3, 10 mM $MgCl_2$, 600 mM NaCl, 1.0 mM A_nUG, 35 mM [^{14}C]UDP, 0.5 Ci/mole, and 4 unit/ml primer-dependent polynucleotide phosphorylase. The mixtures were incubated 2 hr at 37°C, then placed in a boiling water bath for 2 min. Each mixture was diluted tenfold with 7 M urea, 10 mM Tris-HCl pH 8.2, and applied to either a 1.5 × 55 cm column, in the case of A_7UGU and A_8UGU_m, or a 1.1 × 50 cm column, in the case of A_9UGU_m, of DEAE cellulose equilibrated with the latter solvent. Each column was washed with 200 ml of 7 M urea, 10 mM Tris-HCl pH 8.2, 50 mM NaCl, and then re-equilibrated with 7 M urea, 10 mM

$NaCH^{OO}$, 150 mM HOOCH, pH 3.15; the latter required several hundred ml. A_nUGU_m's were eluted with either a 3 l gradient of 0-0.4 M NaCl for n = 7,8, or a 1 l gradient of 0-0.3 M NaCl for n = 9. The effluent A_{260} was monitored, and desired peaks were pooled and desalted as above.

Final desalting of A_nUGU_m's was accomplished by dialyzing 1-5 ml of sample against 3 or 4 changes of 50 ml water; the interval between changes increased with each change, e.g., 2 hr, 4 hr, 8 hr, overnight.

Determination of m for each A_nUGU_m sample involved both ribonuclease A and ribonuclease T1 digestion of 2 or 3 early peaks, followed by paper chromatography. Aliquots of 0.1 to 0.2 A_{260} units of oligonucleotide were digested with either 250 unit/ml ribonuclease T1 or 500 µg/ml ribonuclease A in 100 λ solutions containing 100 mM Tris-HCl pH 8.2, 10 mM $MgCl_2$. The reaction mixtures were incubated 24 hr at 37°C, then spotted on Whatman 3 MM paper with markers U, Up, Up>, UpU, and UpUpU and developed for 20 cm by descending chromatography and dried. The 2 cm wide, 20 cm long strip below each spot was cut into ten 2 cm squares; the [^{14}C] activity of each square was measured in a vial containing 10 ml of 4 g/l PPO, 50 mg/l POPOP dissolved in toluene, using a Beckman LS-250 liquid scintillation spectrometer.

For ribonuclease T1 digestion, the peak of [^{14}C] activity corresponded to U, U_2, or U_3 for a given sample, while for ribonuclease A digestion, the two fastest peaks

corresponded to Up + Up> and U; GpUp is quite slow. For A_nUGU_m, the ratio (Up + Up>)/U must be m-2, allowing the determination of m.

Poly (A,U,G) was synthesized using primer independent polynucleotide phosphorylase, using equal concentrations of ADP, UDP, and GDP. The 0.3 ml reaction mixture contained 200 mM glycine, pH 9.3, 10 mM $MgCl_2$, 0.5 mM ApA, 23 mM [^{3}H]ADP, 14.3 Ci/mole, 23 mM UDP, 23 mM GDP, and 1 mg/ml polynucleotide phosphorylase. The mixture was incubated 24 hr at 37°C, then placed in a boiling water bath for 2 min.

The mixture was added to 0.5 ml water containing 4 mg bentonite in a centrifuge tube, stirred with a vortex mixer, and sedimented at 4000 g for 10 min at 0°C. The supernatant was then dialyzed 24 hr against 250 ml 1 M NaCl, 10 mM Tris-HCl pH 8.2 to remove monomers and short oligomers, and dialyzed 48 hr against 250 ml 100 mM NaCl, 10 mM Tris-HCl pH 8.2. [^{3}H] activity measurements indicated 20% of the original added cpm were TCA-precipitable after the 24 hr incubation, and that 8.8% of the original cpm were retained as TCA-precipitable material after dialysis.

RESULTS AND DISCUSSION

The A_{260} profile of the A_nU column appears in Figure 3-1. Use of a three part gradient hastened elution of the shortest oligonucleotides, which would be quite lengthy with a single, continuous gradient, allowed good

separation of the molecules of interest, and quickly finished the elution of the longest strands.

The poly (A,U) reaction mixture contained 10.5 mmole of nucleoside diphosphates, and about 3 mmole, or a 30% yield, was available as A_nU to be applied to the column. Each A_nU peak of interest gave 0.1 mmole or less, for about a 1% yield from starting material for each of the desired oligonucleotides.

Column profiles for A_7UGp, A_8UGp, and A_9UGp appear in Figures 3-2, 3-3, and 3-4, respectively. The step from 0 to 0.1 M NaCl in starting the gradients removed excess GDP and cleaved GMP, as well as any short contaminants, right away, and then the gradients allowed good separation of A_nUGp from A_nU precursor. Since polynucleotide phosphorylase does not add residues to a terminal phosphate,[10] each A_nUGp produced by ribonuclease T1 hydrolysis no longer participates in the reaction, and one may expect an equilibrium result of 100% addition of Gp to A_nU. In practice, addition was at least 80-90% complete.

Column profiles for A_7UGU_m, A_8UGU_m, and A_9UGU_m appear in Figures 3-5, 3-6, and 3-7, respectively. The columns were re-equilibrated to pH 3.15 before running NaCl gradients in order to titrate most of the AMP residues, whose pK is 3.7, and some of the GMP residues, whose pK is 2.4.[11] When a proton is added to the base, it neutralizes the negative charge on the phosphate, and the residue contributes no charge to the oligonucleotide;

for example, at pH 3.15, A_8UG should elute like $A_{1.8}UG_{0.8}$ or A_4. Since good separation of oligonucleotides differing by only one residue is limited in this system to a chainlength of 12 or less, titration of the AMP's becomes necessary for good separation of A_nUGU_m's.

It may be seen that all or most of the starting A_nUG had U residues added in each reaction. Separation and yield of oligomers with m = 6-10 was good for A_7UGU_m and A_8UGU_m, but only fair for A_9UGU_m.

In determining m for each of the A_7UGU_m peaks in Figure 3-5, ribonuclease A digestion and paper chromatography of the first 3 peaks showing [^{14}C] activity gave (Up + Up>)/U ratios of 0.15 $\pm$ 0.02, 1.00 $\pm$ 0.15, and 2.26 $\pm$ .34, corresponding to m = 2,3, and 4, respectively. Similarly, ribonuclease T1 digests of the first two peaks co-chromatographed with U_2 and U_3.

For A_8UGU_m, ribonuclease T1 digests of the first 3 [^{14}C] peaks co-chromatographed with U, U_2, and U_3; for A_9UGU_m, the second and third [^{14}C] peaks co-chromatographed with U_3 and U_4.

After desalting and dialysis, 30-40 A_{260} units were obtained of each of the largest peaks in Figures 3-5 and 3-6 for the physical and biological studies to follow, with correspondingly smaller amounts from the smaller peaks. Each of the largest peaks, then, represented about 0.03% yield from the original nucleoside diphosphates.

An 8.8% yield, about 20 A_{260} units, was obtained of

poly(A,U,G). Equilibrium sedimentation gave an apparent average molecular weight of 18,000, which may be 30% less than the true weight (see Chapter 4).

REFERENCES

1. Holley, R. W., Apgar, J., Everett, G. A., Madison, J. T., Marquisee, M., Merrill, S. H., Penswick, J. R., and Zamir, A., Science 147 (1965) 1462.
2. Rudland, P. S., and Dube, S. K., J. Mol. Biol. 43 (1969) 273.
3. Steitz, J. A., Nature 224 (1969) 957.
4. Bretscher, M. S., Nature 220 (1968) 1088.
5. Lodish, H. F., and Robertson, H. D., Cold Spring Harbor Symp. Quant. Biol. 34 (1969) 655.
6. Dube, S. K. and Rudland, P.S., Nature 226 (1970) 820.
7. Min Jou, W., Haegeman, G., Ysebaert, M., and Fiers, W., Nature 237 (1972) 82.
8. Martin, F. H., Uhlenbeck, O. C., and Doty, P., J. Mol. Biol. 57 (1971) 201.
9. Uhlenbeck, O. C., Martin, F. H., and Doty, P., J. Mol. Biol. 57 (1971) 217.
10. Thach, R. E., in Procedures in Nucleic Acid Research, eds. G. L. Cantoni and D. R. Davies, Harper and Row, New York, 1966, p. 520.
11. Circular OR-10, P-L Biochemicals, Milwaukee, 1956, p. 20.

Figure 3-1. Elution profile of A_nU separated on a DEAE cellulose column by a NaCl concentration gradient (straight line, right hand ordinate) in 10 mM Tris-HCl, pH 8.2, 7 M urea. Curve showing A_nU peaks, n = 2-12, is effluent A_{260} (left hand ordinate).

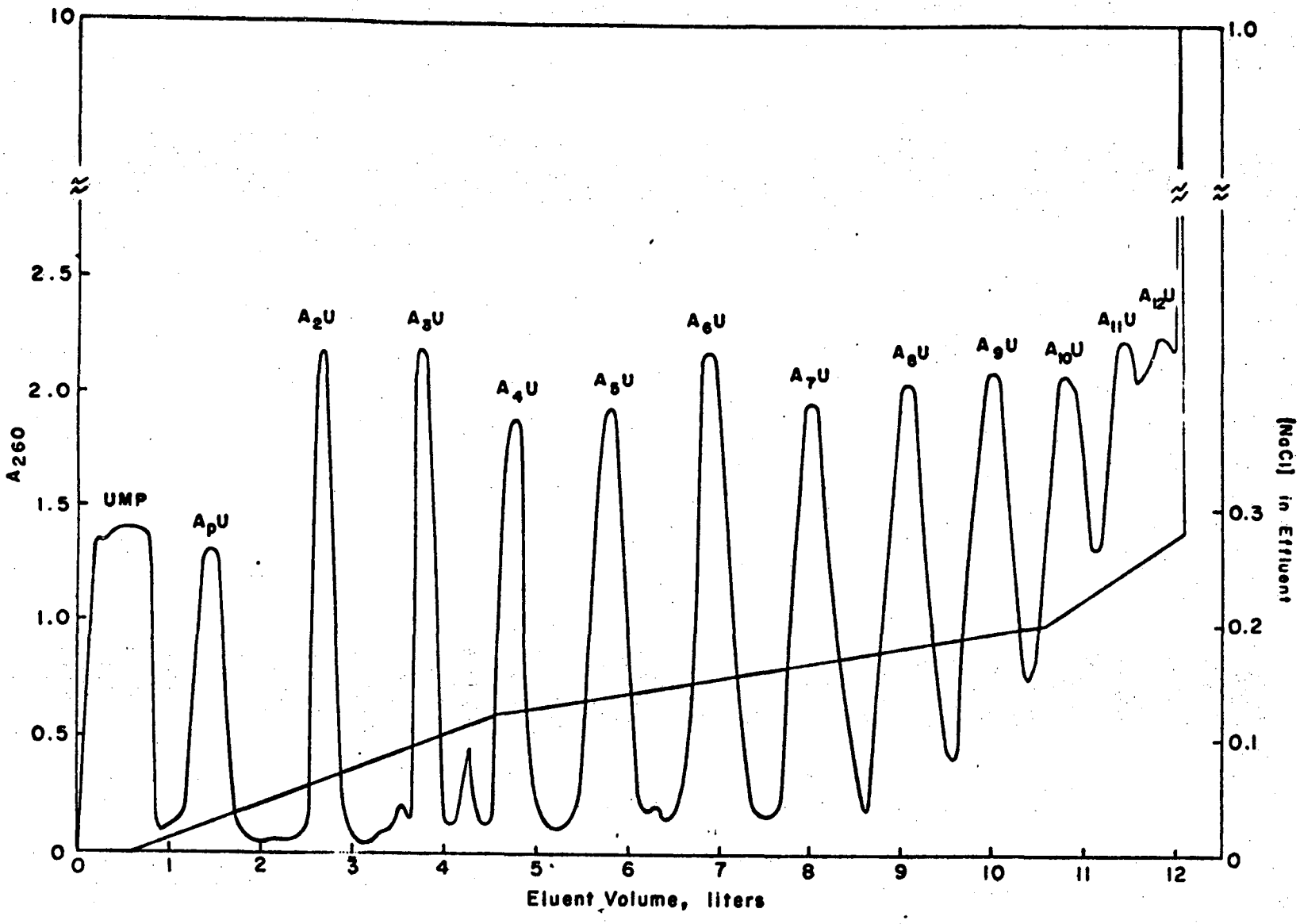
UMP
ApU
A2U
A3U
A4U
A5U
A6U
A7U
A8U
A9U
A10U
A11U
A12U
A260
[NaCl] in Effluent
Eluent Volume, liters
0
0.5
1.0
1.5
2.0
2.5
10
0.1
0.2
0.3
1.0
1
2
3
4
5
6
7
8
9
10
11
12

Figure 3-1

Figures 3-2, 3-3, and 3-4. Elution profiles of A_7UGp, A_8UGp, and A_9UGp, respectively, purified on a DEAE cellulose column by a NaCl concentration gradient in 10 mM Tris-HCl, pH 8.2, 7 M urea.

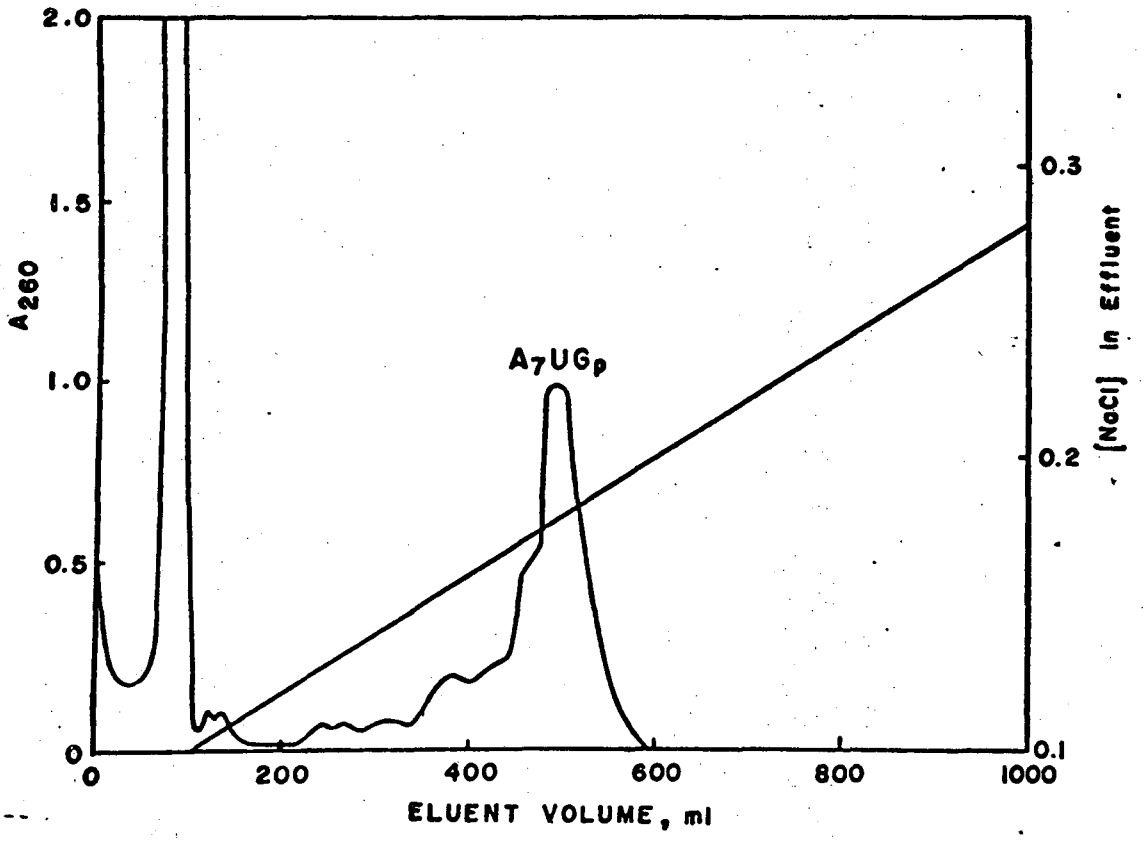
2.0
1.5
1.0
0.5
0
A260
A7UGp
0.3
0.2
0.1
[NaCl] in Effluent
0
200
400
600
800
1000
ELUENT VOLUME, ml

Figure 3-2

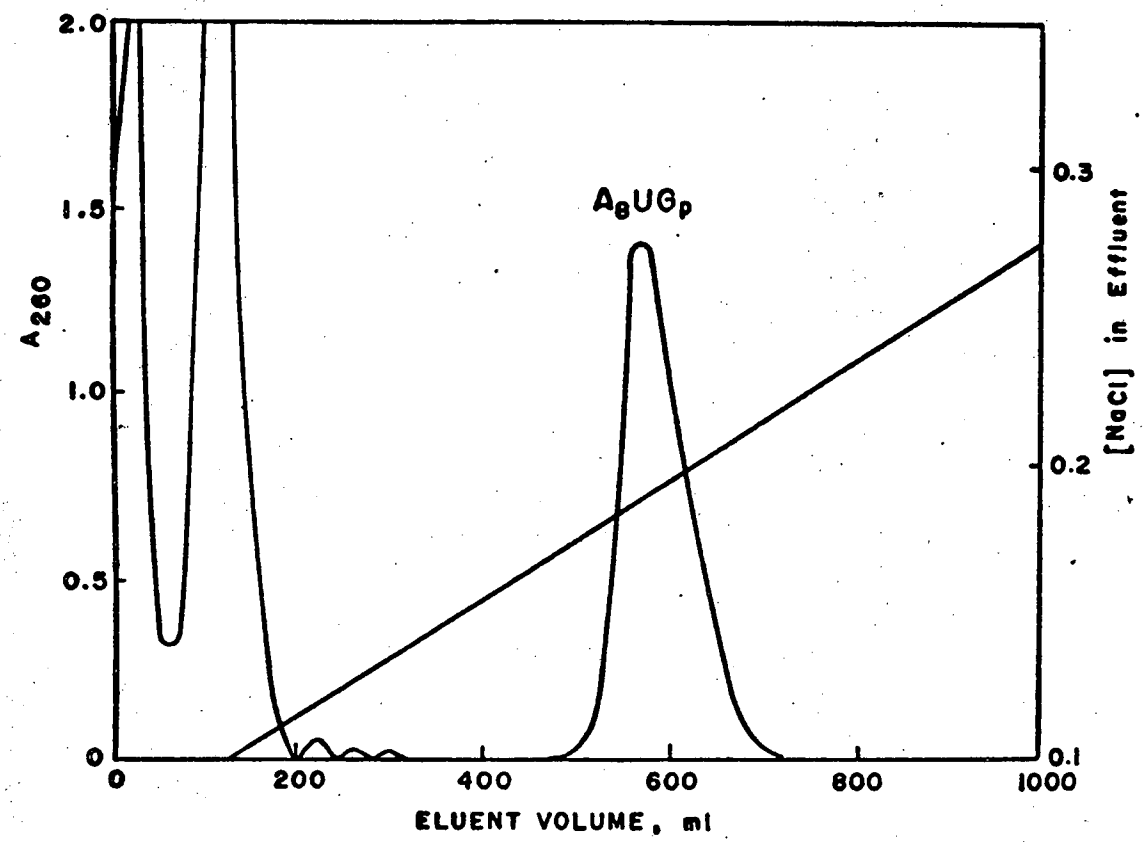
2.0
1.5
1.0
0.5
0
A260
A8UG9
0.3
0.2
0.1
[NaCl] in Effluent
0
200
400
600
800
1000
ELUENT VOLUME, ml

Figure 3-3

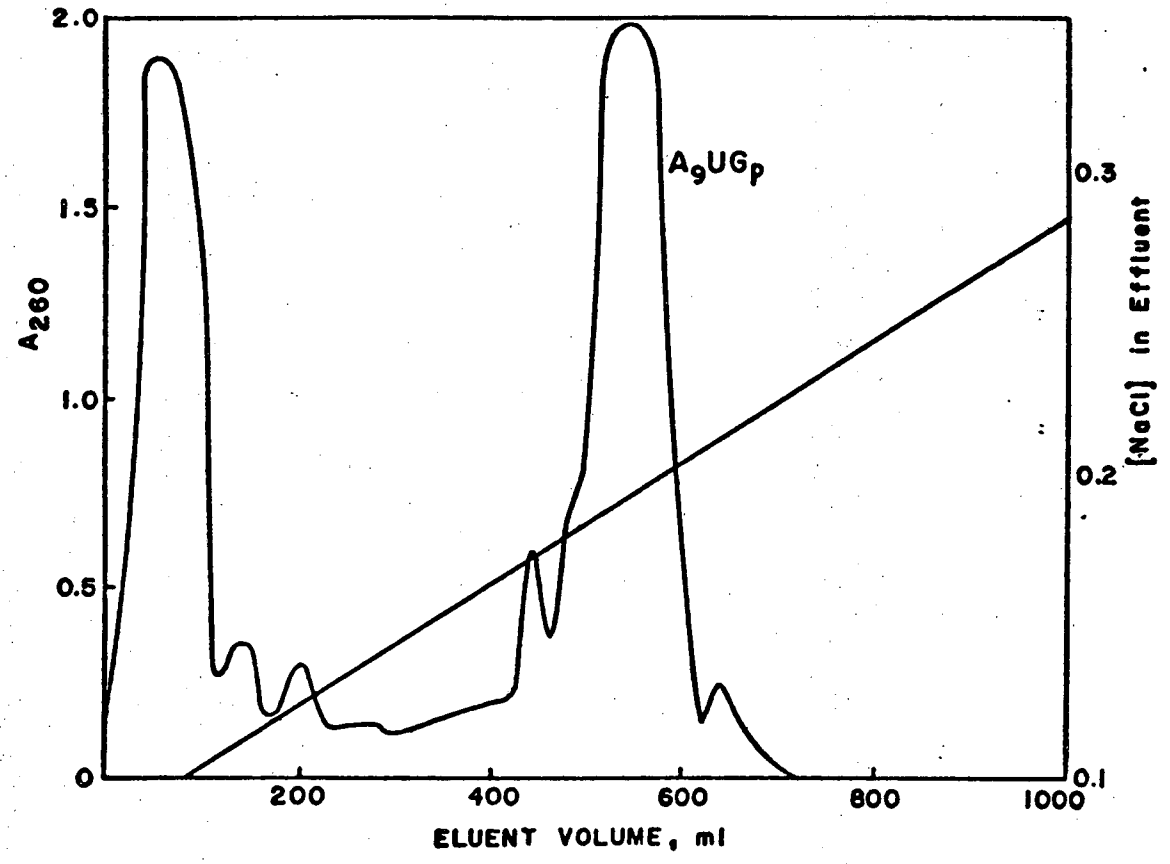
2.0
1.5
1.0
0.5
0
A_{260}
A_9UG_p
0.3
0.2
0.1
[NaCl] in Effluent
200
400
600
800
1000
ELUENT VOLUME, ml

Figure 3-4

Figures 3-5, 3-6, and 3-7. Elution profiles of A_7UGU_m, A_8UGU_m, and A_9UGU_m, respectively, separated on a DEAE cellulose column by a NaCl concentration gradient in 20 mM NaOOCH, .15 M HOOCH, pH 3.15, 7 M urea.

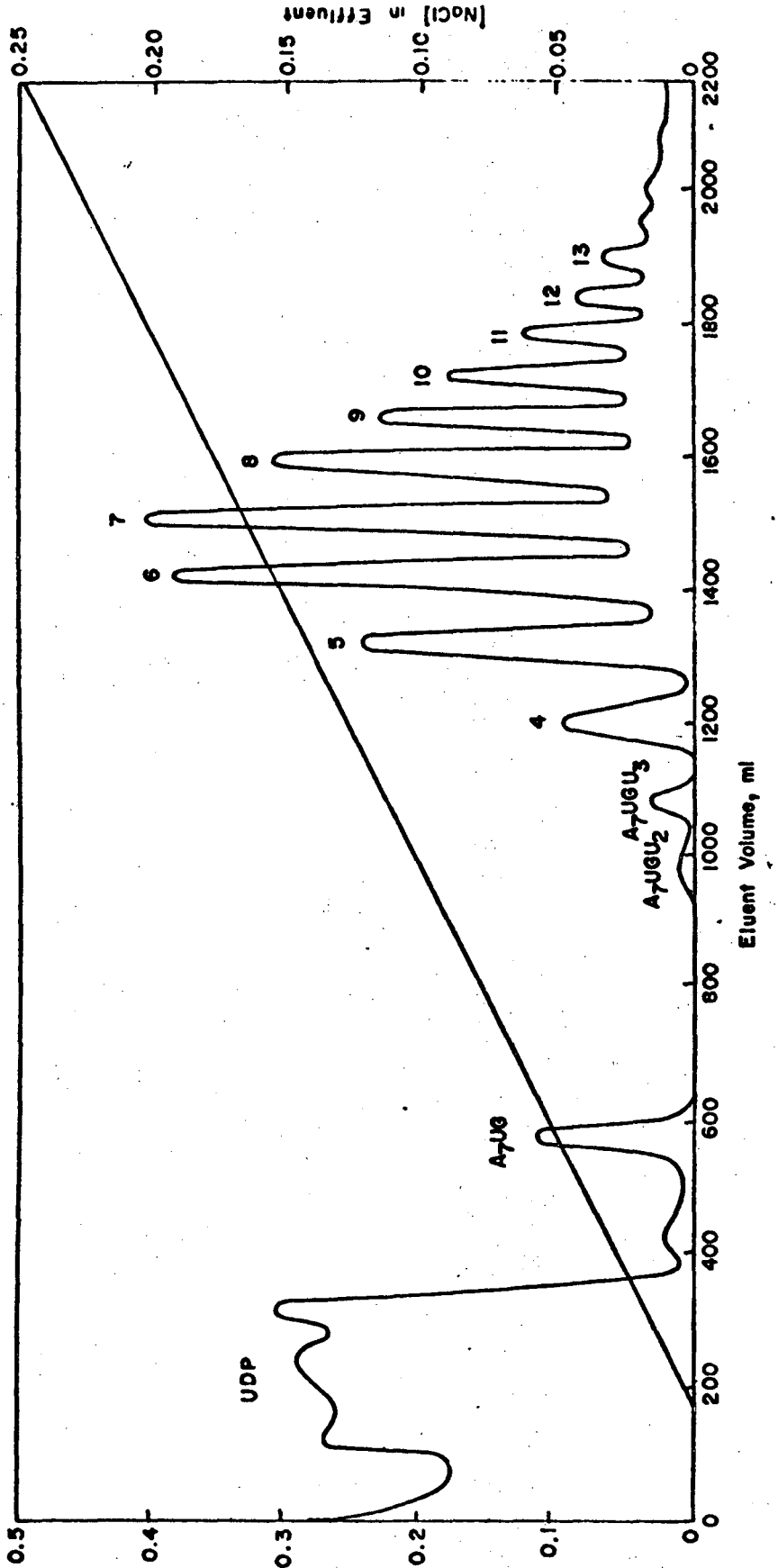
[NaCl] in Effluent
0.25
0.20
0.15
0.10
0.05
0
2200
2000
1800
1600
1400
1200
1000
800
600
400
200
0
Eluent Volume, ml
A260
0.5
0.4
0.3
0.2
0.1
0
UDP
A7UG
A7UGU2
A7UGU3
4
5
6
7
8
9
10
11
12
13

Figure 3-5

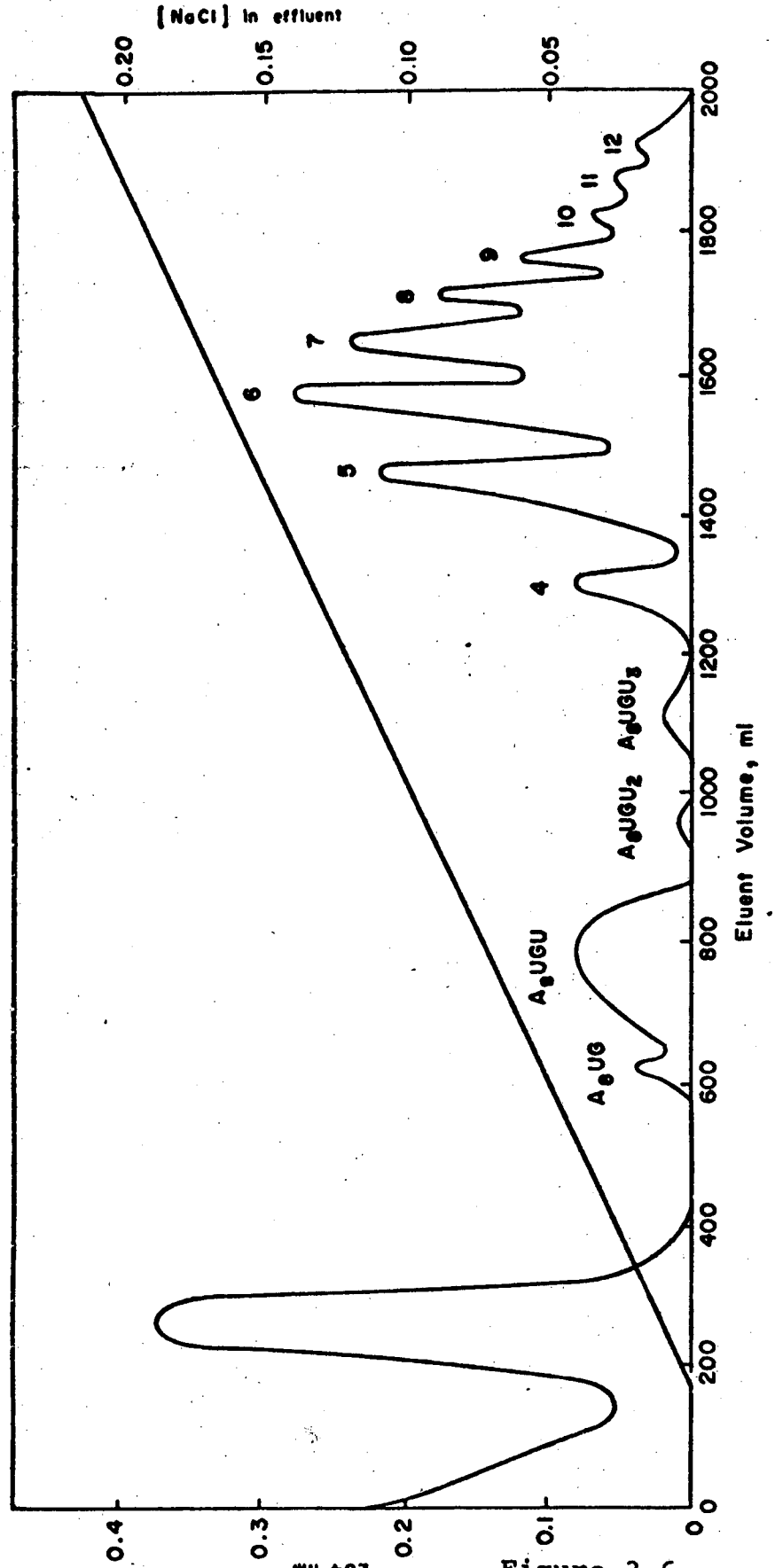
[NaCl] in effluent
0.20
0.15
0.10
0.05
2000
1800
1600
1400
1200
1000
800
600
400
200
0
12
11
10
9
8
7
6
5
4
A_8UGU_3
A_8UGU_2
A_8UGU
A_8UG
Eluent Volume, ml
0.4
0.3
0.2
0.1
0
$A_{264\ nm}$

Figure 3-6

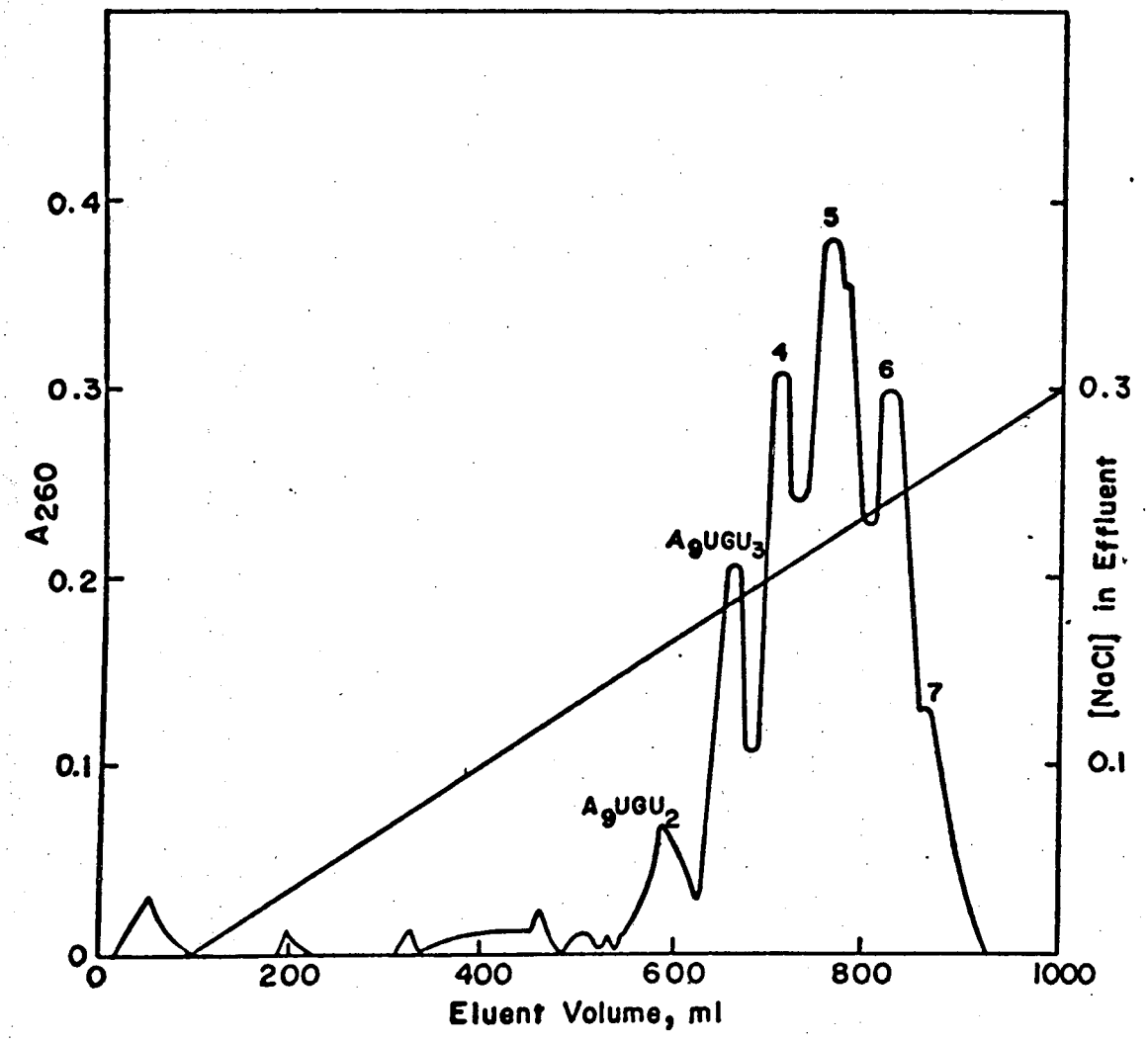
0.4
0.3
0.2
0.1
0
A260
0
200
400
600
800
1000
Eluent Volume, ml
0.3
0.1
[NaCl] in Effluent
A9UGU3
A9UGU2
4
5
6
7

Figure 3-7

CHAPTER 4

THE STABILITY OF RNA HAIRPIN LOOPS AND DIMERS: A_nUGU_m

SUMMARY

RNA oligomers A_nUGU_m, n = 7-9, m = 5-10, have been synthesized and found to form hairpin loops in .02 or .10 M Na^+, and dimers in 1 M Na^+ , or .02 M Na^+ containing 10 mM Mg^{+2}. The hairpin loops displayed T_m's 13 to 29°C greater than that of $A_6C_8U_6$ in the same solvent, and were most stable with a loop size of 6. The increased stability of these loops is attributed to the presence of a U residue in the loop.

INTRODUCTION

Hairpin loops form whenever adjacent regions of an RNA molecule base pair, and most natural RNA's are at least two-thirds base paired.[1-3] Some of the functional properties of tRNA[4], mRNA[5], rRNA[6], and 5S RNA[7] have been attributed to the behavior of hairpin loops. We would like to be able to predict the secondary structure of an RNA molecule on the basis of its sequence, as has been attempted[8-10], but more thermodynamic information is needed about loop stability. A few studies have been made of natural and synthetic hairpin loops[11-15], and we are here continuing the work of Uhlenbeck, et al.[14] on synthetic loops with A-U base paired helices.

RNA oligomers of the form A_nUGU_m, where n = 7-9, and m = 5-10, have been prepared, and are studied as hairpin loops in low salt buffer (.02 and .10 M) and as dimers in 1 M salt and in .02 M salt with .01 M $MgCl_2$. We have found that all A_nUGU_m loops are more stable than $A_6C_8U_6$ in .02 M salt by 13 to 29°C, implying that the presence of a nonstacking U in the loop greatly stabilizes the molecule. Furthermore, the varying stabilities of loops with the same number of bases in the loop but different numbers of A's and U's implies that loop stability depends greatly on sequence.

In 1 M salt, A_8UGU_m dimers with m = 6-8 are only slightly less stable than one would expect for A_8U_8 from the data of Martin, et al.[16] In addition, A_8UGU_6

was found to be surprisingly stable in .02 M salt with .01 M $MgCl_2$.

MATERIALS AND METHODS

The oligomers A_nUGU_m were synthesized as described in Chapter 3. The oligomer $A_6C_8U_6$ was synthesized and characterized by Uhlenbeck, et al.[14]

Measurements were made in four different solvents: 10 mM NaH_2PO_4, 5 mM NaCl, 0.1 mM EDTA, pH 7.00, which will be referred to as 21 mM Na^+ buffer; 10 mM NaH_2PO_4, 10 mM $MgCl_2$, 5 mM NaCl, 0.1 mM EDTA, pH 7.00, or 21 mM Na^+, 10 mM Mg^{+2} buffer; 10 mM NaH_2PO_4, 85 mM NaCl, 0.1 mM EDTA, pH 7.00, or 101 mM Na^+ buffer; 10 mM NaH_2PO_4, 1.0 M NaCl, 0.1 mM EDTA, pH 7.00, or 1 M Na^+ buffer.

Extinction coefficients at 60°C in 21 mM Na^+ buffer were obtained by alkaline hydrolysis of 7 of the 12 oligomers examined here, and agreed within experimental error with extinction coefficients calculated from ε_{260} at 60°C for A_7, A_8, and A_9, extrapolated from the data of Martin, et al.,[16] ε_{260} for U_n's from Simpkins and Richards,[17] and ε_{260} for UMP and GMP from Pabst Circular OR-10.[18] For the sake of consistency, calculated extinction coefficients were used to calculate all oligomer concentrations.

Weight-average molecular weights of oligomers were estimated from sedimentation equilibrium runs in a Spinco Model E analytical ultracentrifuge equipped with UV

scanner. Measurements were made in 21 mM Na^+ buffer at bulk A_{260} of about 0.3 or less, at either 0°C or 20°C or both. To minimize problems of convection in the low salt buffer 25 λ aliquots of oligomer solution were run on top of Beckman FC-43 fluorochemical, giving an aqueous column height of less than 1 mm in the double-sector cell of an ANG rotor. The equilibrium runs were done at 30,000 rpm, and equilibrium was reached in less than an hour (although several hours were allowed before making scans). A $\bar{v}_2$ of 0.53 ml/g[19] was used in the molecular weight calculation.

A_{260} *vs.* temperature profiles were measured on a Gilford 2000 automatic recording spectrophotometer as described by Martin, *et al.*[16] Temperature was controlled by a Neslab constant-temperature bath. Data were treated as previously described,[14] with the low temperature region extrapolated to zero slope.

RESULTS

(a) Extinction Coefficients

The calculated and measured ε_{260} (60°) for each of the A_nUGU_m oligomers studied here appear in Table 4-1. For $A_6C_8U_6$, the previously calculated[4] ε_{260} (47°) of 9.0×10^3 l/mole base·cm was used to calculate concentrations.

Table 4-1

Extinction Coefficients

Oligomer	$\varepsilon_{260}(60°)$, calculated	10^4 ℓ/mole base·cm measured
A_7UGU_5	1.09	--
A_7UGU_6	1.08	1.06
A_7UGU_7	1.07	1.08
A_7UGU_8	1.06	--
A_7UGU_9	1.05	1.05
A_8UGU_5	1.08	1.10
A_8UGU_6	1.07	1.09
A_8UGU_7	1.06	1.03
A_8UGU_8	1.05	--
A_8UGU_{10}	1.04	--
A_9UGU_6	1.05	--
A_9UGU_7	1.04	1.09

(b) Molecular Weights

Weight-average molecular weights were estimated from equilibrium sedimentation as an assay for dimerization or aggregation of oligomers in 21 mM Na^+ buffer. The expected molecular weights were calculated from the sequences of the oligomers and the molecular weights of NaAMP, NaUMP, NaGMP, and uridine. The estimated weight-average molecular weights were calculated from the equation derived from Tanford[20]

$$\bar{M} = \frac{2RT \ln c_b/c_m}{(1-\bar{v}_2\rho)\omega^2(r_b^2-r_m^2)} \qquad (1)$$

where $\bar{M}$ is the weight-average molecular weight, c_b and c_m are the concentrations of oligomer at the bottom and meniscus of the aqueous column, respectively, $\bar{v}_2$ is the partial specific volume of the oligomer, ρ is the solvent density, taken to be 1.0 for 21 mM Na^+ buffer, ω is the angular velocity, and r_b and r_m are the distances in cm from the center of the rotor to the bottom and meniscus of the aqueous column, respectively.

The measured and calculated molecular weights, along with the temperatures at which they were measured, are shown in Table 4-2. The measured molecular weights are all about 30% less than the calculated ones, but are consistent with the model of monomers only for the A_nUGU_m oligomers in 21 mM Na^+ buffer. The consistent values of $\bar{M}$ at 0° and 20°C are a further indication that no dimer to monomer transition occurs with increasing temperature.

Table 4-2

Equilibrium Sedimentation Molecular Weights

Oligomer	T, °C	$\bar{M}_w \pm 10\%$	M_{calc}
A_8UGU_5	20	3600	5326
A_8UGU_6	20	4000	5673
A_8UGU_7	20	4900	6020
A_8UGU_8	20	4300	6367
A_8UGU_8	0	4500	6367
A_8UGU_8	0	4700	6714
A_7UGU_{10}	0	4900	6689

Measurements were made at a nucleotide concentration of about 3×10^{-5} M in 21 mM Na^+ buffer.

One's first reaction to the low measured molecular weights is to attribute them to the effect of low ionic strength on polyelectrolytes. However, an evaluation of the correction terms for ionic strength in Tanford[21] gives no more than a 3% increase in $\bar{M}$; the correction is small because m_3, the Na^+ molality, is still 1000 times m_2, the oligomer molality, while Z, the number of phosphate charges per oligomer, is only 14-18. Rather than ionic strength, the low molecular weights reported must be attributed to signal averaging by the scanner as it scans a 0.5-0.7 mm aqueous column with a 0.05 mm slit; for example, the discontinuity between solvent and underlying oil appears as a sloping line. This effect would be insignificant with a larger sample.

(c) A_{260} vs. Temperature Results

As in the previous paper on hairpin loops,[14] we are studying the reaction

$$\text{single strand} \rightleftharpoons \text{hairpin loop} \qquad (2),$$

which has an equilibrium constant,

$$K(T) = \frac{f}{1-f} \qquad (3),$$

where f is the loop fraction. When $f = 1 - f = 0.5$, $K(T) = 1$, and the temperature at which this occurs is called T_m, the melting temperature.

We will also consider the reaction

$$2 \text{ single strands} \rightleftharpoons \text{dimer} \qquad (4),$$

where f represents the dimer fraction of the oligomers, and define T_m as the temperature where f = 0.5.

The plot of 1 - f vs. T for oligomers should be concentration dependent for dimer formation, shifting to lower T as the concentration decreases, but concentration independent for loop formation. To distinguish the two cases, 1 - f vs. T measurements were made for each of the oligomers studied at three concentrations over a factor of 100, except for A_9UGU_6 and $A_6C_8U_6$, which were done at two concentrations over a factor of 20.

By these criteria, all A_nUGU_m and $A_6C_8U_6$ were found to form loops in 21 mM Na^+ buffer, A_7UGU_8 and A_8UGU_8 formed loops in 101 mM Na^+ buffer, A_8UGU_6 formed dimers in 21 mM Na^+, 10 mM Mg^{+2} buffer, and A_8UGU_6, A_8UGU_7, and A_8UGU_8 formed dimers in 1 M Na^+ buffer.

A_8UGU_9, A_8UGU_{11}, A_8UGU_{12}, and A_7UGU_{11} were also studied in 21 mM Na^+ buffer, but were found to have biphasic A_{260} vs. T profiles, suggestive of populations containing loops, dimers, and/or higher aggregates, although no evidence of this appeared from the molecular weight determnations at the same conditions. In any case, the data for these molecules were impossible to analyze by simple methods. The oligomer A_8UGU_{10} behaved like a hairpin loop in its A_{260} vs. T behavior, but in view of the results for other very similar molecules, and the low average hypochromicity found for A_8UGU_{10} (Table 4-3), we must allow the possibility that the A_{260} vs. T

profile we have observed is only the upper arm of a biphsasic curve. With this caveat in mind, we shall treat this molecule below as a hairpin loop.

The plots of 1 - f vs. T appear in Figure 4-1 for $A_6C_8U_6$, A_7UGU_5, and A_8UGU_5 in 21 mM Na^+ buffer. Figure 4-2 shows plots for A_7UGU_6 and A_8UGU_6 in 21 mM Na^+ buffer. Figure 4-3 shows A_9UGU_6 and A_7UGU_7 in 21 mM Na^+ buffer, while Figure 4-4 presents plots for A_7UGU_8, A_7UGU_9, and A_8UGU_7 in the same buffer, and Figure 4-5, those for A_8UGU_8, A_9UGU_7, and A_8UGU_{10}, also in 21 mM Na^+ buffer. Figure 4-6 presents 1-f plots for A_7UGU_8 and A_8UGU_8 in 101 mM Na^+ buffer.

The results for the dimers, A_8UGU_6, A_8UGU_7, and A_8UGU_8 in 1 M Na^+ buffer, and A_8UGU_6 in 21 mM Na^+, 10 mM Mg^{+2} buffer, are shown in Figure 4-7 as plots of $1/T_m$ vs. log c.

(d) Hairpin Loop Formation Parameters

At T_m,

$$\Delta G^\circ = -RT_m \ln K(T_m) = 0 = \Delta H^\circ - T_m \Delta S^\circ \quad (5),$$

where ΔG° is the total standard free energy, ΔH° the total standard enthalpy, and ΔS° the total standard entropy for the reaction. Our ΔH° is derived from the van't Hoff equation, giving

$$\Delta H^\circ = 4RT_m^2 \, (\partial f/\partial T)_{T_m} \quad (6),$$

which is used for the reasons described previously.[14] Since $\Delta G^\circ = 0$ at T_m,

$$\Delta S^\circ = \Delta H^\circ / T_m \qquad (7).$$

In Table 4-3 appear T_m, ΔH°, ΔS°, and the percent hyperchromicity at 60°C of the oligomers studied in 21 mM Na^+ buffer and 101 mM Na^+ buffer.

From these data, we have three measures of d T_m/d log[Na^+]: A_7UGU_8 and A_8UGU_8 in 21 mM and 101 mM Na^+ buffers, and $A_6C_8U_6$ in 21 mM and 1 M[14] Na^+ buffers. We find an average d T_m/d log [Na^+] of 4.5 $\pm$ 1.1 °C per decade of [Na^+].

(e) Dimer Parameters

Following the treatment of Martin, et al.,[16] we shall determine ΔH°, the total enthalpy of the reaction, which is equal to $N\Delta H_b^\circ$, the number of base pairs, N, in the dimer, times the enthalpy change per base pair added to a helix, ΔH_b°, using d(1/T)/d log c from Figure 4-7 and the equation

$$\frac{1}{T_2} - \frac{1}{T_1} = \frac{R}{N\Delta H_b^\circ} \ln \frac{c_1}{c_2} \qquad (8),$$

where c is the oligomer concentration in mole/l. We shall obtain ΔS_b°, the entropy change per base pair, from the relation $\Delta S_b^\circ = \Delta H_b^\circ / T_m^\infty$, where T_m^∞ is T_m for poly A·poly U in 1 M NaCl, 78°C.[9]

These parameters, ΔH°, ΔH_b°, and ΔS_b° are shown in Table 4-4 for A_8UGU_m, m = 6,7,8 in 1 M Na^+ buffer, and A_8UGU_6 in 21 mM Na^+, 10 mM Mg^{+2} buffer; we have calculated them as a function of all base pairs, and as a

Table 4-3

Thermodynamic Parameters of Hairpin Loop Formation in (a) 21 mM Na^+ Buffer or (b) 101 mM Na^+ Buffer

(a)

Molecule	T_m(°C)	$\Delta H°, \frac{kcal}{mole}$	$\Delta S°$,e.u.	$\%H^{60}$
$A_6C_8U_6$	1.5	-16	-58	20
A_7UGU_5	19.5	-19	-66	19
A_7UGU_6	21.6	-19	-64	21
A_7UGU_7	26.2	-24	-79	22
A_7UGU_8	30.5	-29	-94	21
A_7UGU_9	27.9	-22	-72	20
A_8UGU_5	14.6	-16	-61	15
A_8UGU_6	27.5	-21	-70	21
A_8UGU_7	24.5	-17	-59	21
A_8UGU_8	28.9	-20	-63	21
A_8UGU_{10}	26.4	-14	-48	14
A_9UGU_6	29.5	-25	-81	20
A_9UGU_7	30.5	-22	-71	21

(b)

A_7UGU_8	33.4	-25	-81	21
A_8UGU_8	30.7	-22	-73	20

Table 4-4

Calculated Thermodynamic Parameters of Dimer Formation in (a) 21 mM Na^+ Buffer, and (b) 21 mM Na^+, 10 mM Mg^{+2} Buffer

(a)

		all base pairs		A-U base pairs only	
Molecule	ΔH°, kcal/mole	ΔH°_b, kcal/mole	ΔS°_b, e.u.	ΔH_b, kcal/mole	ΔS°_b, e.u.
A_8UGU_6	-70	-5.0	-14	-5.8	-17
A_8UGU_7	-89	-5.6	-16	-6.4	-18
A_8UGU_8	-97	-5.4	-15	-6.0	-17

(b)

A_8UGU_6	-151	-10.8	-31	-12.6	-36

function of A-U base pairs only, taking the model that G-U base pairs do not contribute to ΔH°.

(f) Loop Initiation Parameters

We would like to separate the effects of base pairing from the effects of loop size and sequence on hairpin loop stability. We shall make some assumptions about the average number of base pairs in a hairpin loop and the enthalpy of base pairing, and then use these assumptions to study the process of loop initiation, the formation of the first base pair in a hairpin loop.

If one writes the equilibrium constant for hairpin loop formation,

$$\frac{f}{1-f} = \gamma s^{N-1} \qquad (9)$$

where γ is the equilibrium constant for loop initiation, and s is the equilibrium constant for subsequent base pair formation, and attempts to solve for γ using the equation

$$\frac{1}{T_m} = \frac{1}{T_m^\infty} + \frac{R}{(N-1)\Delta H_b^\circ} \ln \gamma \qquad (10)$$

where ΔH_b° is the standard enthalpy for adding a base pair to the helix, and T_m^∞ is T_m for poly A·poly U in 1 M NaCl, 78°C.[9] One obtains anomalous results; this is due to electrostatic repulsion of the phosphate charges, which is significant at low ionic strength, destabilizing the infinite polymer more than an oligomer. For example, d T_m/d log $[Na^+]$ for poly A·poly U is 22°C,[22] whereas

for A_7UGU_8, A_8UGU_8, and $A_6C_8U_6$, it only averages 5°C (see above).

As an alternative, we take the approximation proposed by Elson, et al.,[23] which involves estimating a $\Delta H^*(N)$ of base pairing which depends on the number of base pairs, N, formed by the oligomer, and using $\Delta H^*(N)$ to determine a length-dependent base-pairing constant $s^*(N)$, according to the relationship

$$RT \ln s^*(N) = \Delta H^*(N) - T\Delta S^\circ \qquad (11)$$

where ΔS° is taken to be $\Delta H_b^\circ/T_m^\infty$ for poly A·poly U in 1 M NaCl, independent of electrostatic interactions.

Let us estimate $\Delta H^*(N)$ starting with the $\Delta\bar{H}_b^\circ$ for poly A·poly U found by Krakauer and Sturtevant[24] in 18 mM NaCl, which is -7.38 ± 0.08 kcal/mole. We shall adjust this figure by looking at the calculation made by Elson, et al.[23] for the electrostatic free energy change of all the phosphates, ΔG_{el}°, in $d(TA)_{50}$ between the fully extended single strand and each hairpin loop as a function of N, the number of base pairs. Their calculation assumed $d(TA)_2$ in the loop, N base pairs in the helix, and l_1 and l_2 residues in each fully extended, unbase-paired arm. They used the conditions $[Na^+]$ = 10 mM, γ = .003, and the electrostatic interaction parameter z_p^2/D = .004, where z_p is the effective charge on each phosphate, and D is the dielectric constant in the vicinity of the molecule. No attempt was made to evaluate z_p or D directly; the quantity z_p^2/D =

.004 gave the best fit to their data for ionic strength .01 - .06 M. While this is not the same system we are studying, it is sufficiently similar for the purpose of adjusting ΔH°_b for the infinite polymer to $\Delta H^*(N)$ for a short (N = 5,6,7) hairpin loop.

Elson, et al. calculated that $\Delta G^\circ_{el}(50 = +0.7$ kcal/mole, compared with $\Delta G^\circ_{el}(5,6,7) = 0.53, 0.55, 0.57$ kcal/mole, respectively, giving an average correction to $\Delta\bar{H}^\circ$ of $\Delta G^\circ_{el}(5,6,7) - \Delta G^\circ_{el}(50) = -0.15 \pm 0.02$ kcal/mole, with the further assumption that $\Delta S^\circ_{el}(50)$ does not differ significantly from $\Delta S^\circ_{el}(5,6,7)$, allowing us to equate the free energy difference to an enthalpy difference.

Finally, we estimate $\Delta H^*(5,6,7) = -7.38 \pm 0.08 - 0.15 \pm 0.02 = -7.53 \pm 0.10$ kcal/mole, which we shall round off to -7.5 kcal/mole and refer to as ΔH^*, the standard enthalpy per base pair for our oligomers in 21 mM Na^+ buffer.

From Equation (10), we may now calculate s*(5,6,7):

$$s^*(5,6,7) = e^{\frac{\Delta H^*}{RT} - \frac{\Delta S^\circ_b}{R}} \qquad (12),$$

where $\Delta S^\circ_b = -8.0$ kcal/mole/351°K, using values of ΔH°_b and T^∞_m for poly A·poly U from Tinoco, et al.[9] We may now apply the equilibrium Equation (8) at T_m where f = 0.5 to obtain

$$\gamma = [s^*(5,6,7)(T_m)]^{1-N} \qquad (13).$$

For the free energy of loop initiation, we shall use the equation

$$\Delta G_i^\circ = \Delta H_i^\circ - T\Delta S_i^\circ = -RT \ln \gamma (T) \qquad (14),$$

where ΔH_i°, the enthalpy of loop initiation, is the difference between ΔH°, the total enthalpy of the reaction, and $(N-1)\Delta H^*$, the total enthalpy of the base pairs in the hairpin loop, and where ΔS_i° will be obtained from Equation (14). From the middle and right side of Equation (14), we obtain

$$\gamma(T_2) = \gamma(T_1)\ e^{-(\frac{\Delta H_i^\circ}{R})(\frac{1}{T_2} - \frac{1}{T_1})} \qquad (15),$$

which we shall use to convert $\gamma(T_m)$ to $\gamma(25°C)$.

In Table 4-5 we show N, the presumed number of base pairs in each hairpin loop, the sequence of unbase-paired bases in the loop, $\gamma(25°C)$, ΔH_i°, ΔS_i°, and ΔG_i° for each oligomer studied in 21 mM Na^+ buffer. No calculations were made for the two oligomers studied in 101 mM Na^+ buffer because this would have involved estimating a different ΔH^*.

DISCUSSION

(a) Dimers

When the T_m's of A_8UGU_m in 1 M Na^+ buffer are extrapolated to $c = 10^{-4}$ M and plotted as a function of the number of base pairs (Figure 4-8) along with the data of Martin, et al.,[16] for A_nU_n and Uhlenbeck, et al.,[25] for A_nUGU_n, it may be seen (i) that the stability of A_nUGU_n

Table 4-5

Calculated Thermodynamic Parameters of Loop Initiation at 25°C in 21 mM Na^+ Buffer

Molecule	N	Loop	γ	ΔH°_i, kcal/mole	ΔS°_i, e.u.	ΔG°_i, kcal/mole
$A_6C_8U_6$	6	CCCCCCCC	2.5×10^{-4}	21.5	56	4.9
A_7UGU_5	5	AAUG	4.7×10^{-3}	11	26	3.2
A_8UGU_5	5	AAAUG	3.2×10^{-3}	14	36	3.4
A_7UGU_6	5	AAUGU	5.9×10^{-3}	11	27	3.1
A_7UGU_7	5	AAUGUU	9.9×10^{-3}	6	11	2.7
A_8UGU_6	5	AAAUGU	11.5×10^{-3}	9	21	2.7
A_8UGU_7	6	AAUGU	2.5×10^{-3}	20.5	57	3.6
A_9UGU_6	6	AAAUG	4.8×10^{-3}	12.5	31	3.2
A_7UGU_8	6	AUGUU	6.3×10^{-3}	8.5	18	3.0
A_7UGU_9	6	AUGUUU	3.6×10^{-3}	15.5	41	3.3
A_8UGU_8	6	AAUGUU	4.0×10^{-3}	17.5	48	3.3
A_9UGU_7	6	AAAUGU	4.9×10^{-3}	15.5	42	3.1
A_8UGU_{10}	6	AAUGUUUU	3.0×10^{-3}	23.5	67	3.5

nearly catches up to the stability of $A_{n+1}U_{n+1}$ at n = 5, but then continues to lag behind, and (ii) that trailing adenylate residues significantly stabilize A_8UGU_6 and A_8UGU_7 over A_6UGU_6 and A_7UGU_7. The stabilization due to one extra adenylate in A_8UGU_7 appears to balance the destabilization due to the two G-U base pairs in the middle of the molecule, relative to A_7U_7.

If one compares the values for ΔH°_b in Table 4-5 for counting A-U base pairs only, with the value of -6.4 kcal/mole found by Martin, et al.[16] for A_4U_4 using the same method, one may conclude that A_8UGU_m dimers behave like two $A_4 + U_m$ dimers joined by a UG + GU region. The G-U bonded region is itself quite weak, but causes the linked dimers to melt cooperatively.

A_8UGU_6 was studied in 21 mM Na^+, 10 mM Mg^{+2} buffer with no sure expectation of whether loops would be favored, as in low salt, or dimers, as in high salt; either result would have been reasonable. The unusual result is the high enthalpy of base pairing, -10.8 kcal/mole residue; this implies that the coordination and charge shielding by the Mg^{+2} cation of two adjacent phosphates imposes much more order than the charge shielding alone caused by an Na^+ cation.

(b) Hairpin Loops

The primary result to be seen in Table 4-5 is that hairpin loops with A, U, and G in the loop are much more stable than a loop containing only C's. Using d T_m/d

log $[Na^+]$, one would predict that all the hairpin loops studied by Uhlenbeck, et al.,[14] $A_6C_mU_6$, m = 4,5,6,8 and $A_5GC_5U_5$, are less stable than all the A_nUGU_m hairpin loops studied here.

Furthermore, we ascribe the greater stability of A_nUGU_m loops to the presence of a uridine residue, which does not stack, unlike A, G, or C, and hence need not be unstacked to form a loop. The very low circular dichroism shown by AUG[26,27] provides additional evidence that there is no stacking for this particular trimer, and therefore that it should provide little resistance to loop formation. In contrast, C_n oligomers and the C's in $A_6C_6U_6$ and $A_6C_8U_6$[14] show similar CD spectra with considerable stacking, while the smaller loop in $A_5C_5U_6$ shows evidence of strain. We shall report elsewhere[27] (Chapter 5) studies on the A_nUGU_m oligomers studied here, but in brief these molecules display spectra similar to those of A_6U_6,[28] and show indications of partial stacking of the loop adenines.

The uridine residue, then, appears to function as a universal joint in a hairpin loop. This behavior may well be the reason for the presence of U on the 5' side of the anticodon in all tRNA molecules which have been sequenced, and also in the next adjacent position in half of these tRNA molecules. The selection of AUG as the codon for initiating protein synthesis, if this process involves selection of a particular hairpin loop,[5] could be due to its stabilizing of loop formation.

The affinity of initiation factor f_3 for the A_nUGU_m hairpin loops has been measured by us,[29] as well as its affinity for AUG, $A_5GC_5U_5$, A_8U, poly (A,U,G), and f2 viral RNA, and we found that f_3 will bind to any oligomer containing AUG, but not to those tested lacking AUG, yet will bind much more strongly to the two polymers tested.

The interpretation of the fine structure of loop sequence effects is more involved than the clear effect of U. The number of base pairs indicated for each oligomer in Table 4-5 is only presumed; we chose not to attempt the analysis of a partition function containing all the likely partially bonded intermediate states, in view of our experience[14] that this approach gave results little different from the all-or-none model, and that whatever results we might obtain about the effective fractions of base-paired states would be entirely dependent on the particular model and parameters used.

One may make two classes of comparisons: among identical loops with different numbers of base pairs, and among different loops of the same size and same number of base pairs. For the loop AAAUGU with 5 or 6 base pairs, ΔG°_i increases with the number of base pairs, as it does for the loop AAUGU with 5 and 6 base pairs; this effect could be due to the electrostatic repulsion which increases with the number of charges,[23] but is not reflected in the average ΔH^* we have used. However, the opposite effect occurs for the loop AAAUG

with 5 and 6 base pairs. If we compare the two loops AAUGUU and AAAUGU, both with 5 and with 6 base pairs, we find that AAAUGU is slightly favored in both cases; similarly, the loop AAAUG is slightly favored over AAUGU for loops with 6 base pairs. These results indicate that after the first A and U in a loop, added A's are more stabilizing than added U's. On the other hand, the loop AUGUU in a molecule with 6 base pairs, has a slight edge over the loop AAUGU in a molecule with 5 base pairs, even with the disadvantage of extra electrostatic repulsion.

When the ΔG_i°'s of the different 5- and 6-membered loops are averaged, one finds ΔG_i°'s of 3.4 and 3.0 kcal/mole, respectively; the one 8-membered loop has a ΔG_i° of 3.5 kcal/mole, although this loop is A_8UGU_{10}, whose authenticity has been questioned above. The one 4-membered loop has a ΔG_i° of 3.2 kcal/mole, which may reflect either the benefit of fewer electrostatic interactions, or a true configuration with 4 base pairs and a 6-membered loop. We may tentatively assert that a 6-membered loop is the most stable size for this class of loops.

If one chooses to treat all the loops with 6 base pairs as having 7, with one less A and U in the loop, ΔG_i° increases by 0.7 kcal/mole, and ΔH_i° by 7.5 kcal/mole, for each one, but the above conclusions are unaffected, except that 5-membered loops are most favored, and larger loops are disfavored.

In order to complete the exploration of the size and

sequence dependence of loop stability, loops must be synthesized with varying numbers of G's and C's in conjunction with different bases; furthermore, it would be desirable to synthesize loops with G-C base pairs in the helical region, in order to determine whether the sequence dependence in the loop is affected. The accurate prediction of secondary structures will clearly be possible only when the sequence dependence has been exhaustively studied.

REFERENCES

1. Englander, S. W., and Englander, J. J., Proc. Natl. Acad. Sci. U.S., 53 (1965) 370.
2. McMullen, D. W., Jaskunas, S. R., and Tinoco, I., Jr., Biopolymers 5 (1967) 589.
3. Cantor, C., Proc. Natl. Acad. Sci. U.S., 59 (1968) 478.
4. Cramer, F., Progress in Nucleic Acid Research and Molecular Biology 11 (1971) 391.
5. Steitz, J. A., Nature 224 (1969) 957.
6. Eilam, Y. and Elson, D., Biochemistry 10 (1971) 1491.
7. Lewis, J. B. and Doty, P., Nature 225 (1970) 510.
8. Kallenbach, N. R., J. Mol. Biol. 37 (1968) 445.
9. Tinoco, I., Jr., Uhlenbeck, O. C., and Levine, M. D., Nature 230 (1971) 362.
10. DeLisi, C. and Crothers, D. M., Proc. Natl. Acad. Sci. U.S. 68 (1971) 2682.
11. Römer, R., Riesner, P., Maass, G., Wintermeyer, W., Thiebe, R., and Zachau, H. G., FEBS Letters 5 (1969) 15.
12. Coutts, S. M., Biochim. Biophys. Acta 232 (1971) 94.
13. Scheffler, I. E., Elson, E. L., and Baldsin, R. L., J. Mol. Biol. 48 (1970) 145.
14. Uhlenbeck, O. C., Borer, P. N., and Dengler, B., and Tinoco, I., Jr., J. Mol. Biol., in press.

15. Gralla, J. and Crothers, D. M., J. Mol. Biol., in press.

16. Martin, F. H., Uhlenbeck, O. C., and Doty, P., J. Mol. Biol. 57 (1971) 201.

17. Simpkins, H. and Richards, E. G., J. Mol. Biol. 29 (1967) 349.

18. Circular OR-10, P-L Biochemicals, Milwaukee, 1956, pp. 12,16.

19. Mahler, H. R. and Cordes, E. H., Biological Chemistry, Harper and Row, New York, 1966, p. 145.

20. Tanford, C., Physical Chemistry of Macromolecules, Wiley and Sons, New York, 1961, p. 260.

21. op. cit., p. 267.

22. Inman, R. B. and Baldwin, R. L., J. Mol. Biol. 8 (1964) 452.

23. Elson, E. L., Scheffler, I. E., and Baldwin, R. L., J. Mol. Biol. 54 (1970) 401.

24. Krakauer, H. and Sturtevant, J. M., Biopolymers 6 (1968) 491.

25. Uhlenbeck, O. C., Martin, F. H., and Doty, P., J. Mol. Biol. 57 (1971) 217.

26. Gray, D. M., Tinoco, I., Jr., and Chamberlin, M. J., Biopolymers 11 (1972) 1235.

27. Wickstrom, E. and Tinoco, I., Jr., submitted to Biopolymers.

28. Borer, P. N., Ph.D. Thesis, University of California, Berkeley, 1972.

29. Wickstrom, E., submitted to Nature.

Figures 4-1, 4-2, 4-3, 4-4, and 4-5. Single strand fraction, 1-f, vs. temperature, ^{o}C, for $A_6C_8U_6$ and A_nUGU_m in 10 mM NaH_2PO_4, 5 mM NaCl, 0.1 mM EDTA, pH 7.00 (21 mM Na^+ buffer).

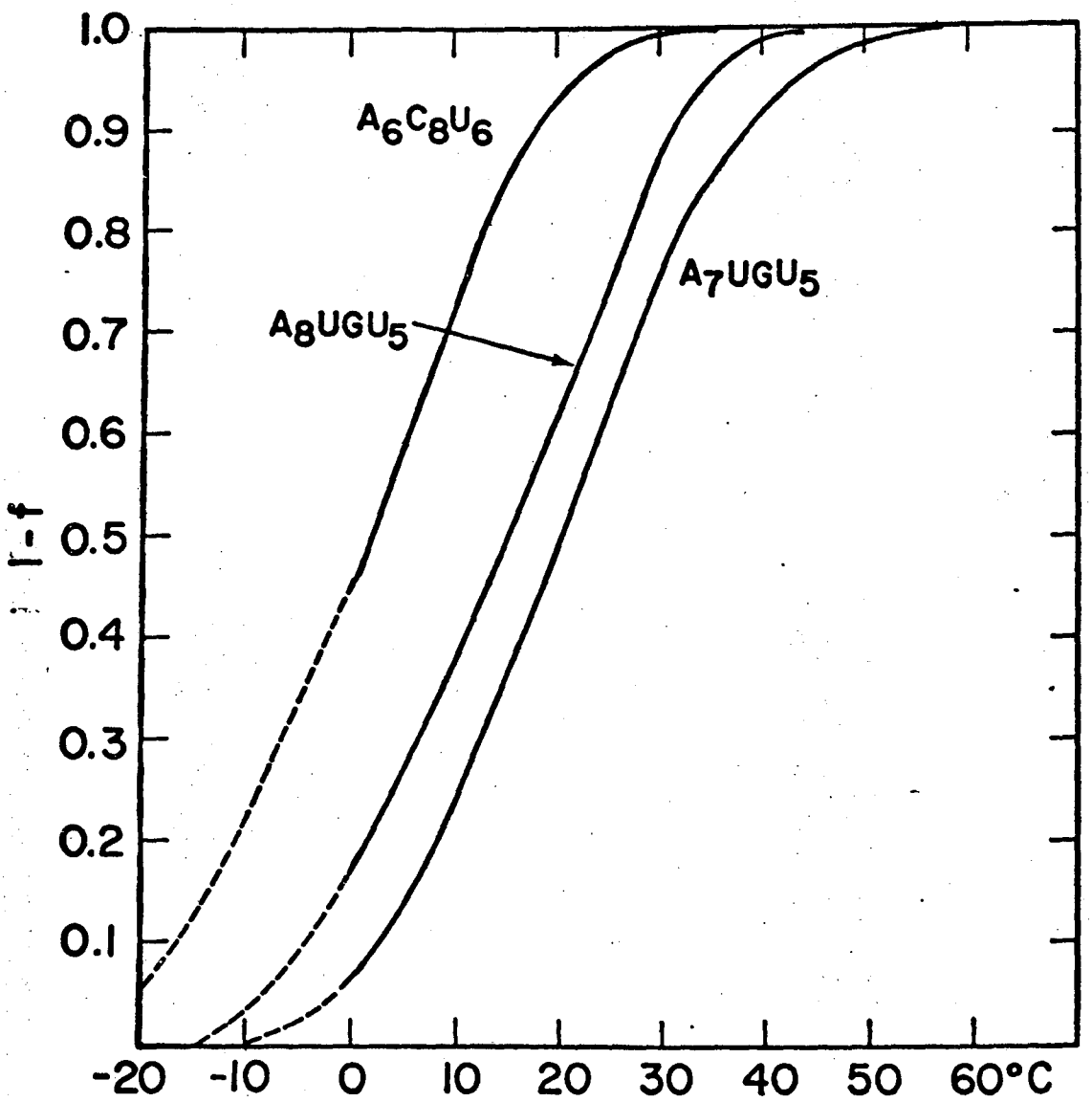
1.0
0.9
0.8
0.7
0.6
0.5
0.4
0.3
0.2
0.1
1-f
A6C8U6
A8UGU5
A7UGU5
-20
-10
0
10
20
30
40
50
60°C

Figure 4-1

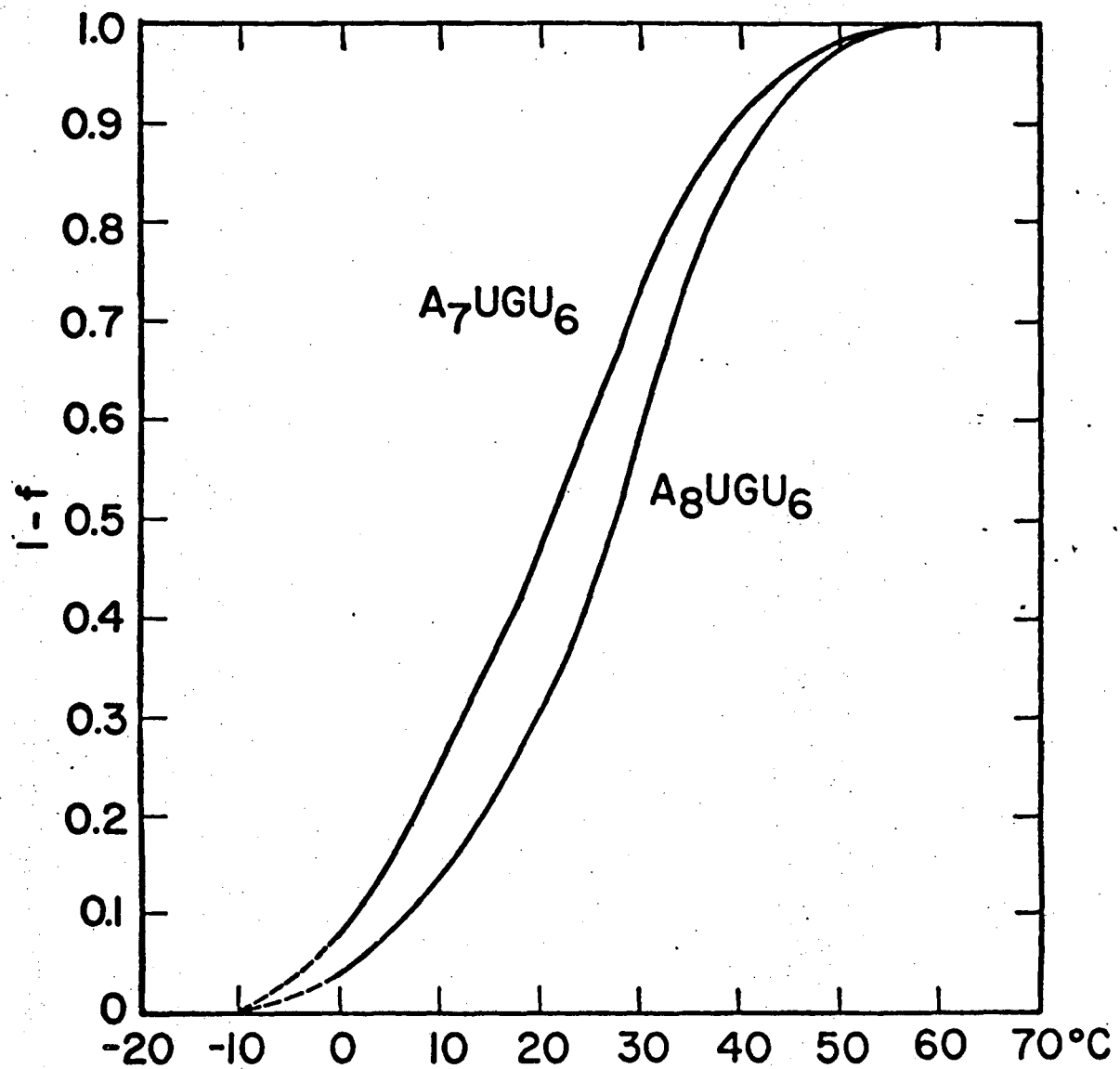
1.0
0.9
0.8
0.7
0.6
0.5
0.4
0.3
0.2
0.1
0
1-f
A7UGU6
A8UGU6
-20
-10
0
10
20
30
40
50
60
70°C

Figure 4-2

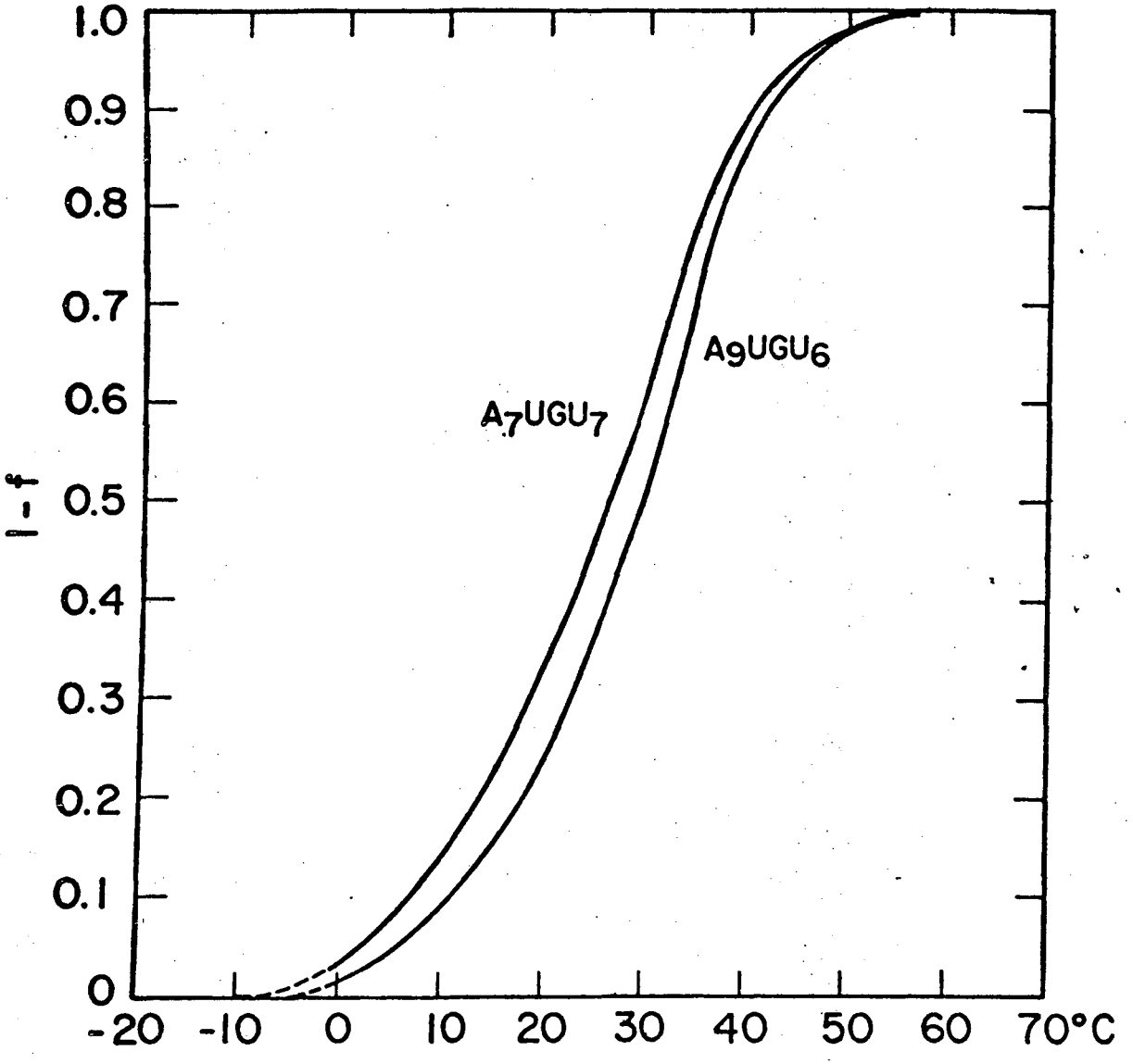
1.0
0.9
0.8
0.7
0.6
0.5
0.4
0.3
0.2
0.1
0
1-f
A9UGU6
A7UGU7
-20
-10
0
10
20
30
40
50
60
70°C

Figure 4-3

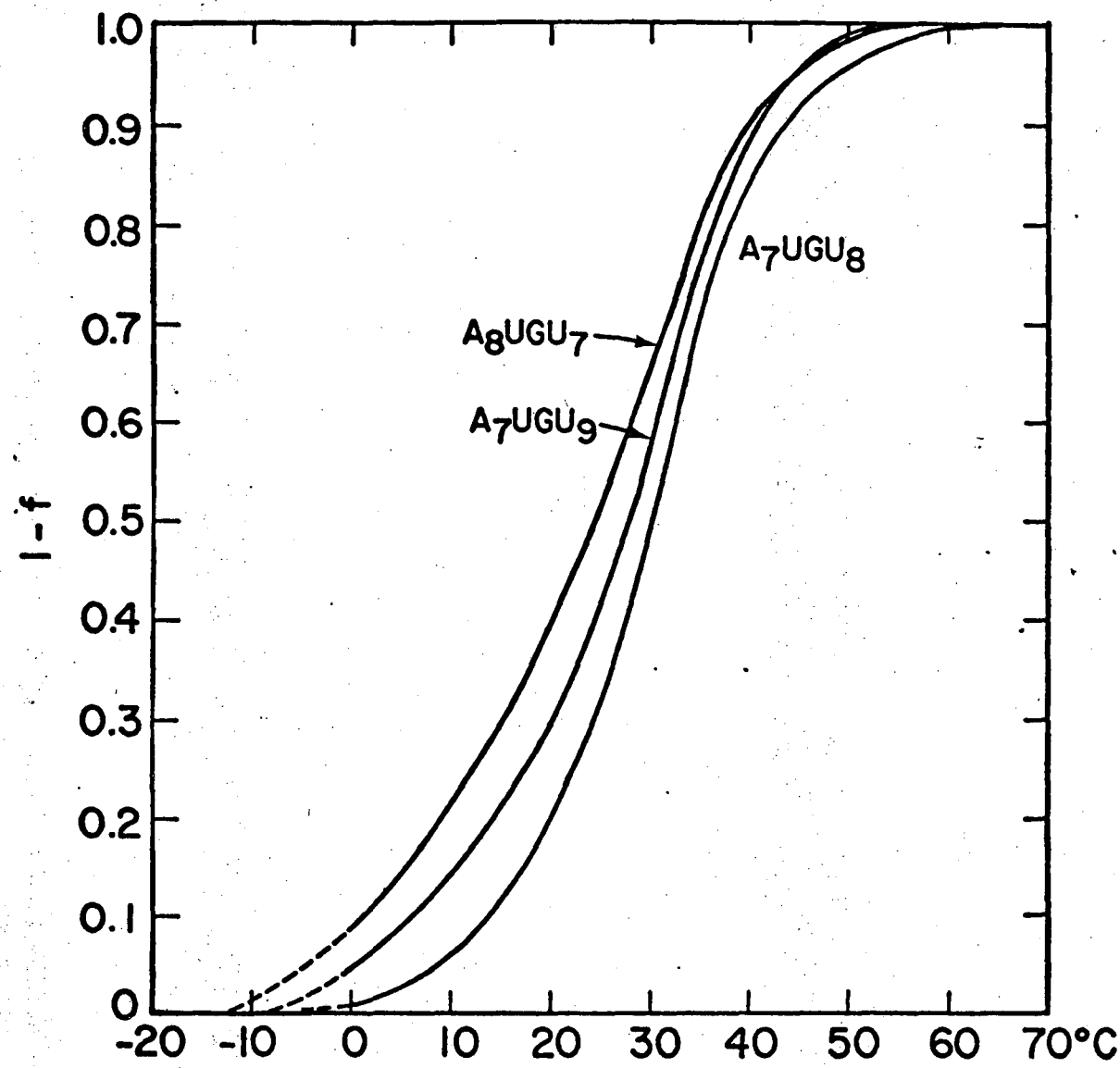
1.0
0.9
0.8
0.7
0.6
0.5
0.4
0.3
0.2
0.1
0
1-f
-20
-10
0
10
20
30
40
50
60
70°C
A7UGU8
A8UGU7
A7UGU9

Figure 4-4

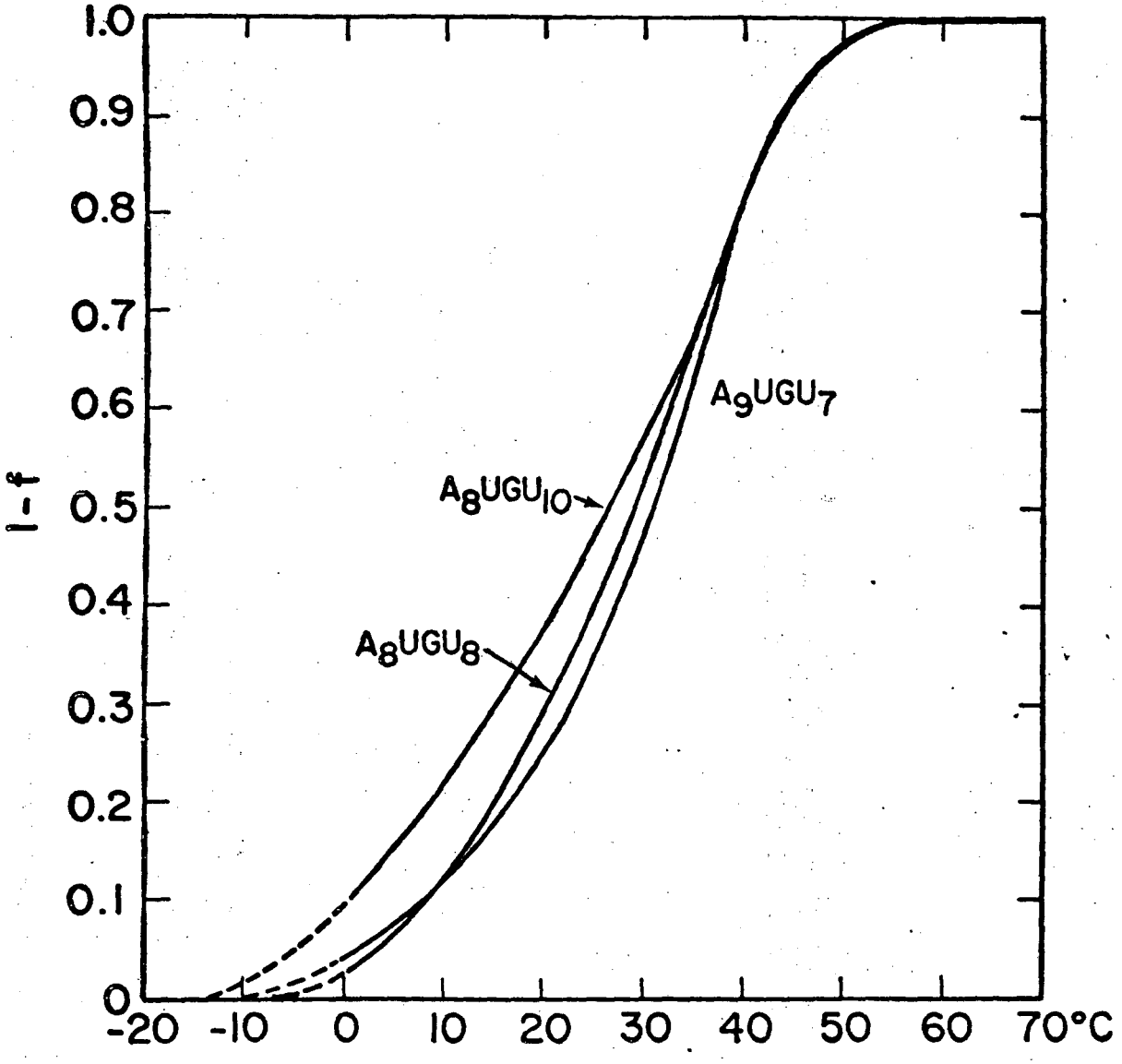
1.0
0.9
0.8
0.7
0.6
0.5
0.4
0.3
0.2
0.1
0
1-f
-20
-10
0
10
20
30
40
50
60
70°C
A9UGU7
A8UGU10
A8UGU8

Figure 4-5

Figure 4-6. Single strand fraction vs. temperature for A_7UGU_8 and A_8UGU_8 in 10 mM NaH_2PO_4, 85 mM NaCl, 0.1 mM EDTA, pH 7.00 (101 mM Na^+ buffer).

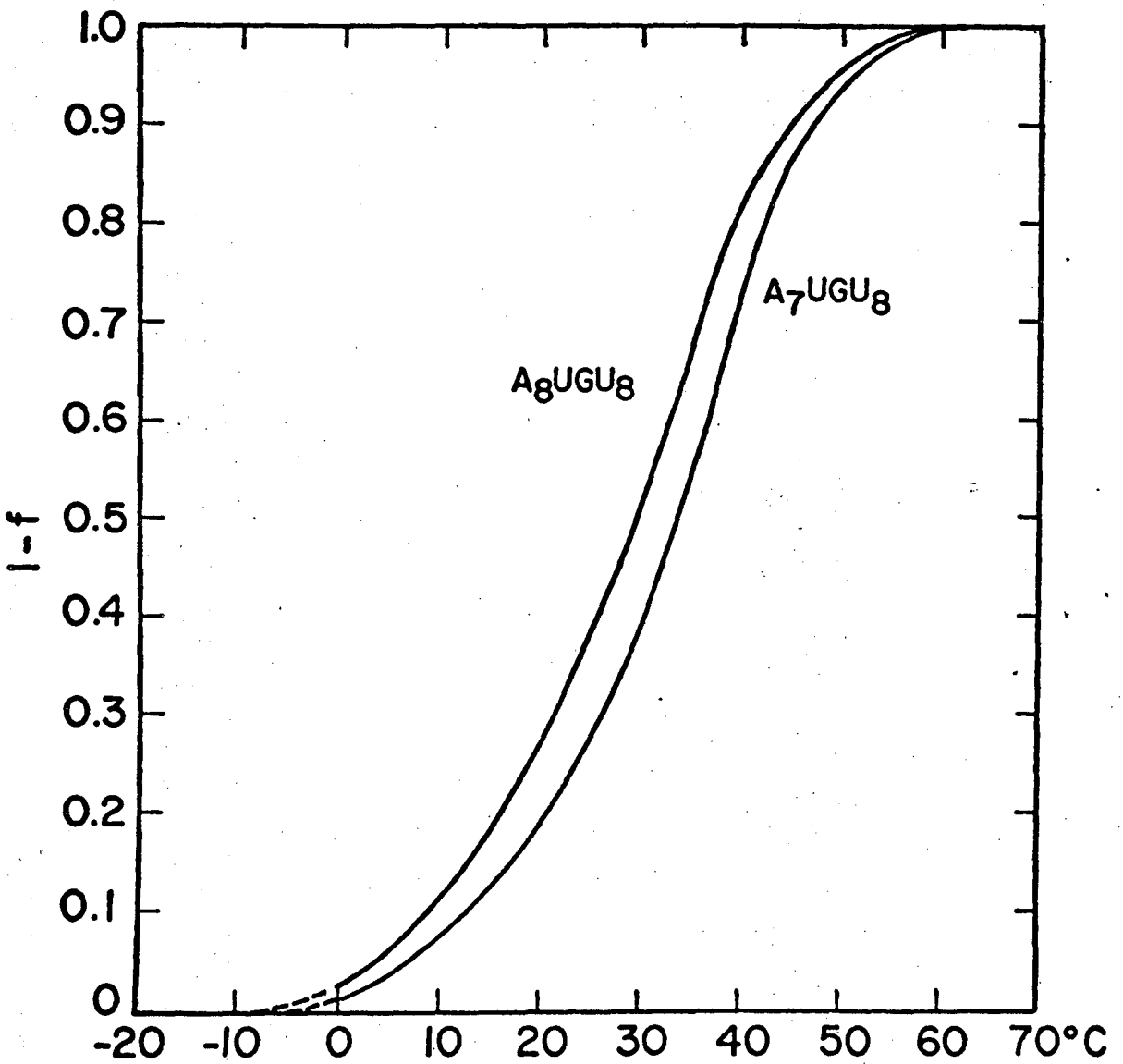
1.0
0.9
0.8
0.7
0.6
0.5
0.4
0.3
0.2
0.1
0
1-f
A7UGU8
A8UGU8
-20
-10
0
10
20
30
40
50
60
70°C

Figure 4-6

Figure 4-7. Dependence of T_m of A_nUGU_m on strand concentration. (○), A_8UGU_6 in 21 mM Na^+, 10 mM Mg^{+2} buffer. (■), A_8UGU_6, (●), A_8UGU_7, and (▲), A_8UGU_8, in 1 M Na^+ buffer.

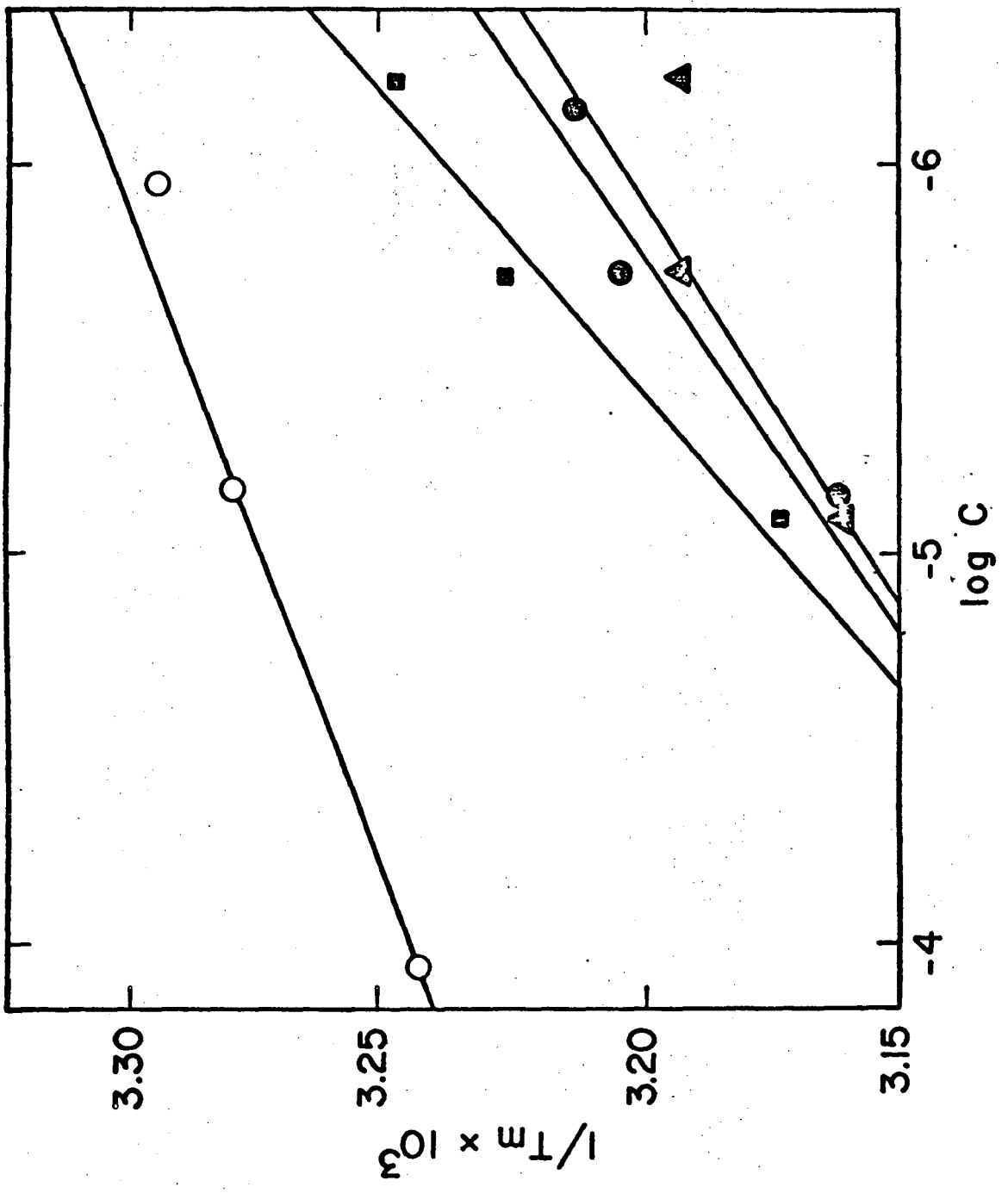

Figure 4-7

Figure 4-8. Dependence of T_m on helix length. Oligomers at 10^{-4}M in 1 M Na^+ buffer. Solid line and open circles: A_nU_n, n = 4-7, from Martin, et al.[16] Dotted line and filled squares: A_8UGU_m, m = 6-8 (extrapolated). Dashed line: A_nUGU_n, n = 4,5,8; open squares from Uhlenbeck, et al.[25]

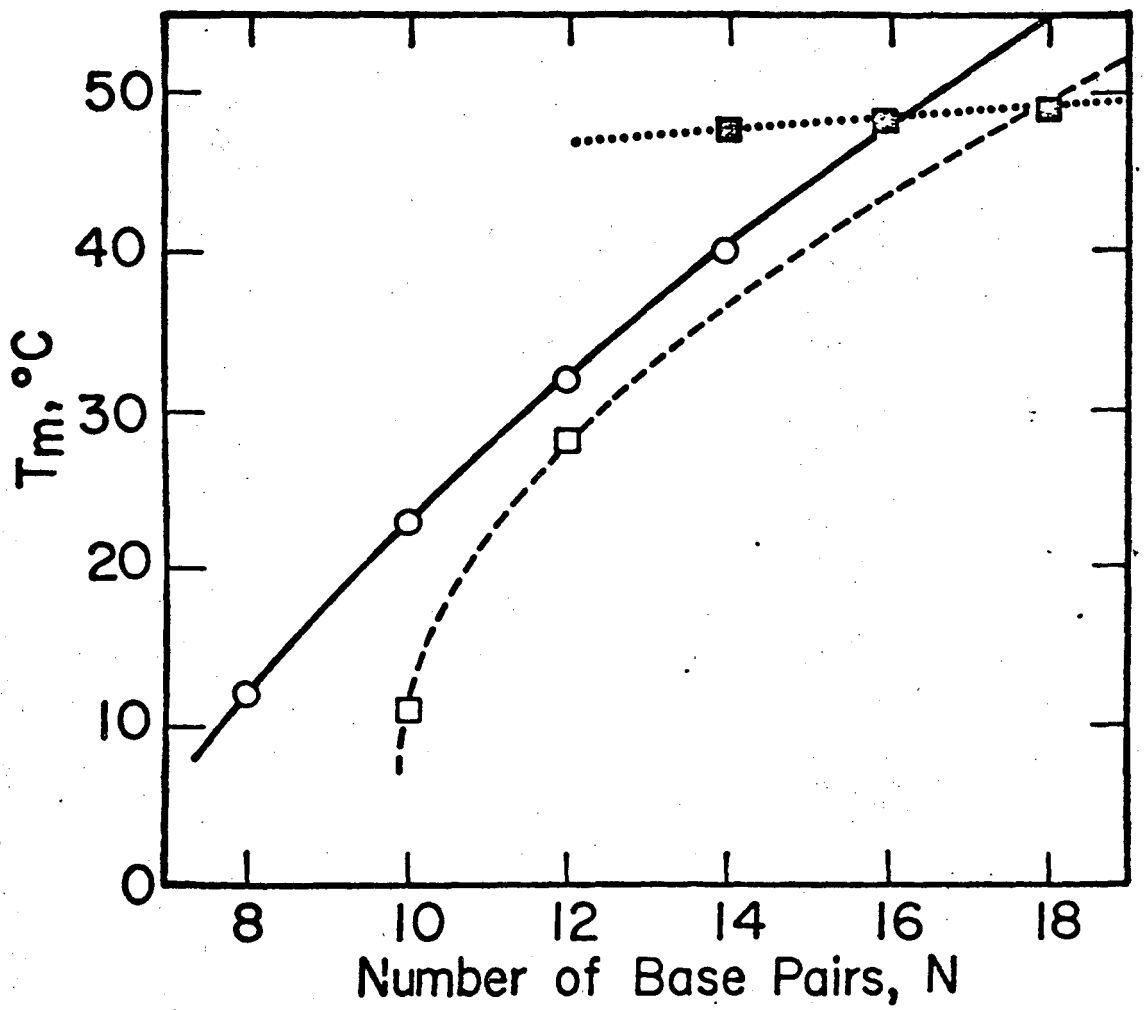

Figure 4-8

CHAPTER 5

CIRCULAR DICHROISM OF HAIRPIN LOOPS CONTAINING AUG: A_nUGU_m

SUMMARY

Circular dichroism spectra were taken of the hairpin loops $A_7UGU_{6,7,8}$, $A_8UGU_{6,7,8}$, and A_9UGU_6 in .02 M NaCl, and compared with circular dichroism spectra of A_6U_6 in 1 M NaCl. Difference spectra were calculated between each A_nUGU_m and A_6U_6 at similar temperatures and identical single strand fractions. Appropriate weighting factors were used for the assumption of 5,6, or 7 base pairs in the hairpin loops, to give the presumed CD spectrum of the unbasepaired nucleotides in the loop, for each assumed number of base pairs. Using the measured CD spectra of ApA, ApUpGp, A, and U, CD spectra were calculated for each of the presumed unbasepaired sequences, and compared with the difference spectra. The best agreement was found for hairpin loop models containing 5 base pairs and 5-8 unbasepaired nucleotides.

INTRODUCTION

The structure of RNA hairpin loops has attracted considerable interest in recent years.[1-9] The stability of the hairpin loops $A_6C_mU_6$, m = 4,5,6,8 was studied previously[10], and we recently studied the sequence dependent stability of the hairpin loops A_nUGU_m, n = 7-9, m = 5-10, in low salt buffer.[11] These molecules were shown to form hairpin loops in 21 mM Na^+ buffer by the criteria of monomeric molecular weights from equilibrium sedimentation at 0° and 20°C, and constant A_{260} vs. temperature profiles at three concentrations over two orders of magnitude.

In this paper we report the circular dichroism spectra of A_7UGU_{6-8}, A_8UGU_{6-8}, and A_9UGU_6 in 21 mM Na^+ buffer at various temperatures. We have compared the spectrum of each molecule at its lowest single strand fraction with the CD spectrum of A_6U_6 at the same single strand fraction, measured in 1 M Na^+ buffer, using weighting factors which represent different arbitrary numbers of base pairs. The resulting difference spectra are compared with model CD spectra for the bases in the unbasepaired loop, calculated from the measured spectra of ApA, ApUpGp, A, and U.

These comparisons give the best agreement for hairpin loops assumed to have 5 base pairs and 5-8 unbasepaired loop residues. The results imply that the adenosines in the loops of A_nUGU_m hairpin loops are partially

stacked.

MATERIALS AND METHODS

A_nUGU_m oligomers were synthesized and characterized as described previously.[11] All measurements on A_nUGU_m oligomers were made in 10 mM NaH_2PO_4, 5 mM NaCl, 0.1 mM EDTA, pH 7.00 (21 mM Na^+ buffer).

A_6U_6 measurements were done in 10 mM NaH_2PO_4, 1 M NaCl, 0.1 mM EDTA, pH 7.00 (1 M Na^+ buffer). The A_{260} vs. temperature profile was measured by Martin, et al.,[12] and the circular dichroism was measured by Borer.[13] Circular dichroism spectra were taken by Warshaw and Cantor[14] of ApA, A, and U in 10 mM NaH_2PO_4, 0.1 M $NaClO_4$, pH 7.2, at 26°C.

ApUpGp was prepared by ribonuclease T1 digestion of TMV RNA, followed by separation of different length oligonucleotides on a DEAE Sephadex column, using a NaCl concentration gradient in 7 M urea.[15] ApUpGp was separated from other trimers by the method of Inoue, et al.[16] on a Dowex 1x2 column, using a NaCl concentration gradient in .01 M HCl. The circular dichroism of ApUpGp was measured in 10 mM Tris-HCl, 10 mM $MgCl_2$, 60 mM NH_4Cl, pH 7.4, at 25°C.

Ultraviolet absorption spectra were taken with a Cary 15 recording spectrophotometer. Circular dichroism spectra were taken with a Cary 60 spectropolarimeter with a Cary 6001 CD accessory. Spectra were digitized by a Digital Equipment Corp. PDP-8/S computer interfaced

to the Cary 60.[17] Cell holder temperature was controlled by a thermostatted thermoelectric cooler.[18] The spectra are presented as both circular dichroism ($\epsilon_L - \epsilon_R$), and ellipticity, per mole of base.

Digitized spectra were smoothed and analyzed using programs written by Dr. Philip N. Borer[13] and Dr. Martin Itzkowitz. Spectra were computer-plotted using a program written by Dr. Burt Dorman and modified by Borer.

The A_{260} vs. temperature profiles measured by Martin, et al.[12] for A_6U_6 in 1 M Na^+ buffer, and for A_nUGU_m in 21 mM Na^+ buffer[11] allowed calculation of the fraction of molecules which are single-stranded, 1-f, at any temperature. Hence, it was possible to measure the CD of the A_nUGU_m hairpin loops at temperatures where 1-f for A_nUGU_m equalled 1-f for A_6U_6 at temperatures where its CD had already been measured. In this way, one could compare the CD spectra of A_nUGU_m and A_6U_6 with the same proportions of helical and single-stranded states. Furthermore, the temperatures at which 1-f for A_nUGU_m and A_6U_6 were the same were quite close, e.g., 1-f = .04 for A_7UGU_7 at 0°C and A_6U_6 at 0°C, or 1-f = .02 for A_7UGU_8 at 0°C and A_6U_6 at -3.5°C. For this reason, the temperature dependent CD of single-stranded A_n regions should be very close, if not identical, for A_nUGU_m and A_6U_6 at a given single strand fraction.

In order to study the CD of the unbasepaired nucleotides in the hairpin loops, difference spectra were

calculated between A_nUGU_m and A_6U_6 at the lowest single strand fraction measured, .02 - .08, depending on the A_nUGU_m molecule. Difference spectra in terms of $\epsilon_L - \epsilon_R$ per mole of nucleotide in the loop were obtained by using weighting factors which assumed different numbers of base pairs, K, and unbasepaired residues, L, for each molecule. For example, A_7UGU_6 has 15 residues, so 15 = 2K + L. If K = 5 and L = 5, then only 10/15 of the molecule is helical, compared with A_6U_6, and 5/15 is in the loop. Hence, per mole of nucleotide,

$$\epsilon_L - \epsilon_R(AAUGU) = \frac{15}{5}\{\epsilon_L - \epsilon_R(A_7UGU_6) - \frac{10}{15}[\epsilon_L - \epsilon_R(A_6U_6)]\} \quad (1)$$

$$= 3[\epsilon_L - \epsilon_R(A_7UGU_6)] - 2[\epsilon_L - \epsilon_R(A_6U_6)] \quad (2).$$

If one assumes K = 6 and L = 3, one obtains

$$\epsilon_L - \epsilon_R(AUG) = 5[\epsilon_L - \epsilon_R(A_7UGU_6)] - 4[\epsilon_L - \epsilon_R(A_6U_6)] \quad (3).$$

In general, the weighting factor for the CD of A_nUGU_m is (2K + L)/L, and that for the CD of A_6U_6 is 2K/L.

We shall compare the difference spectra obtained for 5,6, or where applicable, 7 base pairs for each of the 7 hairpin loops studied, with model spectra calculated from the measured spectra of ApA, ApUpGp, A, and U. If we assume ApA stacking interactions between adjacent A's, including the last A in the helix and the first A in the loop, we then calculate a model CD spectrum for the short single strand A_nUGU_m, where now n + m = L. We obtain

$$\epsilon_L - \epsilon_R(A_nUGU_m) = \frac{1}{L}\{2n[\epsilon_L - \epsilon_R(ApA)] - (n+1)[\epsilon_L - \epsilon_R(A)] + 3[\epsilon_L - \epsilon_R(ApUpGp)] + m[\epsilon_L - \epsilon_R(U)]\} \quad (4).$$

RESULTS

The measured CD spectra of A_7UGU_{6-8}, A_8UGU_{6-8}, and A_9UGU_6 in 21 mM Na^+ buffer appear in Figures 5-1 - 5-7. The temperature and single strand fraction, 1-f, for each spectrum are shown in each figure. In Figures 5-8 and 5-9 we show the CD spectra measured by Borer[13] of A_6U_6 in 1 M Na^+ buffer. The spectra in Figure 5-8 are those used in calculating difference spectra. Figure 5-10 shows the CD spectra of ApA, A, and U measured by Warshaw and Cantor,[14] and that of ApUpGp used to calculate model spectra for the unbasepaired nucleotides in each loop.

In calculating difference spectra between A_nUGU_m hairpin loops and A_6U_6 double strands, we are making a crucial assumption that the CD of the helical portion of each hairpin loop, measured in 21 mM Na^+ buffer, is the same as that for A_6U_6 helical dimers in 1 M Na^+ buffer. While we may say that the single strand fraction of each molecule is identical, and small, and that the temperature dependent stacking of single stranded A regions is almost identical, we cannot be sure of the effects of differing ionic strength. At low ionic strength, electrostatic repulsion among phosphates charges becomes significant. If the electrostatic interaction affects only the enthalpy of base pairing, and not the double helical structure, our assumptions are justified,

since we have already seen that our hairpin loops and A_6U_6 are about equally stable in their different solvents. If, however, the separation along the helical axis or the orientation of adjacent base pairs changes due to lowered ionic strength, one would expect the optical characteristics of the helix to change.

The difference spectra and the model loop spectra are presented in Figures 5-11 - 5-20. In each figure, a difference spectrum and model spectrum appear for two pairs of values of K and L.

In no case do we see exact agreement between a particular difference and model spectrum. However, the most marked disagreements occur for the most strained model loops, and the closest agreement is seen for K = 5 and L = 5 (A_7UGU_6), 6 (A_7UGU_7, and A_8UGU_6), 7 (A_7UGU_8, A_8UGU_7, and A_9UGU_6), and 8 (A_8UGU_8).

For A_7UGU_6, with 6 base pairs, and A_8UGU_7, with 7 base pairs, both with AUG in the loop, and for A_7UGU_8, with UGU in the loop, the difference spectra are all quite large; the two presumed AUG spectra are somewhat similar. With K = 6 for A_7UGU_8 and A_8UGU_7, the difference spectra are not very large, but do not resemble either the model loop spectra or the sum of the monomers. For K = 5 for all 3 molecules, one sees good agreement between model and difference spectra for A_7UGU_6 and A_8UGU_7, and fair agreement for A_7UGU_8. In each case, the 220 nm peak agrees very well.

A_7UGU_7 shows difference spectra of opposite symmetry in the 250 and 270 nm regions, with the same symmetry as the model spectra in the case where K = 5. A_8UGU_8, which might be expected to act like A_7UGU_7 with K greater by one, acts instead like A_8UGU_7. It is interesting that the difference spectrum for K = L = 6, which is a large loop, is small and nondescript in the 250 and 270 nm regions, while the difference spectrum for 5 base pairs and an 8-membered loop shows a reasonable resemblance to the model spectrum.

A_8UGU_6 and A_9UGU_6 are molecules with one and two more adenosines, respectively, than A_7UGU_6. Like the latter, their difference spectra are most like the model spectra for K = 5. Comparing all 3, the difference spectra show about the same magnitudes with increasing A's in the loop, but the crossover around 260 nm shifts progressively to the blue, and the 250 nm trough decreases in magnitude. It is noteworthy that the increasing ApA contribution to the model spectra is not reflected in the difference spectra.

Overall, for the values of K and L where the agreement between difference and model spectra is good, the best fit is seen for the 220 nm peak, and the magnitudes of the 250 nm trough and 270 nm peak are uniformly lower than those of the model spectra. Furthermore, the crossover around 260 nm shifts to the blue as L increases, with added U's showing a more pronounced effect than added A's.

DISCUSSION

Bearing in mind the assumption that the CD per base of the base pairs in the A_nUGU_m hairpin loops measured in 21 mM Na^+ buffer equals the CD per base of A_6U_6, measured in 1 M Na^+ buffer, we shall attempt to interpret the fit, or lack of fit, between the difference spectra and model loop spectra for the A_nUGU_m hairpin loops.

In each case, we find that the more strained the loop, the greater the divergence between difference spectrum and model spectrum. In the cases where L = 3 or 4, we expect steric strain to greatly reduce the possibility of stacking interactions between neighboring bases. This effect should, in turn, greatly reduce the circular dichroism due to such a loop, approaching the sum of the CD spectra of the component nucleotides, unless the orientations of the nucleotides produced by steric strain allow transitions previously unseen, and give rise to an entirely new CD spectrum. While the latter is a possible explanation for the fairly large difference spectra calculated for small loops, we consider it unlikely.

We conclude that large loops are favored over maximal base pairing, although we cannot determine from these data the ideal loop size or an upper limit where base pairing is again favored over larger loop size. A_{260} vs. temperature studies on these same hairpin loops[9]

in the same solvent showed that A_7UGU_8 is more stable than A_7UGU_9, and that A_8UGU_8 is more stable than A_8UGU_{10}. If K is set equal to 5 for all these molecules, we may say that L = 7 is preferred over L = 8, which is preferred over L = 10. However, we have made no absolute determination of K for any of these molecules, such as might be possible using proton magnetic resonance or rapid tritium exchange, so we may speak only of theoretical loop sizes for a given K.

From the degree of agreement seen between difference and model spectra for K = 5, we conclude that the adenosines in the loops of A_nUGU_m hairpin loops are partially stacked, but that the average amount of stacking per residue in a given size loop decreases with increasing A's. This suggests that the first one or two A's in the loop are partially stacked relative to ApA at 26°C, but that subsequent ones are not.

These results invite the following speculations: (i) that the Fuller and Hodgson model[1] for the anticodon loop of tRNA is partially correct, in that at most two of the loop purines are stacked, and the other 5 residues are not; (ii) that the Woese model[6] for reciprocating stacking structures in the anticodon loop of a tRNA undergoing translocation on a ribosome is not possible, due to the lack of stacking by uridines on the 5' side of the anticodon loop; (iii) that one function of the bulky residues commonly found on purines adjacent to the 3' end of the anticodon in tRNA molecules is to inhibit

REFERENCES

1. Fuller, W. and Hodgson, A., Nature 215 (1967) 817.
2. Romer, R., Riesner, P., Maass, G., Wintermeyer, W., Thiebe, R., and Zachau, H. G., FEBS Letters 5 (1969) 15.
3. Coutts, S. M., Biochim. Biophys. Acta, 232 (1971) 94.
4. Scheffler, I. E., Elson, E. L., and Baldwin, R. L., J. Mol. Biol. 48 (1970) 145.
5. Elson, E. L., Scheffler, I. E., and Baldwin, R. L., J. Mol. Biol. 54 (1970) 401.
6. Woese, C., Nature 226 (1970) 817.
7. Tinoco, I., Jr., Uhlenbeck, O. C., and Levine, M. D., Nature 230 (1971) 362.
8. DeLisi, C. and Crothers, D. M., Proc. Natl. Acad. Sci. U.S. 68 (1971) 2682.
9. Gralla, J. and Crothers, D. M., J. Mol. Biol., in press.
10. Uhlenbeck, O. C., Borer, P. N., Dengler, B., and Tinoco, I., Jr., J. Mol. Biol., in press.
11. Wickstrom, E. and Tinoco, I., Jr., submitted to
12. Martin, F. M., Uhlenbeck, O. C., and Doty, P., J. Mol. Biol. 57 (1971) 201.
13. Borer, P. N., Ph.D. Thesis, University of California, (1972).
14. Warshaw, M. M. and Cantor, C. R., Biopolymers 9 (1970) 1079.
15. Lloyd, D., Ph.D. Thesis, University of California, (1969).

16. Inoue, Y., Aoyagi, S., and Nakanishi, K., J. Amer. Chem. Soc. 89 (1967) 5701.

17. Tomlinson, B. L., Ph.D. Thesis, University of California, (1968).

18. Allen, F. S., Gray, D. M., Roberts, G., and Tinoco, I., Jr., Biopolymers 11 (1972) 853.

Figures 5-1 through 5-7. Circular dichroism spectra of A_nUGU_m in 21 mM Na^+ buffer at different temperatures, ^oC, and single strand fractions, 1-f, at the concentrations indicated.

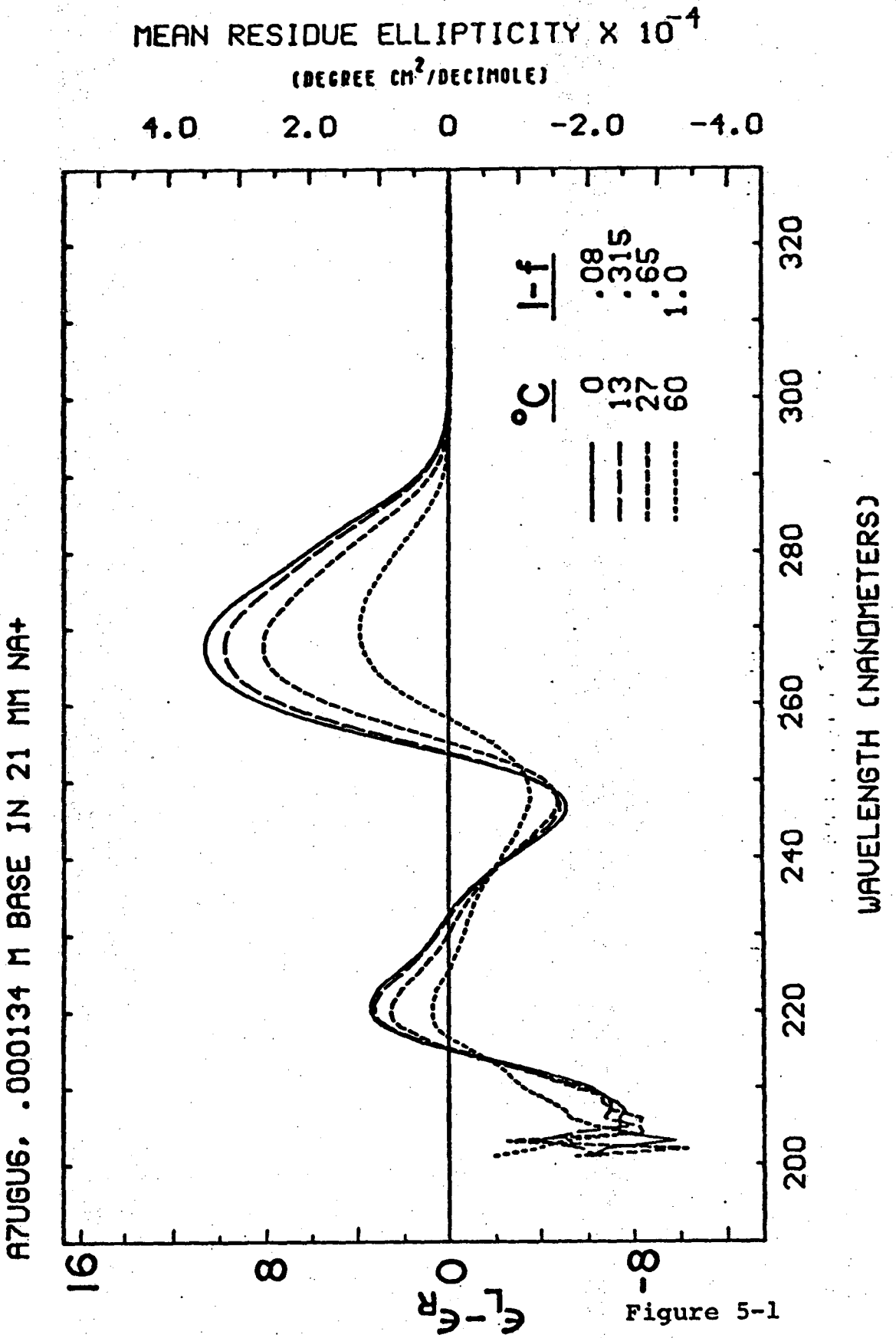
MEAN RESIDUE ELLIPTICITY X 10^{-4}
(DEGREE CM^2/DECIMOLE)
4.0
2.0
0
-2.0
-4.0
1-f
.08
.315
.65
1.0
°C
0
13
27
60
320
300
280
260
240
220
200
WAVELENGTH (NANOMETERS)
16
8
0
-8
$\epsilon_L - \epsilon_R$
A7UGU6. .000134 M BASE IN 21 MM NA+

Figure 5-1

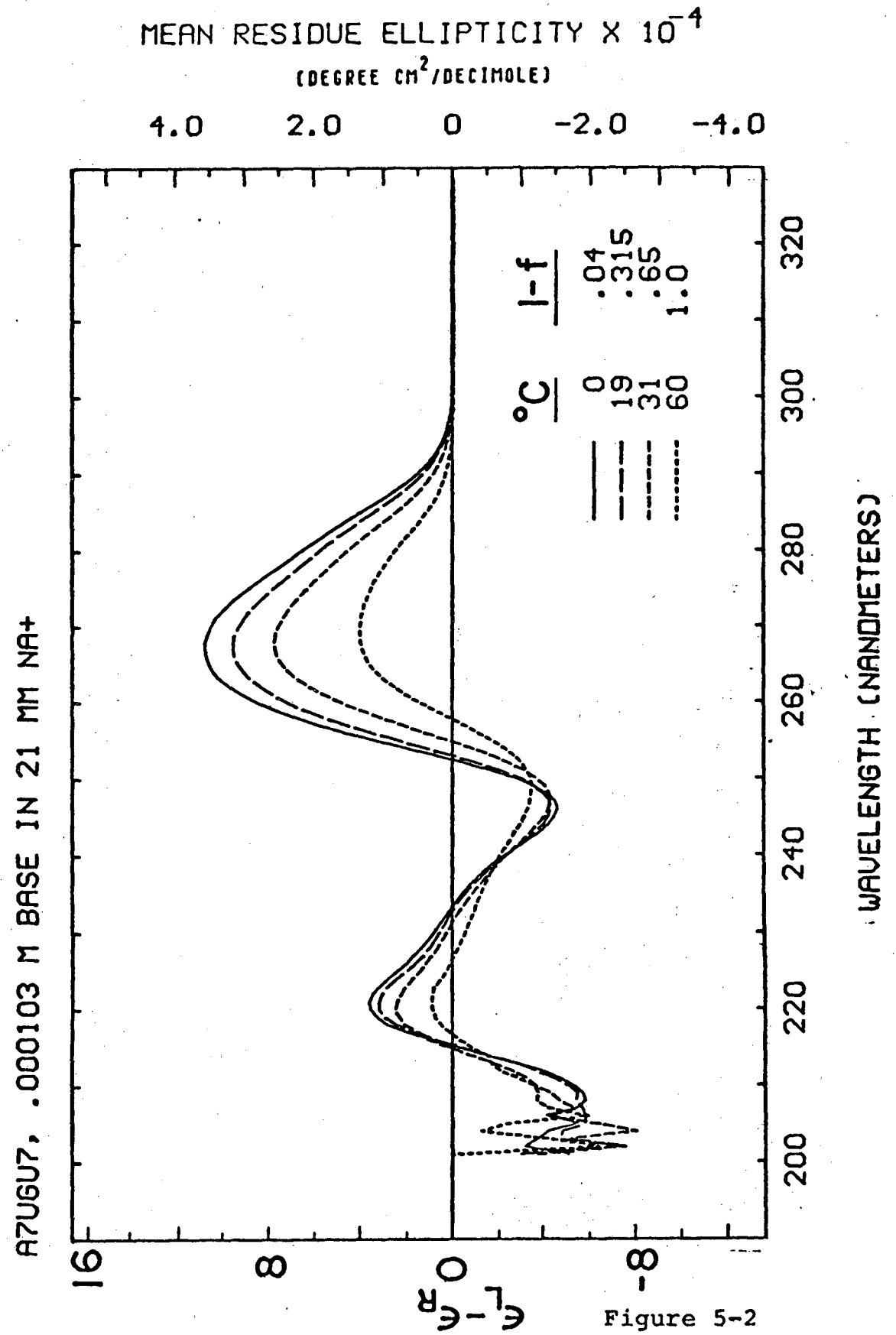
MEAN RESIDUE ELLIPTICITY X 10^{-4}
(DEGREE CM^2/DECIMOLE)
4.0
2.0
0
-2.0
-4.0
°C
0
19
31
60
1-f
.04
.315
.65
1.0
320
300
280
260
240
220
200
WAVELENGTH (NANOMETERS)
A7UGU7, .000103 M BASE IN 21 MM NA+
16
8
0
-8
$\epsilon_L - \epsilon_R$

Figure 5-2

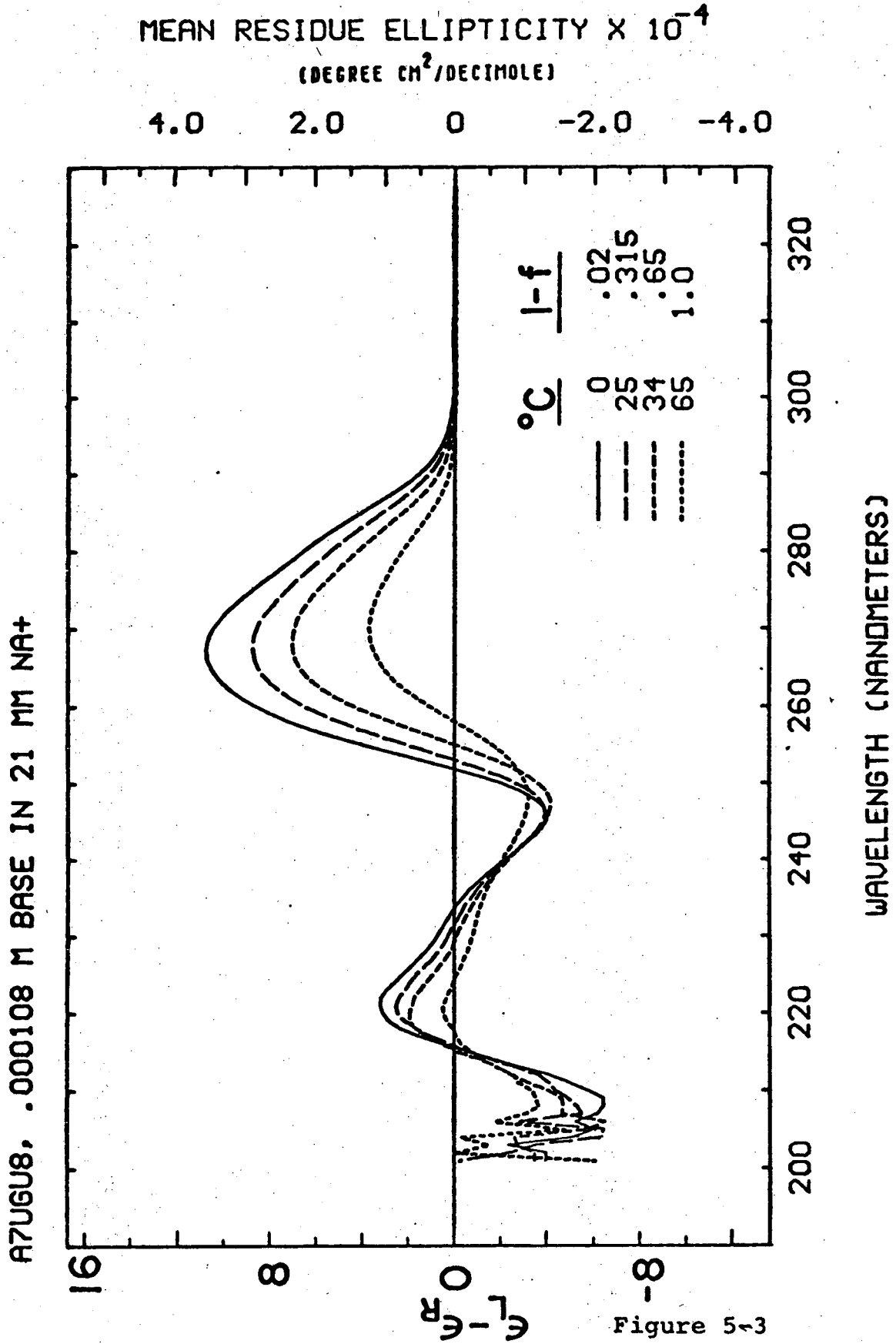
MEAN RESIDUE ELLIPTICITY X 10^{-4}
(DEGREE CM^2/DECIMOLE)
4.0
2.0
0
-2.0
-4.0
°C
0
25
34
65
l-f
.02
.315
.65
1.0
320
300
280
260
240
220
200
WAVELENGTH (NANOMETERS)
16
8
0
-8
$\epsilon_L - \epsilon_R$
A7UGU8, .000108 M BASE IN 21 MM NA+

Figure 5-3

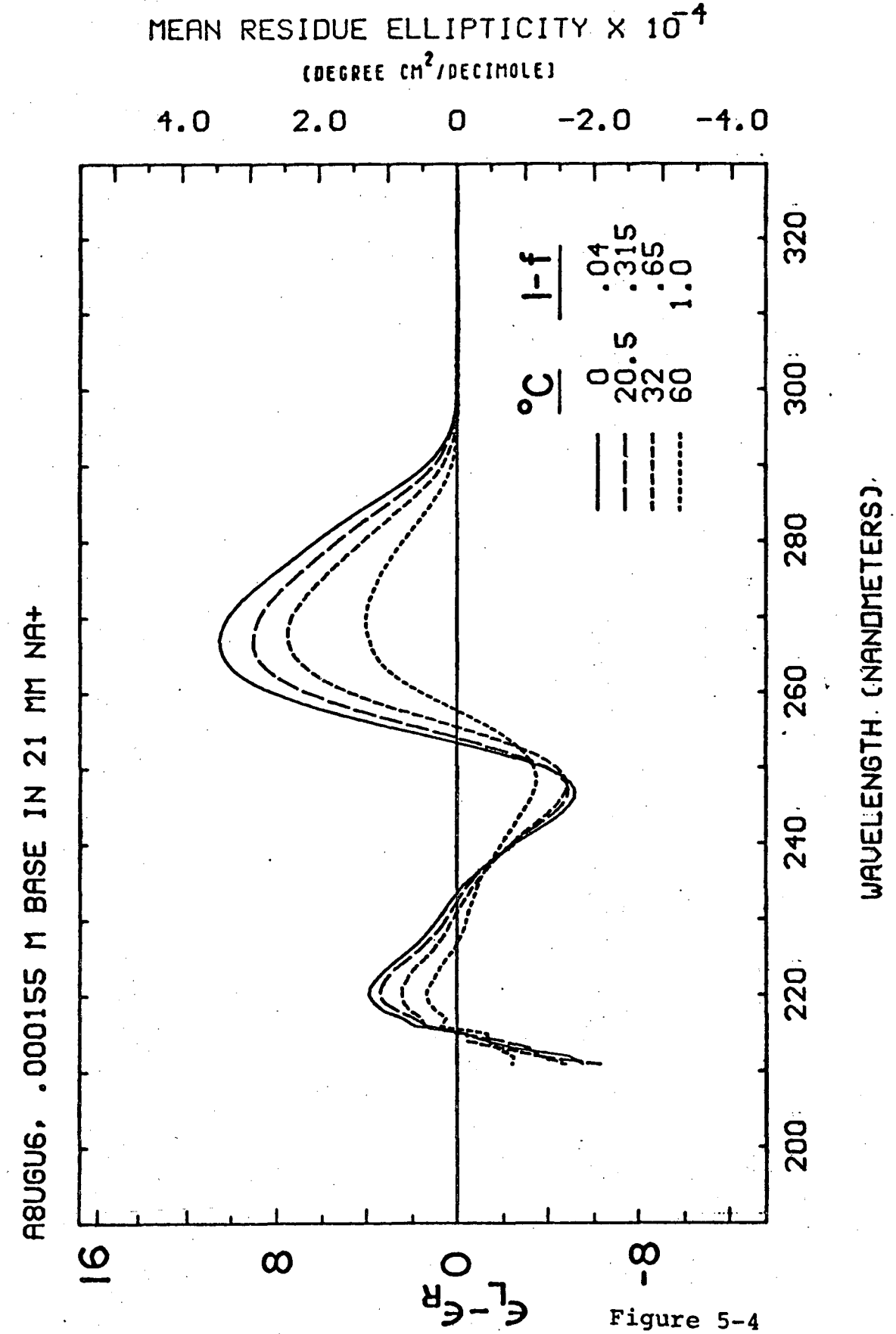
MEAN RESIDUE ELLIPTICITY X 10^{-4}
(DEGREE CM^2/DECIMOLE)
4.0
2.0
0
-2.0
-4.0
°C
0
20.5
32
60
1-f
.04
.315
.65
1.0
320
300
280
260
240
220
200
WAVELENGTH (NANOMETERS)
A8UGU6, .000155 M BASE IN 21 MM NA+
16
8
0
-8
$\epsilon_L - \epsilon_R$

Figure 5-4

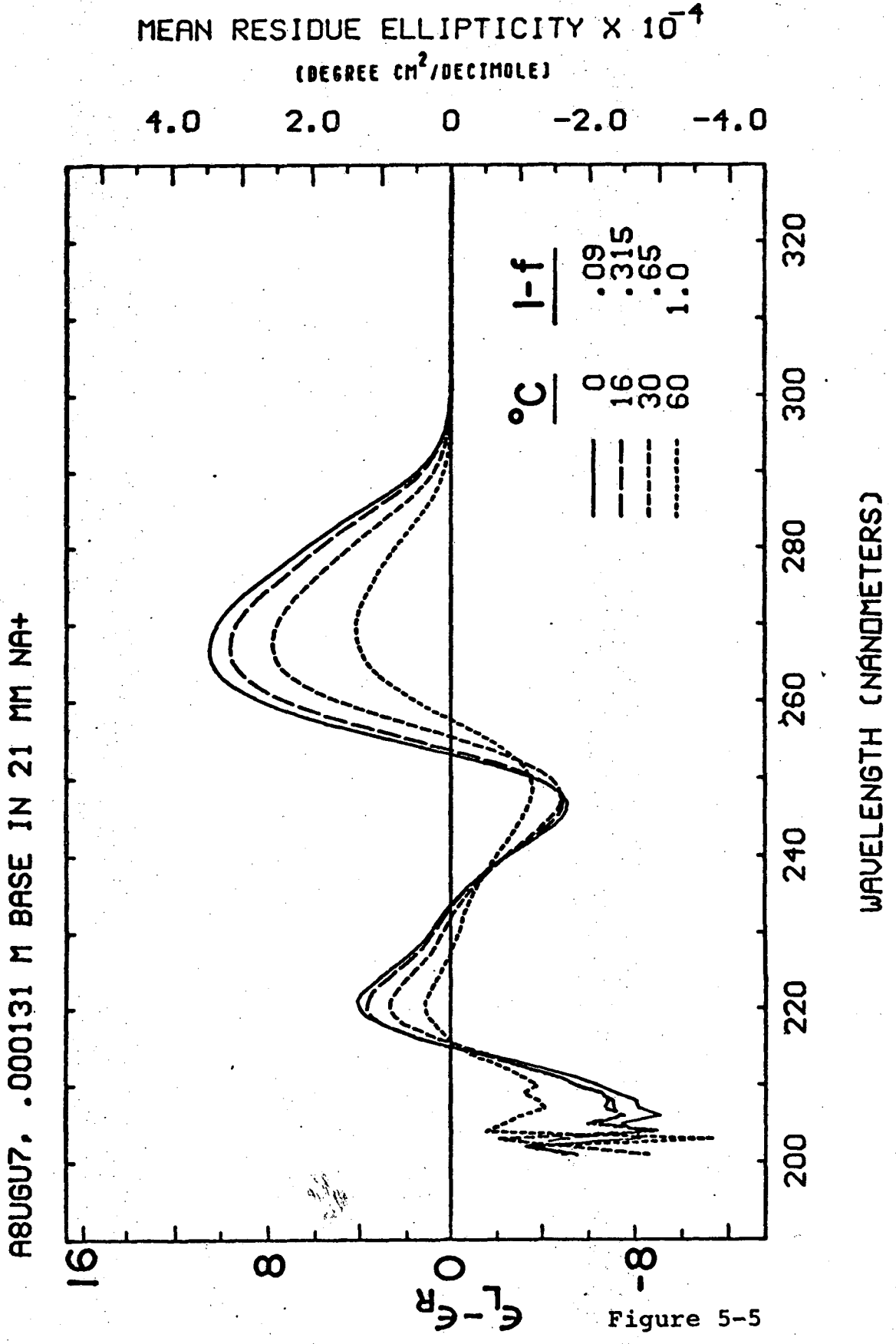
MEAN RESIDUE ELLIPTICITY X 10^{-4}
(DEGREE CM^2/DECIMOLE)
4.0
2.0
0
-2.0
-4.0
°C
0
16
30
60
1-f
.09
.315
.65
1.0
320
300
280
260
240
220
200
WAVELENGTH (NANOMETERS)
16
8
0
-8
$\epsilon_L - \epsilon_R$
A8UGU7, .000131 M BASE IN 21 MM NA+

Figure 5-5

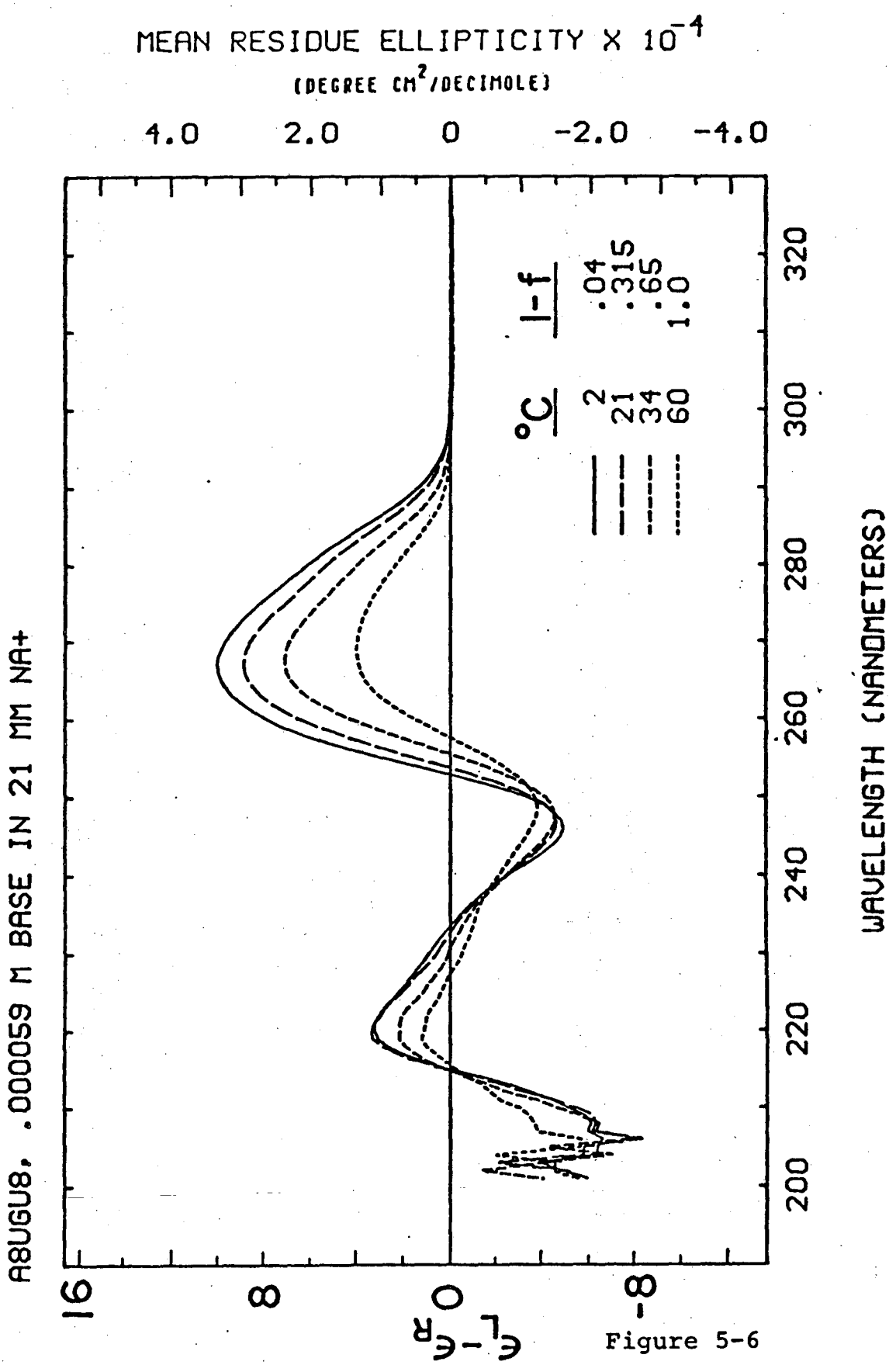
MEAN RESIDUE ELLIPTICITY X 10^{-4}
(DEGREE CM^2/DECIMOLE)
4.0
2.0
0
-2.0
-4.0
°C
2
21
34
60
1-f
.04
.315
.65
1.0
320
300
280
260
240
220
200
WAVELENGTH (NANOMETERS)
16
8
0
-8
$\epsilon_L - \epsilon_R$
A8UGU8, .000059 M BASE IN 21 MM NA+

Figure 5-6

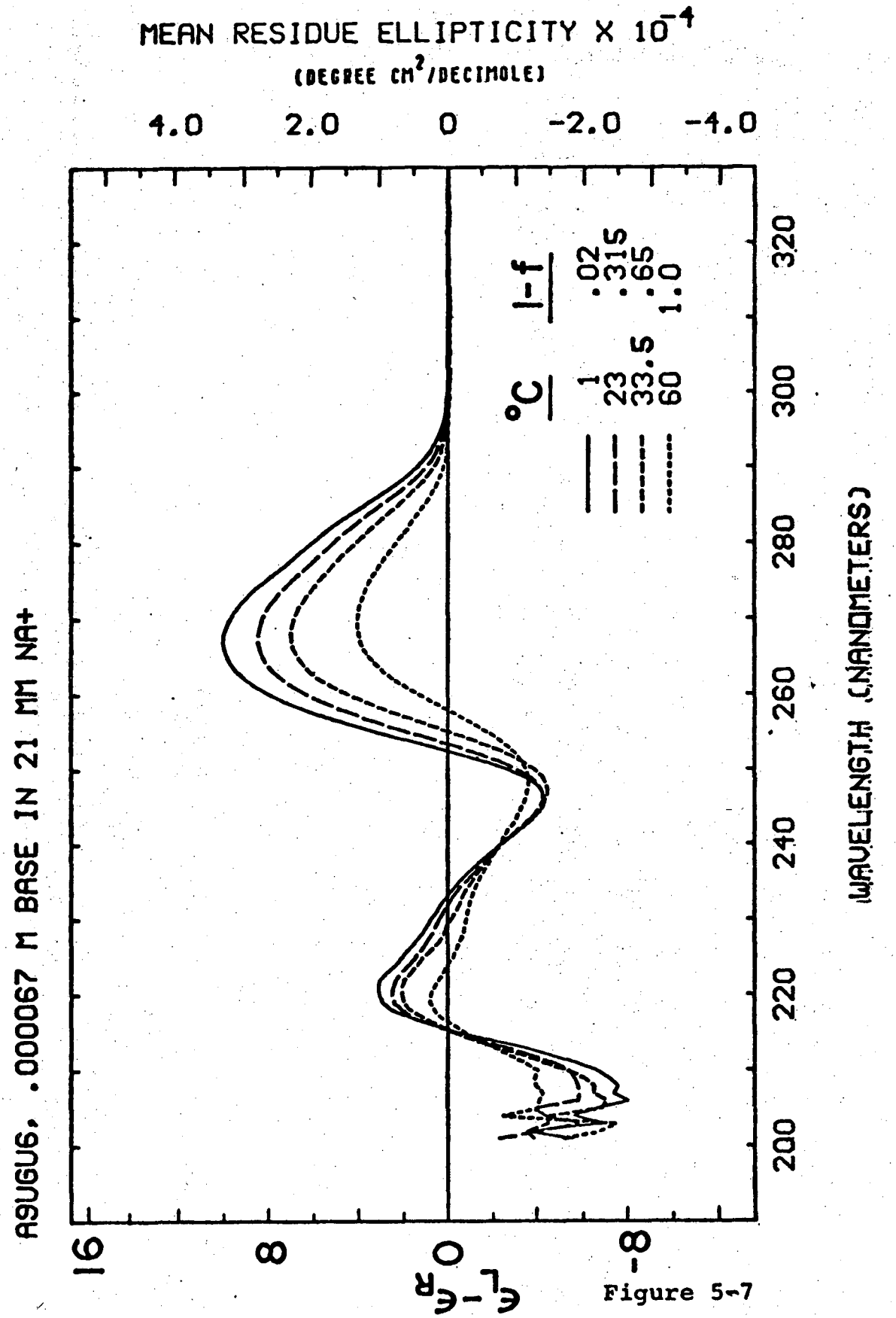
MEAN RESIDUE ELLIPTICITY X 10^{-4}
(DEGREE CM^2/DECIMOLE)
4.0
2.0
0
-2.0
-4.0
°C
1
23
33.5
60
1-f
.02
.315
.65
1.0
320
300
280
260
240
220
200
WAVELENGTH (NANOMETERS)
A9UGU6. .000067 M BASE IN 21 MM NA+
16
8
0
-8
$\epsilon_L - \epsilon_R$

Figure 5-7

Figures 5-8 and 5-9. Circular dichroism spectra of A_6U_6 in 1 M Na^+ buffer at different temperatures and single strand fractions, measured by Borer.[13]

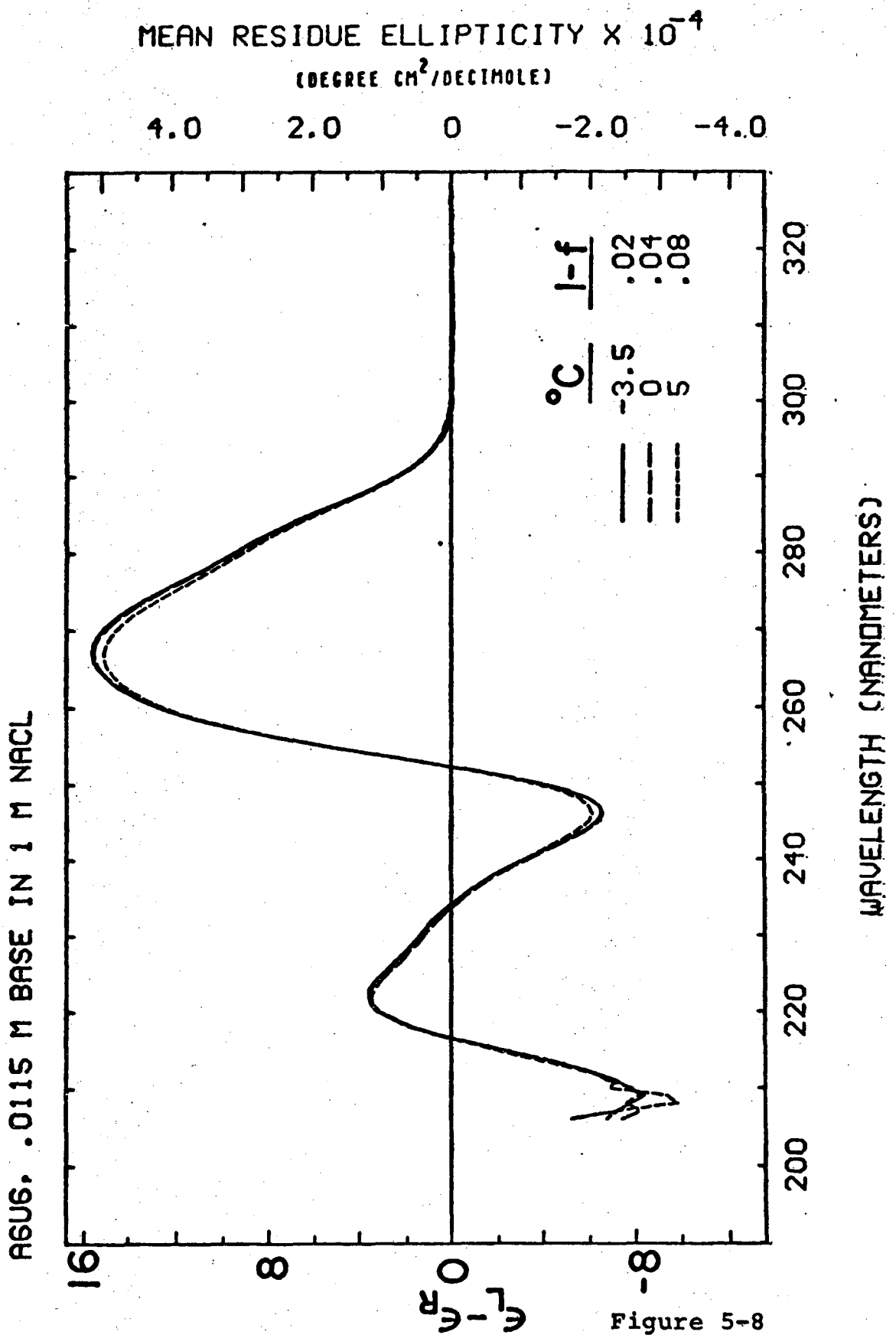
MEAN RESIDUE ELLIPTICITY X 10^{-4}
(DEGREE CM^2/DECIMOLE)
4.0
2.0
0
-2.0
-4.0
16
8
0
-8
$\epsilon_L - \epsilon_R$
200
220
240
260
280
300
320
WAVELENGTH (NANOMETERS)
°C
-3.5
0
5
f
.02
.04
.08
AGUG. .0115 M BASE IN 1 M NACL

Figure 5-8

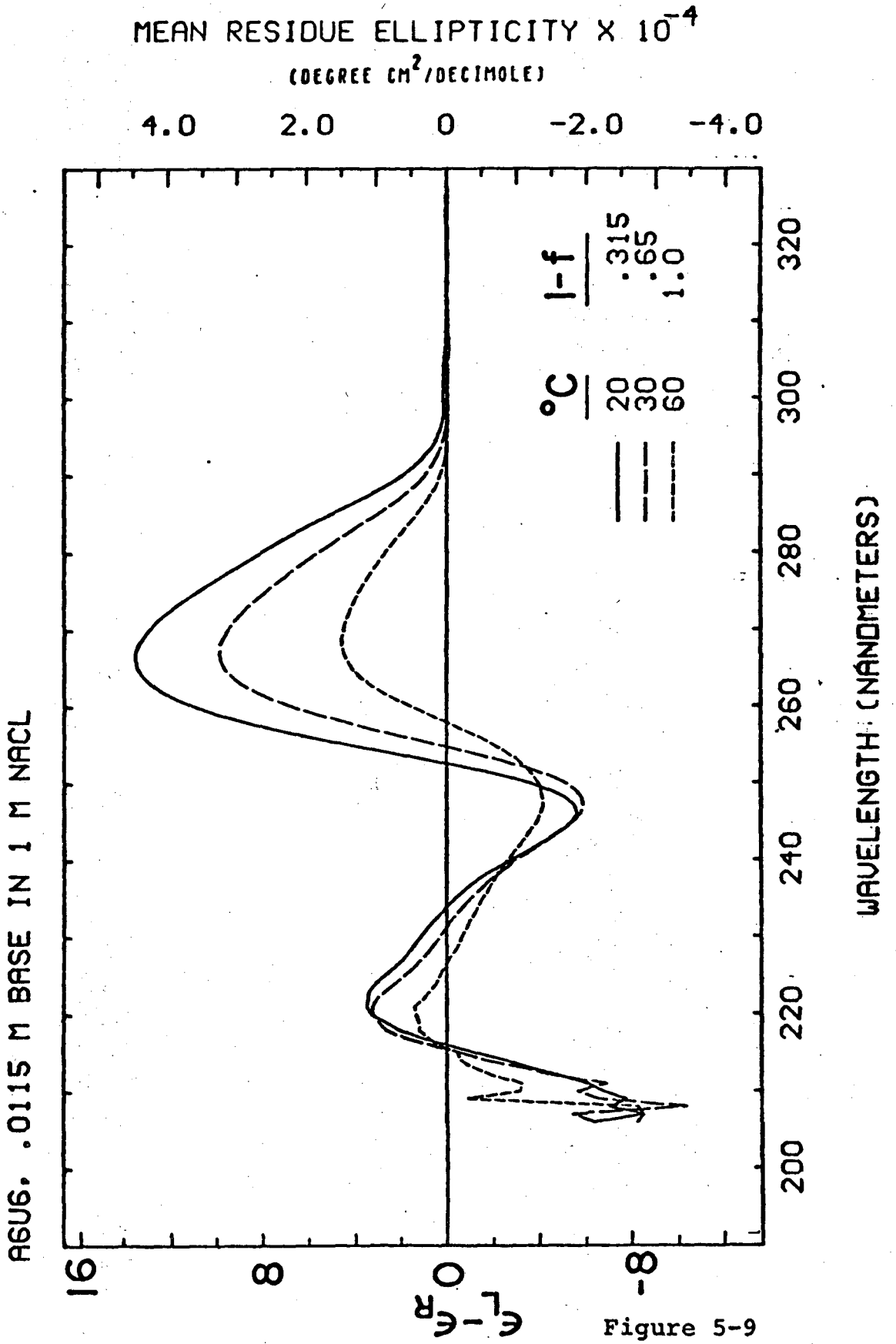
MEAN RESIDUE ELLIPTICITY X 10^{-4}
(DEGREE CM^2/DECIMOLE)
4.0
2.0
0
-2.0
-4.0
1-f
.315
.65
1.0
°C
20
30
60
320
300
280
260
240
220
200
WAVELENGTH (NANOMETERS)
AGUG. .0115 M BASE IN 1 M NACL
16
8
0
-8
$\epsilon_L - \epsilon_R$

Figure 5-9

Figure 5-10. Circular dichroism spectra of ApA, A, and U in 10 mM NaH_2PO_4, 0.1 M $NaClO_4$, pH 7.2, at 26°C, measured by Warshaw and Cantor,[14] and of ApUpGp in 10 mM Tris-HCl, 60 mM NH_4Cl, 10 mM $MgCl_2$, pH 7.4, at 25°C.

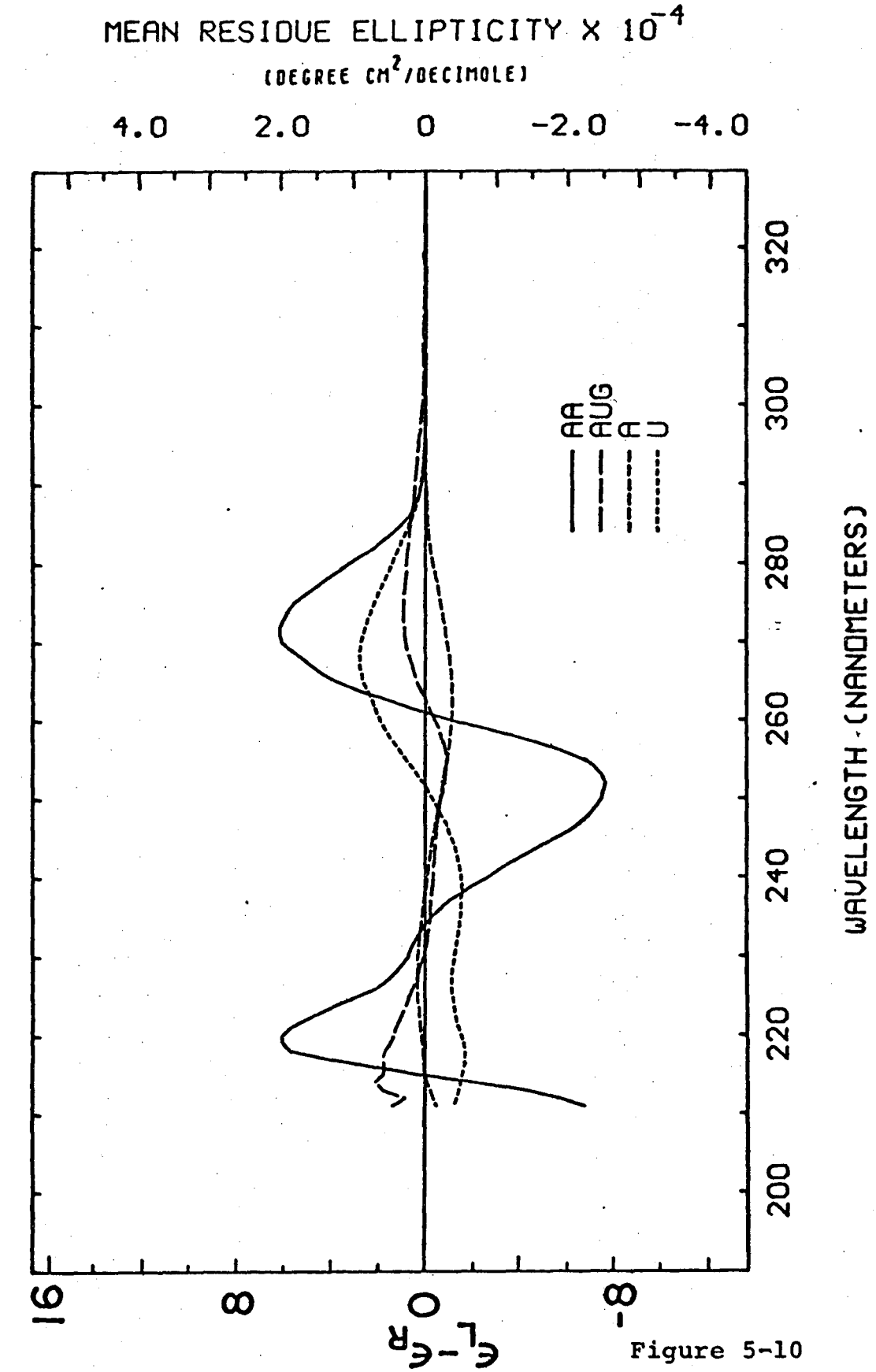
MEAN RESIDUE ELLIPTICITY X 10^{-4}
(DEGREE CM^2/DECIMOLE)
4.0
2.0
0
-2.0
-4.0
AA
AUG
A
U
320
300
280
260
240
220
200
WAVELENGTH (NANOMETERS)
16
8
0
-8
$\epsilon_L - \epsilon_R$

Figure 5-10

Figures 5-11 through 5-20. Difference circular dichroism spectra and model loop circular dichroism spectra for A_nUGU_m at the indicated values of K and L (see text).

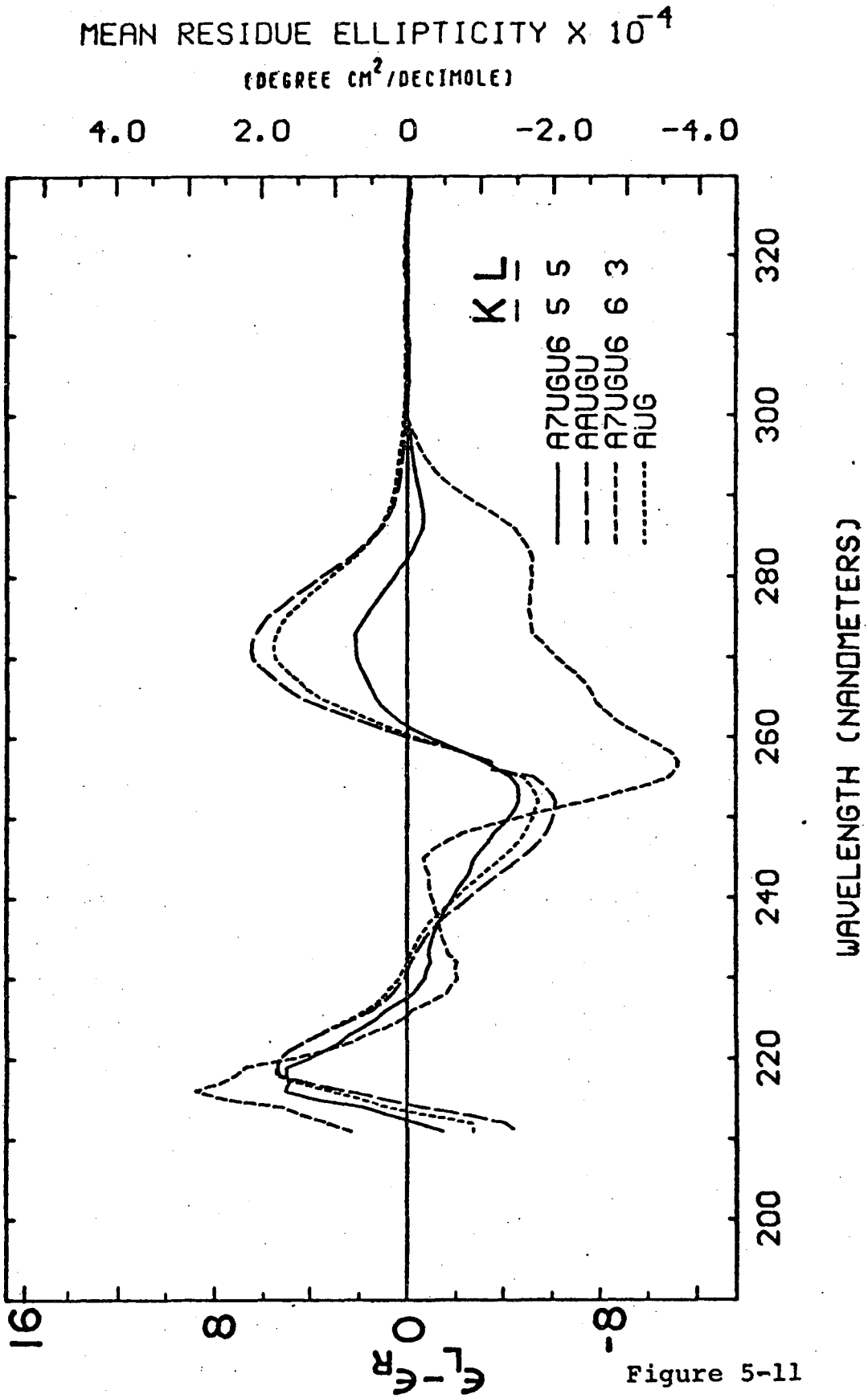
MEAN RESIDUE ELLIPTICITY X 10^{-4}
(DEGREE CM^2/DECIMOLE)
4.0
2.0
0
-2.0
-4.0
KL
55
63
A7UGU6
AAUGU
A7UGU6
AUG
320
300
280
260
240
220
200
WAVELENGTH (NANOMETERS)
16
8
0
-8
$\epsilon_L - \epsilon_R$

Figure 5-11

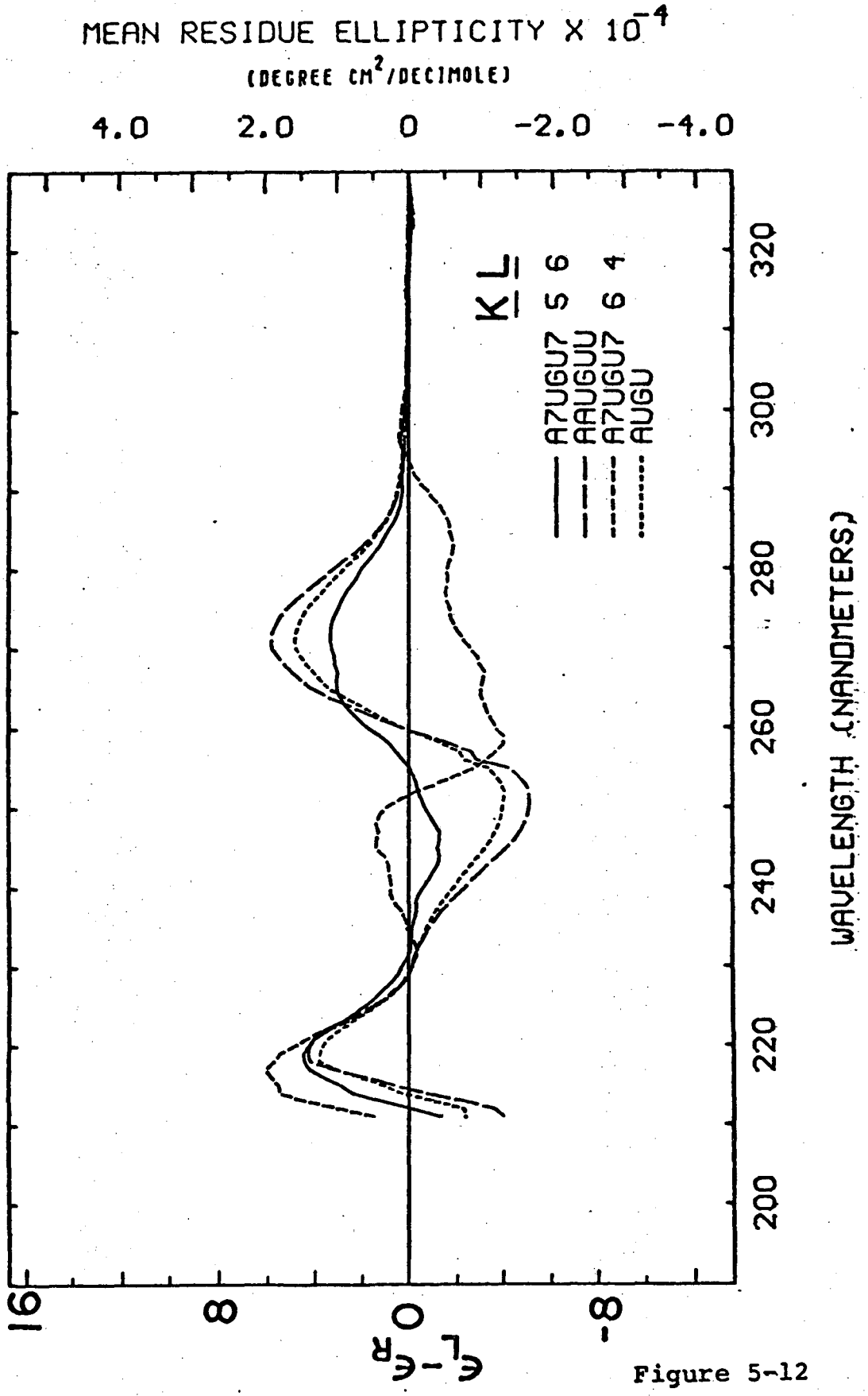
MEAN RESIDUE ELLIPTICITY X 10^{-4}
(DEGREE CM^2/DECIMOLE)
4.0
2.0
0
-2.0
-4.0
K L
5 6
6 4
A7UGU7
AAUGUU
A7UGU7
AUGU
320
300
280
260
240
220
200
WAVELENGTH (NANOMETERS)
16
8
0
-8
$\epsilon_L - \epsilon_R$

Figure 5-12

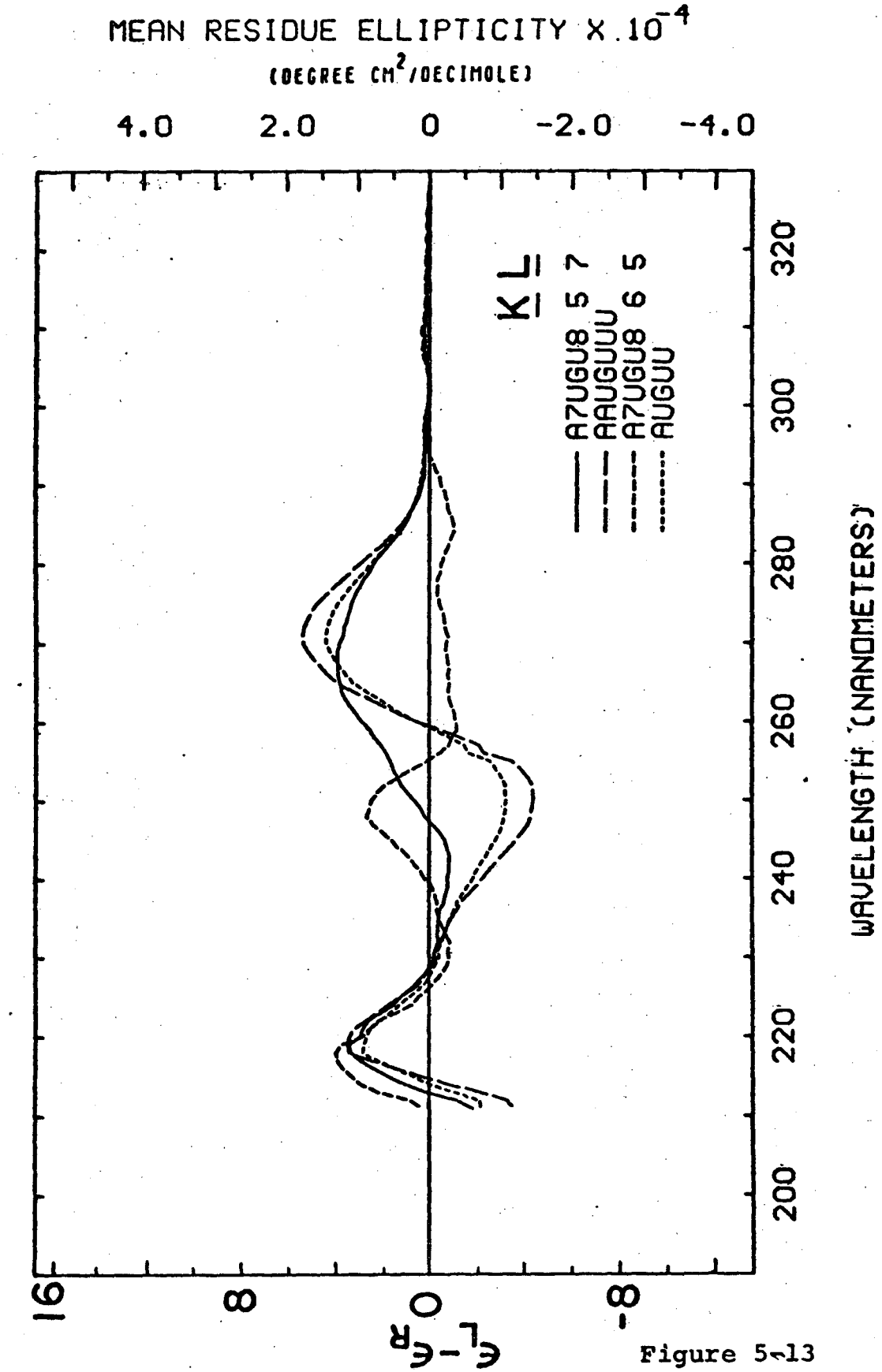
MEAN RESIDUE ELLIPTICITY X.10⁻⁴
(DEGREE CM²/DECIMOLE)
4.0
2.0
0
-2.0
-4.0
KL
A7UGU8 5 7
AAUGUUU
A7UGU8 6 5
AUGUU
320
300
280
260
240
220
200
WAVELENGTH (NANOMETERS)
16
8
0
-8
εL-εR

Figure 5-13

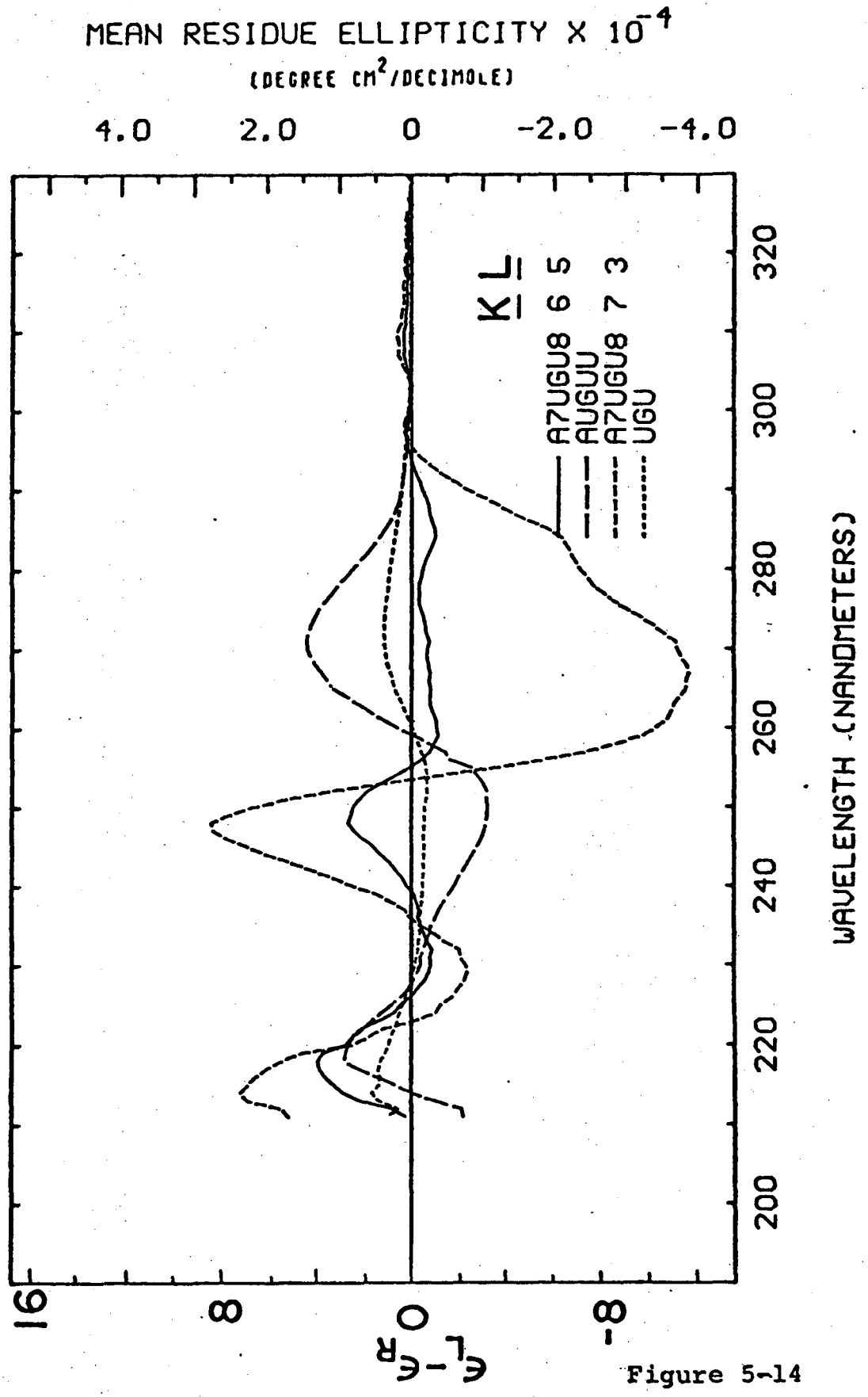
MEAN RESIDUE ELLIPTICITY X 10^{-4}
(DEGREE CM^2/DECIMOLE)
4.0
2.0
0
-2.0
-4.0
KL
6 5
7 3
A7UGU8
AUGUU
A7UGU8
UGU
320
300
280
260
240
220
200
WAVELENGTH (NANOMETERS)
16
8
0
-8
$\epsilon_L - \epsilon_R$

Figure 5-14

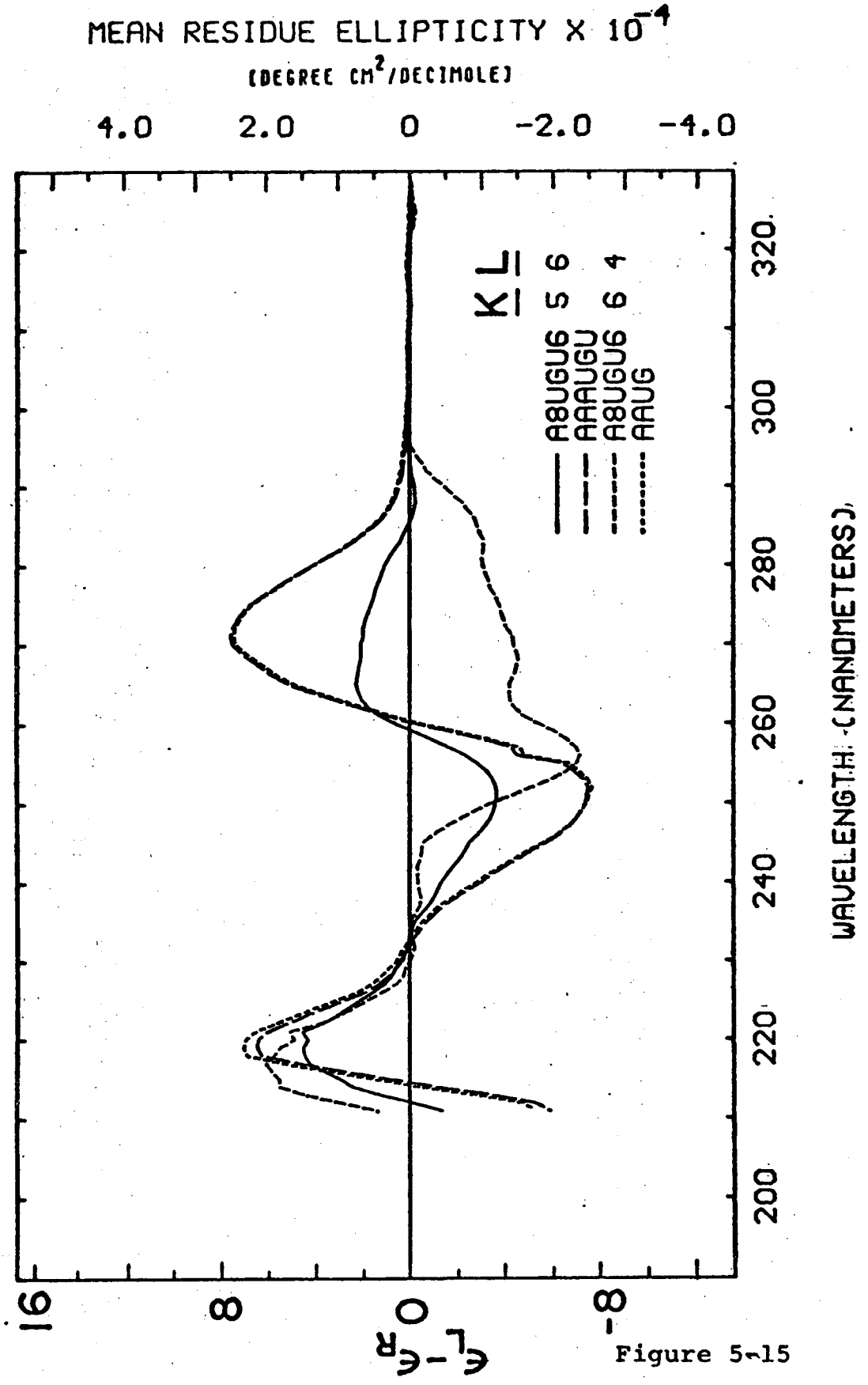
MEAN RESIDUE ELLIPTICITY X 10^{-4}
(DEGREE CM^2/DECIMOLE)
4.0
2.0
0
-2.0
-4.0
KL
5 6
6 4
A8UGU6
AAAUGU
A8UGU6
AAUG
320.
300
280
260
240
220
200
WAVELENGTH (NANOMETERS)
16
8
0
-8
$\epsilon_L - \epsilon_R$

Figure 5-15

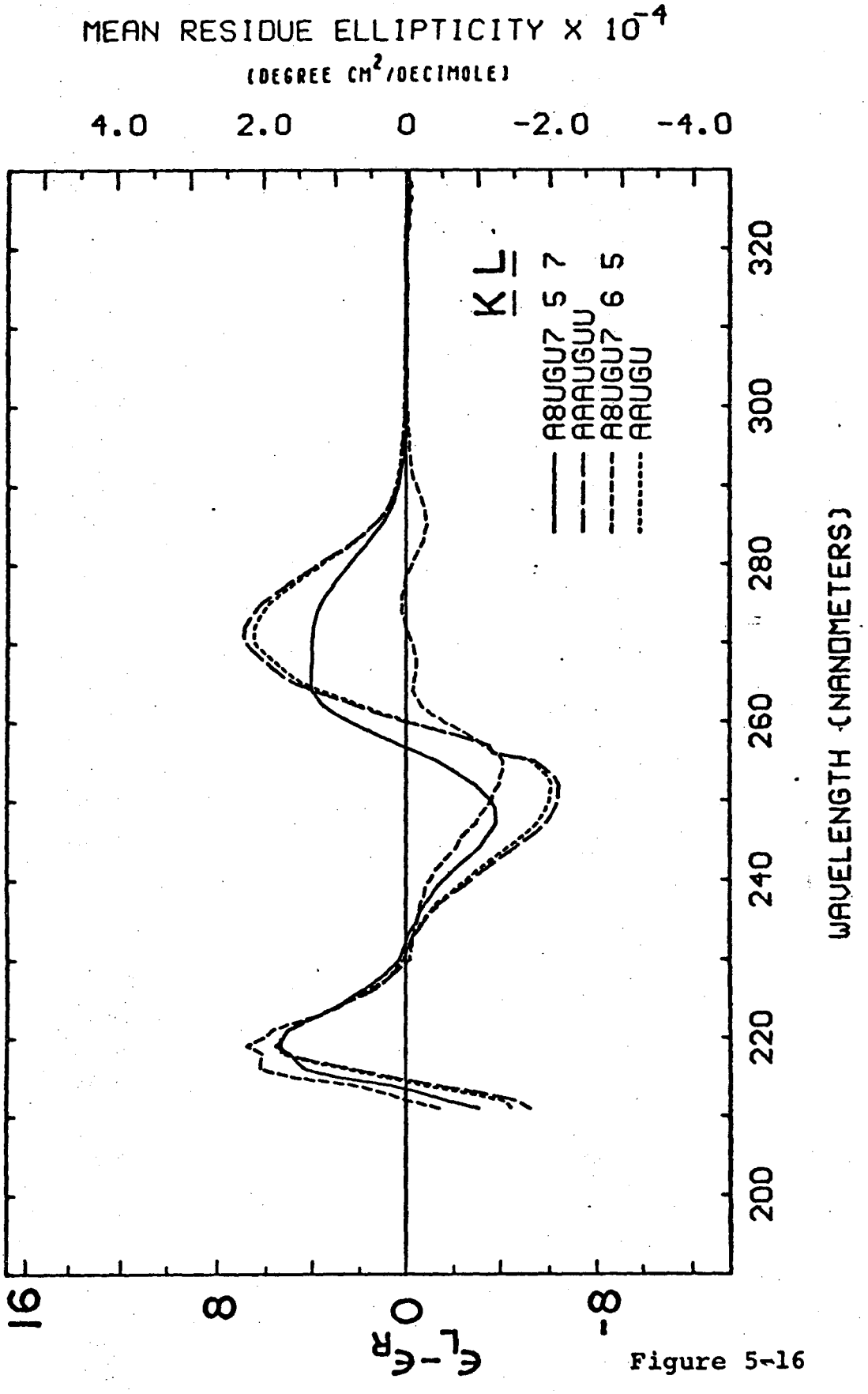
MEAN RESIDUE ELLIPTICITY X 10^{-4}
(DEGREE CM^2/DECIMOLE)
4.0
2.0
0
-2.0
-4.0
KL
A8UGU7 5 7
AAAUGUU
A8UGU7 6 5
AAUGU
320
300
280
260
240
220
200
WAVELENGTH (NANOMETERS)
16
8
0
-8
$\epsilon_L - \epsilon_R$

Figure 5-16

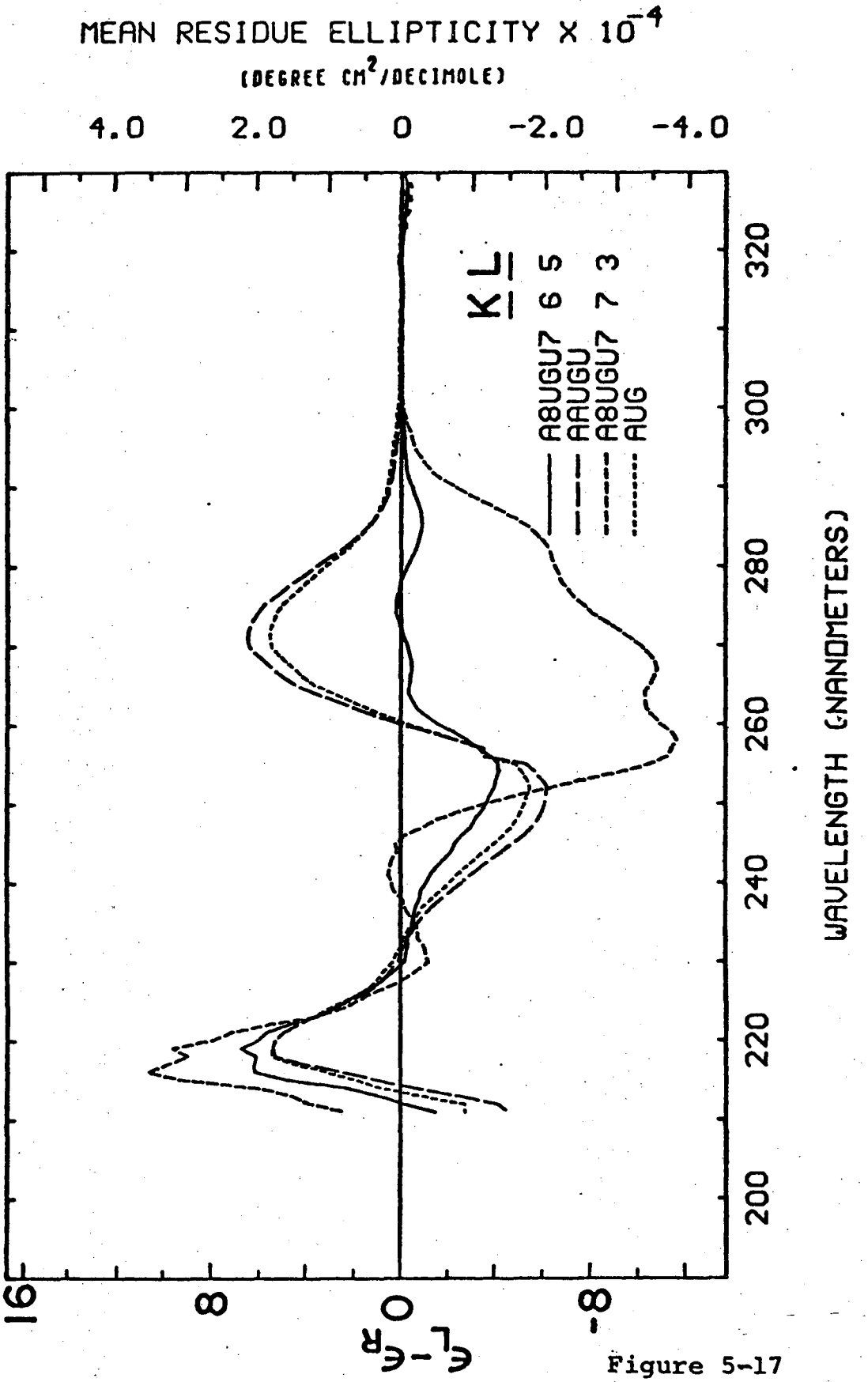
MEAN RESIDUE ELLIPTICITY X 10^{-4}
(DEGREE CM^2/DECIMOLE)
4.0
2.0
0
-2.0
-4.0
KL
6 5
7 3
A8UGU7
AAUGU
A8UGU7
AUG
320
300
280
260
240
220
200
WAVELENGTH (NANOMETERS)
16
8
0
-8
$\epsilon_L - \epsilon_R$

Figure 5-17

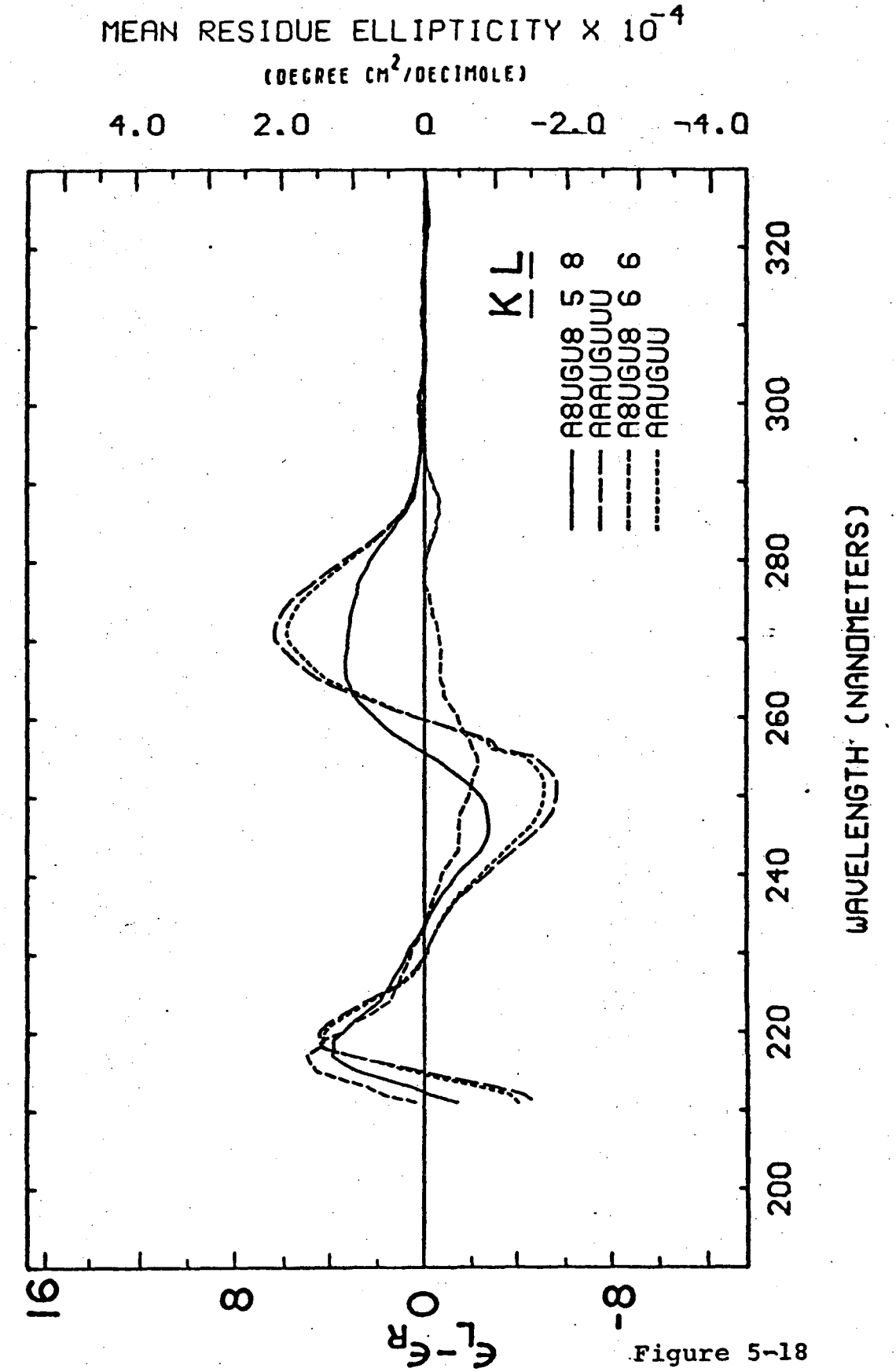
MEAN RESIDUE ELLIPTICITY X 10^{-4}
(DEGREE CM^2/DECIMOLE)
4.0
2.0
0
-2.0
-4.0
K L
A8UGU8 5 8
AAAUGUUU
A8UGU8 6 6
AAUGUU
320
300
280
260
240
220
200
WAVELENGTH (NANOMETERS)
16
8
0
-8
$\epsilon_L - \epsilon_R$

Figure 5-18

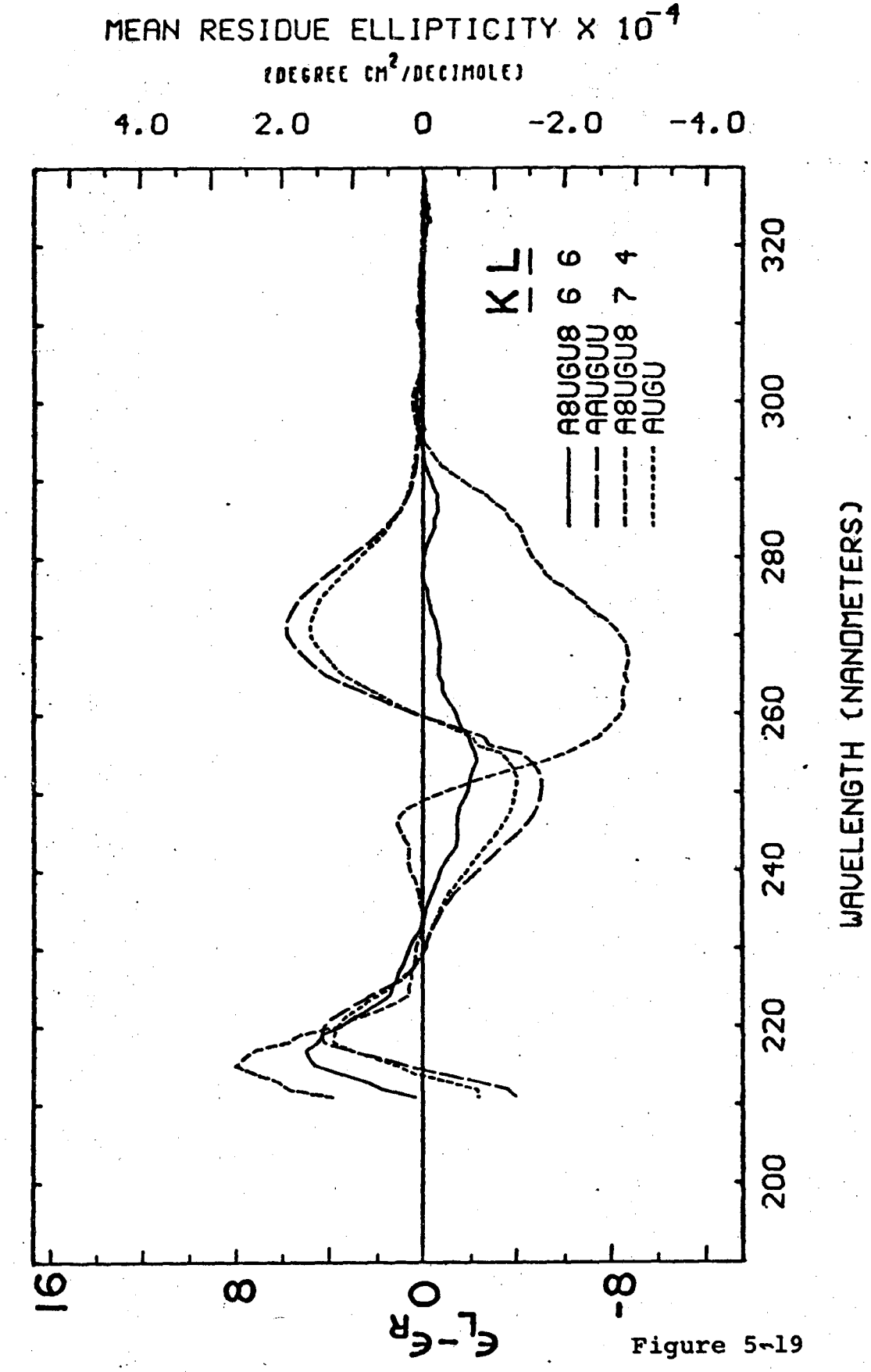
MEAN RESIDUE ELLIPTICITY X 10^{-4}
(DEGREE CM^2/DECIMOLE)
4.0
2.0
0
-2.0
-4.0
KL
6 6
7 4
A8UGU8
AAUGUU
A8UGU8
AUGU
320
300
280
260
240
220
200
WAVELENGTH (NANOMETERS)
16
8
0
-8
$\epsilon_L - \epsilon_R$

Figure 5-19

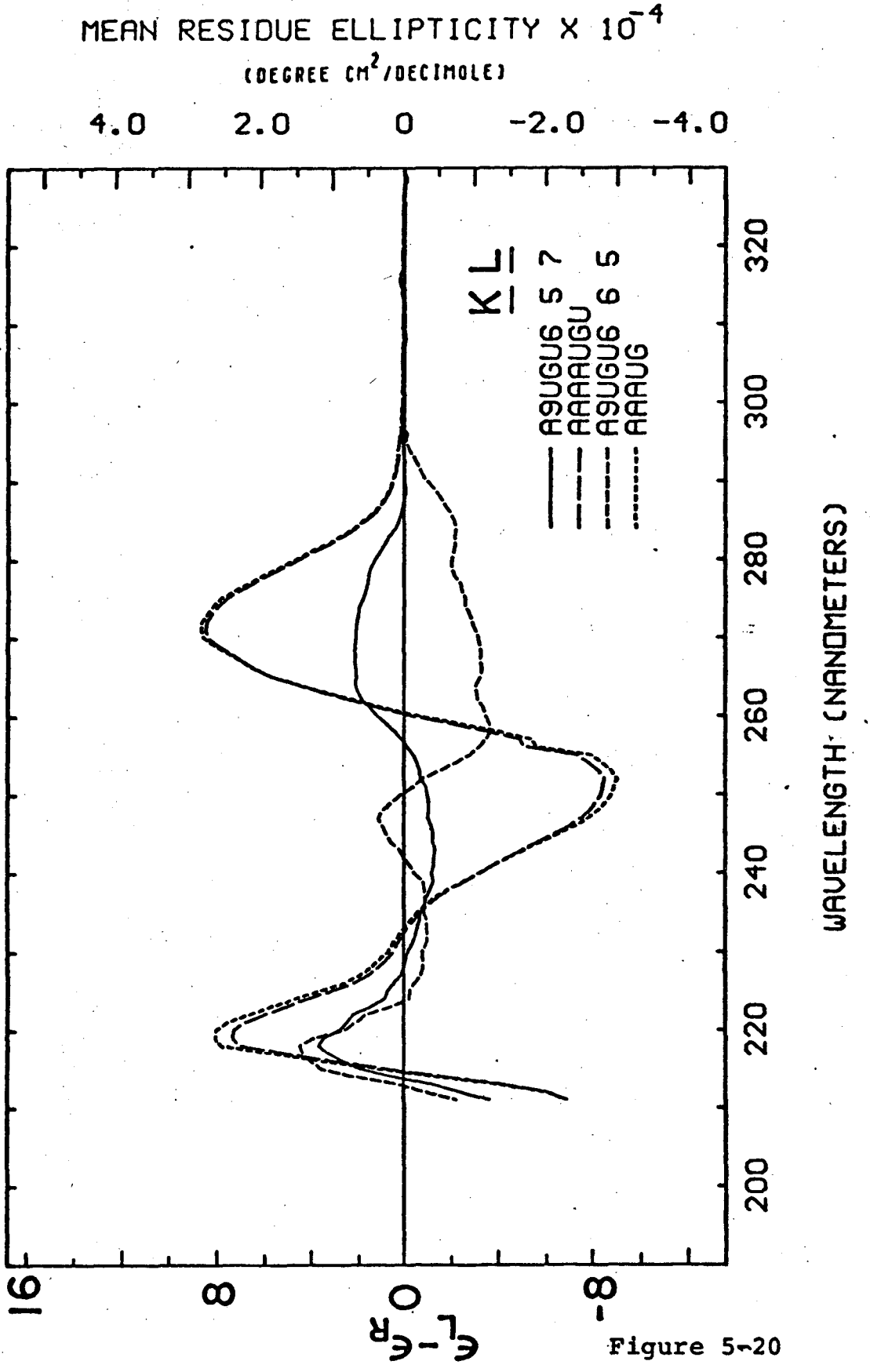
MEAN RESIDUE ELLIPTICITY X 10^{-4}
(DEGREE CM^2/DECIMOLE)
4.0
2.0
0
-2.0
-4.0
K L
5 7
6 5
A9UGU6
AAAAUGU
A9UGU6
AAAUG
320
300
280
260
240
220
200
WAVELENGTH (NANOMETERS)
16
8
0
-8
$\epsilon_L - \epsilon_R$

Figure 5-20

CHAPTER 6

INITIATION FACTOR f_3 BINDING TO AUG AND AUG-CONTAINING SINGLE STRANDS, HAIRPIN LOOPS, AND POLYMERS

SUMMARY

A nitrocellulose filter assay has been used to detect the binding of f_3 to AUG, A_nUGU_m single strands and hairpin loops, poly (A,U,G), and f2 RNA. No binding could be found for A_8U or $A_5GC_5U_5$. AUG-containing oligonucleotides showed a weak binding with a K of 10^3 - 10^4 M^{-1}, whereas AUG-containing polymers showed strong binding with a K of 10^5 and greater.

INTRODUCTION

Initiation factor f_3 from E. coli appears to be essential for the translation of natural messenger RNA's in vitro.[1-4] Evidence exists for two f_3 functions: recognition of specific mRNA's, and dissociation of single ribosomes.[5-13] Studies in eukaryotes have found a factor analogous to f_3 which shows a specific mRNA recognition function.[14,15] While there are several reports that T4 infection of E. coli changes mRNA specificity of the initiation factors,[5-7] contrary results have been reported[16] which indicate no change in initiation factor specificity upon T4 infection.

Steitz's sequencing of the initiation regions of R17 RNA,[17] as well as other viral RNA sequencing efforts,[18-20] suggested the possibility that initiation AUG codons existed in hairpin loops, each of which could be bound by a specific f_3. In this model, methionine AUG codons could exist either in single- or double-stranded regions without causing initiation errors. The differing ratios of gene products from R17 RNA translated in vitro by E. coli ribosomes, 20 coat: 6 synthetase: 1 maturation protein,[21] in contrast with the gene order, maturation - coat - synthetase,[22] imply different rates of initiation and/or elongation for each cistron. Furthermore, the finding of Fukami and Imahori[23] that preincubation of R17 RNA in the presence of 10 mM Mg^{+2} at 0°, 50°, 60°, and 70°C prior to in

vitro protein synthesis gave different amounts and ratios of gene products in each case, compared with the normal assay, definitely implies conformational control over translation. All of these results suggested an initiation experiment measuring the affinity of f_3 alone for various RNA's, with and without AUG.

Utilizing a nitrocellulose filter assay,[9] f_3 has been found to bind about equally well to AUG, A_7UGU_2, A_7UGU_3, A_7UGU_8, A_7UGU_9, A_8UGU_6, A_8UGU_7, A_8UGU_8, and A_8UGU_{10}, but not at all to A_8U or $A_5GC_5U_5$. All the A_nUGU_m where n=7,8 and $m \geq 6$ are considered to be hairpin loops in the conditions of the assay,[24] as well as $A_5GC_5U_5$,[25] by the criteria of constant A_{260} *vs.* T profiles at three concentrations over two orders of magnitude, and approximately monomeric molecular weights from equilibrium sedimentation. Initiation factor f_1 failed to bind AUG, and inhibited AUG binding by f_3.

MATERIALS AND METHODS

Initiation factors f_1 and f_3 were the generous gift of Professor John Hershey. f_3 was 99% pure and nuclease-free. f2 viral RNA was the kind gift of Mr. Michael Stallcup. All other RNA's were prepared with polynucleotide phosphorylase and primer dependent polynucleotide phosphorylase by standard methods.[26-28] Sequences were determined by ribonuclease T1 and ribonuclease A digestion and paper chromatography. Physical characterization of hairpin loops was done by absorbance

vs. temperature curves on a Gilford 2000 absorbance recorder,[28] and equilibrium sedimentation in a Spinco Model E analytical ultracentrifuge equipped with ultraviolet scanner. Full details of the synthesis and physical characterization of the hairpin loops will be published elsewhere.[24] All of the hairpin loops used here displayed T_m's between 20° and 30°C in 10 mM NaH_2PO_4 pH 7.00, 5 mM NaCl, 0.1 mM EDTA ($[Na^+]$ = 21 mM), and continue to form hairpin loops in the same solvent with 85 mM NaCl ($[Na^+]$ = 101 mM), with T_m's about 3° higher.

Each nitrocellulose filter assay[9] consisted of incubating for 20 min at 0°C a sample reaction mixture and a background reaction mixture of 100λ each containing 10 mM NaH_2PO_4 pH 7.00, 1 mM DTT, 0.1 mM EDTA, 40 mM NaCl, 1 mg/ml BSA, radioactively labeled and unlabeled RNA at the indicated concentrations, and, in the sample mixtures, initiation factors at the indicated concentrations. Each mixture was then diluted with 1 ml of 0.2 M Tris-H_3PO_4 pH 7.25, 5% glycerol (PTG) and immediately filtered through a PTG-soaked HAWP 25 Millipore filter at 1 ml/15 sec, followed by a 1 ml PTG rinse of the reaction tube and filter. The filters were dried and counted in 10 ml of toluene containing 4g/l PPO and 50 mg/l POPOP with a Beckman LS-250 liquid scintillation spectrometer. To obtain the total cpm in a reaction mixture at the same counting efficiency as the assay, a 10λ aliquot of labeled RNA

was placed on a filter treated as in the assay.

Each filter received only one rinse because low f_3-RNA equilibrium constants were expected, and several rinses could wash away any cpm bound to initiation factor, compared with nonspecific binding to BSA or nitrocellulose. Even one dilution and one rinse may be expected to reduce the bound cpm from equilibrium conditions, and hence the calculated equilibrium constants must be considered lower bounds.

Concentrations of initiation factors were calculated from $E_{280}^{1\%} = 10$ and molecular weights of 21,000 for f_3 and 9700 for f_1. Concentrations of RNA were calculated from extinction coefficients at 60°C, except for [AUG], which was calculated from the specific activity of [^{3}H]-GDP.

RESULTS

Table 6-1 shows the results of the assays. The first column lists the RNA and isotope measured, the second the cpm retained on the sample filter, the third the cpm retained on the background filter, and the fourth the difference between sample and background, which is presumed to represent cpm bound to factor f_3. The next column gives the cpm available in each 100λ reaction mixture, followed by a column with the initial RNA concentration in each reaction mixture. The f_3·RNA complex concentration in the seventh column derives from the initial RNA concentration and the ratio of

cpm bound to factor and cpm in reaction mixture. Since [f_3·RNA] << [RNA], except for experiments with poly (A,U,G), final [RNA] differs negligibly from initial [RNA]; in the case of poly (A,U,G), final [RNA] = initial [RNA] - [f_3·RNA]. [f_3], the final f_3 concentration in the eighth column, is the difference between the initial f_3 concentration of 24×10^{-7} M and [f_3·RNA]. K is the association constant for the reaction, f_3 + RNA $\rightleftharpoons$ f_3·RNA.

From these data the binding of poly (A,U,G) to f_3 appears quite strong, as does the binding of f2 RNA, judging from its effect on the binding of poly (A,U,G). If one assumes a competitive inhibition model for the effect of f2 RNA, its association constant with f_3 may be calculated. Using an average K of 4.8×10^5 M^{-1} for uninhibited poly (A,U,G) binding, and the measured binding in the presence of f2 RNA, one derives a final [f_3] of 8.5×10^{-7} M, which implies [f_3·f2 RNA] = 9.7×10^{-7} M. This result is six times as great as the initial [f2 RNA], and may reflect inaccuracies in the calculations leading to it, for example in the initial [f_3] or [poly (A,U,G)]. On the other hand, Sabol et al.[9] found 100% binding of [^{3}H] MS2 RNA using the same assay with an [RNA] of about 2×10^{-8} M and 5 to 25 times less f_3. Since there are three naturally occurring initiation sites, an f_3 complex to RNA ratio of 3 would not be surprising; the calculated ratio of 6 is either erroneous or shows the existence of more than three f_3

binding sites on f2 RNA in low ionic strength and the absence of Mg^{+2}.

The association constants for AUG-containing hairpin loops and single strands, and AUG trimer vary considerably, but are all of the same order of magnitude. Since these constants are lower limits, derived from the differences of large numbers, the principal conclusion to be made from them is that AUG in a single-stranded region binds to f_3, while A_8U and $A_5GC_5U_5$ do not. These two controls rule out the binding of AAA, AAG, AGC, GCC, CCC, CCU, and UUU.

AUG does not bind to f_1, and it is significant that f_1 inhibits the binding of AUG to f_3. The most likely explanation of this result lies in an $f_1 \cdot f_3$ complex involving most of the f_3.

DISCUSSION

Two contrasting results appear from this work: a weak binding of AUG to f_3, and a strong binding of AUG-containing polymer to f_3. The factor clearly shows no preference for AUG in a hairpin loop, and no inclination to bind a hairpin loop without AUG. Thus, one is led on the one hand to reject specific f_3 binding to hairpin loops, and on the other to hypothesize a secondary structural basis for the strong f_3 binding to polymer.

The first possibility is that any long single-stranded RNA with an AUG, e.g., $A_{50}UGA_{50}$, can bind

strongly due to non-specific RNA binding to f_3 on either side of the AUG site. The second is that f_3 binds strongly to two (or three) hairpin loops at once: the loop containing AUG, and the one(s) immediately adjacent. The first possibility requires that initiator AUG's be located in single-stranded regions, or that f_3 be capable of melting base-paired regions. The second requires abundant hairpin loops in natural mRNA's and a more complex specificity for f_3.

The first possibility, virtually a straw man, is unlikely from the known sequences of mRNA regions, the stability of hairpin loops,[29] and the findings that most natural RNA's are at least two-thirds base-paired.[30-32] These same reasons, on the other hand, support the second possibility. Indeed, initiator AUG hairpin loops with immediately adjacent loops on the 5' side which would be stable even in the assay conditions used here may be deduced from the sequence of the R17 coat protein initiator region of Steitz,[17] or that of R17 from the 5' end to the maturation protein as determined by Adams et al.[33] (Figure 6-1).

These results create the need for a host of further studies. What affinity will f_3 show for GUG, UAG, UAA, or CAU? Does f_1 merely inhibit RNA binding by f_3, or does it impose greater specificity on the f_3? Can a single-stranded RNA be synthesized which will bind to f_3 as well as poly (A,U,G), or alternatively, can a double hairpin be devised which will do the same trick?

Studies such as these will be limited primarily by the supply of pure f_1 and f_3, and by the talents of the RNA synthesizers.

This work was performed in the laboratory of Professor I. Tinoco, Jr., to whom I am greatly indebted, and was supported by the National Institutes of Health Grant No. GM 10840. The author would also like to acknowledge the excellent technical assistance of Ernest Foxman.

REFERENCES

1. Stanley, W., Salas, M., Wahba, A. J., and Ochoa, S., Proc. Natl. Acad. Sci. U.S. 56 (1966) 290.
2. Revel, M., Lelong, J. C., Brawerman, G., and Gros, F., Nature 219 (1968) 1016.
3. Iwasaki, K., Sabol, S., Wahba, A. J., and Ochoa, S., Arch. Biochem. Biophys. 125 (1968) 542.
4. Revel, M., Greenshpan, M., and Herzberg, M., Cold Spring Harbor Symp. Quant. Biol. 34 (1969) 261.
5. Dube, S. K. and Rudland, P. S., Nature 226 (1970) 820.
6. Steitz, J. A., Dube, S. K., and Rudland, P. S., Nature 226 (1970) 824.
7. Ihler, G. and Nakada, D., J. Mol. Biol. 62 (1971) 419.
8. Revel, M., Aviv (Greenshpan), H., Groner, Y., and Pollack, Y., FEBS Letters 9 (1970) 213.
9. Sabol, S., Sillero, M. A. G., Iwasaki, K., and Ochoa, S., Nature 228 (1970) 1269.
10. Dubnoff, J. S. and Maitra, U., Proc. Natl. Acad. Sci. U.S. 68 (1971) 318.
11. Kaempfer, R., Proc. Natl. Acad. Sci. U.S. 68 (1971) 2458.
12. Grunberg-Manago, M., Rabinowitz, J. C., Dondon, J., Lelong, J. C., and Gros, F., FEBS Letters 19 (1971) 193.

13. Vermeer, C., Talens, J., Bloemsma-Jonkman, F., and Bosch, L., FEBS Letters 19 (1971) 201.

14. Heywood, S. M., Proc. Natl. Acad. Sci. U.S. 67 (1970) 1782.

15. Crystal, R. G., Shafritz, D. A., Prichard, P. M., and Anderson, W. F., Proc. Natl. Acad. Sci. U.S. 68 (1971) 1810.

16. Goldman, E. and Lodish, H. F., J. Mol. Biol. 67 (1972) 35.

17. Steitz, J. A., Nature 224 (1969) 957.

18. Nichols, J. L., Nature 225 (1970) 147.

19. DeWachter, R., Vandenberghe, A., Merregaert, J., Contreras, R., and Fiers, W., Proc. Natl. Acad. Sci. U.S. 68 (1971) 585.

20. Min Jou, W., Haegeman, G., Ysebaert, M., and Fiers, W., Nature 237 (1972) 82.

21. Lodish, H. F., Nature 220 (1968) 345.

22. Jeppesen, P.G.N., Steitz, J. A., Gesteland, R. F., and Spahr, P. F., Nature 226 (1970) 230.

23. Fukami, H. and Imahori, K., Proc. Natl. Acad. Sci. U.S. 68 (1971) 570.

24. Wickstrom, E. and Tinoco, I., Jr., manuscript in preparation.

25. Cech, C., unpublished observation.

26. Thach, R. E., in Procedures in Nucleic Acid Research, ed. by G. L. Cantoni and D. R. Davies, Harper & Row, New York, 1966, 520.

27. Thach, R. E., Sundararajan, T. A., Dewey, K. F., Brown, J. C., and Doty, P., Cold Spring Harbor Symp. Quant. Biol. 31 (1966) 85.

28. Martin, F. H., Uhlenbeck, O. C., and Doty, P., J. Mol. Biol. 57 (1971) 201.

29. Uhlenbeck, O. C., Borer, P. N., Dengler, B., and Tinoco, I., Jr., J. Mol. Biol.,in press.

30. Englander, S. W., and Englander, J. J., Proc. Natl. Acad. Sci. U.S. 53 (1965) 370.

31. McMullen, D. W., Jaskunas, S. R., and Tinoco, I., Jr., Biopolymers 5 (1967) 589.

32. Cantor, C., Proc. Natl. Acad. Sci. U.S. 59 (1968) 478.

33. Adams, J. M., Spahr, P.-F., and Cory, S., Biochemistry 11 (1972) 976.

Table 6-1

RNA	Sample cpm	Background cpm	cpm Bound to Factor	cpm in Rxn. Mix.	[RNA], M	$[f_3 \cdot RNA]$, M	$[f_3]$, M	K, M^{-1}
[^{3}H]poly(A,U,G)	7874.3	487.0	7387.3	16,730	2×10^{-6}	8.8×10^{-7}	15.2×10^{-7}	5.2×10^{5}
[^{3}H]poly(A,U,G)	7324.1	364.7	6959.4	16,730	2×10^{-6}	8.3×10^{-7}	15.7×10^{-7}	4.4×10^{5}
[^{3}H]poly(A,U,G) + f2 RNA	5257.0	401.6	4855.4	16,730	2×10^{-6} 1.6×10^{-7}	5.8×10^{-7}	18.2×10^{-7}	2.3×10^{5}
[^{14}C]A_8UGU_6	1289.7	469.4	820.3	106,050	3.6×10^{-5}	2.8×10^{-7}	21.2×10^{-7}	3.7×10^{3}
[^{14}C]A_8UGU_6 + A_8U	1115.3	326.4	788.9	106,050	3.6×10^{-5} 17×10^{-5}	2.7×10^{-7}	21.3×10^{-7}	3.5×10^{3}
[^{14}C]A_8UGU_7	908.0	608.9	299.1	124,250	8.6×10^{-5}	2.1×10^{-7}	21.9×10^{-7}	1.1×10^{3}
[^{14}C]A_8UGU_8	807.9	385.8	422.1	60,700	4.5×10^{-5}	3.1×10^{-7}	20.9×10^{-7}	3.3×10^{3}
[^{14}C]A_8UGU_{10}	873.2	491.3	381.9	87,860	6.3×10^{-5}	2.7×10^{-7}	21.3×10^{-7}	2.0×10^{3}
[^{14}C]A_7UGU_2	141.3	97.2	44.1	9,136	3.2×10^{-5}	1.5×10^{-7}	22.5×10^{-7}	2.1×10^{3}
[^{14}C]A_7UGU_3	231.0	107.0	124.0	18,120	2.8×10^{-5}	1.9×10^{-7}	22.1×10^{-7}	3.1×10^{3}
[^{14}C]A_7UGU_8	1279.6	241.9	1037.7	102,770	7.0×10^{-5}	7.1×10^{-7}	16.9×10^{-7}	6.0×10^{3}
[^{14}C]A_7UGU_9	1363.8	832.1	531.7	155,430	9.6×10^{-5}	3.3×10^{-7}	20.7×10^{-7}	1.7×10^{3}
[^{3}H]$A_5GC_5U_5$	286.1	289.0	-2.9	51,750	5.7×10^{-5}	0	24×10^{-7}	0
[^{3}H]$A_5GC_5U_5$	216.0	242.5	-26.5	41,850	4.6×10^{-5}	0	24×10^{-7}	0
[^{3}H]AUG	741.6	634.6	107.0	66,020	2.1×10^{-7}	3.4×10^{-9}	24×10^{-7}	6.7×10^{3}
[^{3}H]AUG + 27×10^{-7} M f_1	604.1	634.6	-30.5	66,020	2.1×10^{-7}	0	0	0
[^{3}H]AUG + 27×10^{-7} M f_1	596.8	634.6	-37.8	66,020	2.1×10^{-7}	0	24×10^{-7}	0

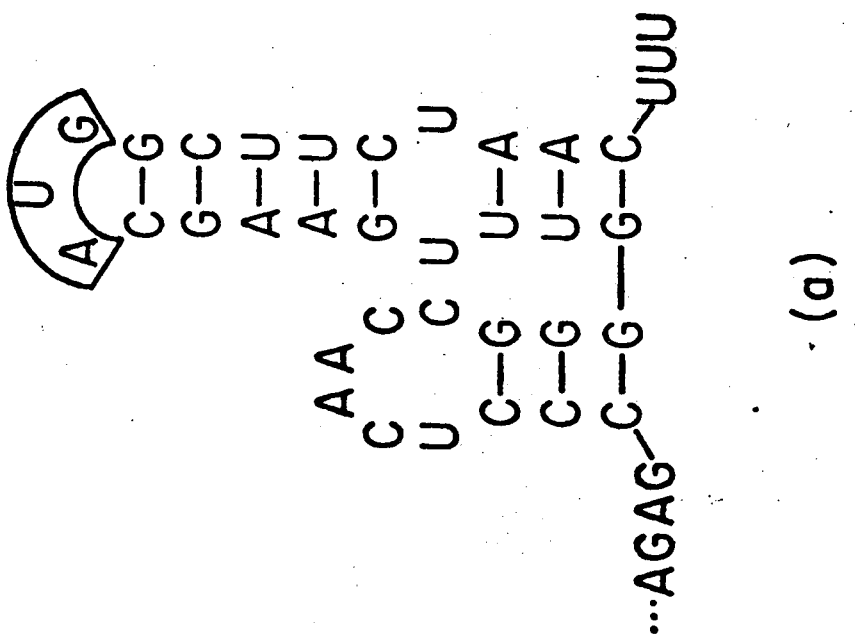

Figure 6-1. (a) Possible secondary structure for the nucleotide sequence of the coat protein initiation region of R17 RNA from Steitz.[17]

(b) Possible secondary structure for the nucleotide sequence of R17 RNA from the 5' end up to the maturation protein initiation region from Adams, et al.[33]

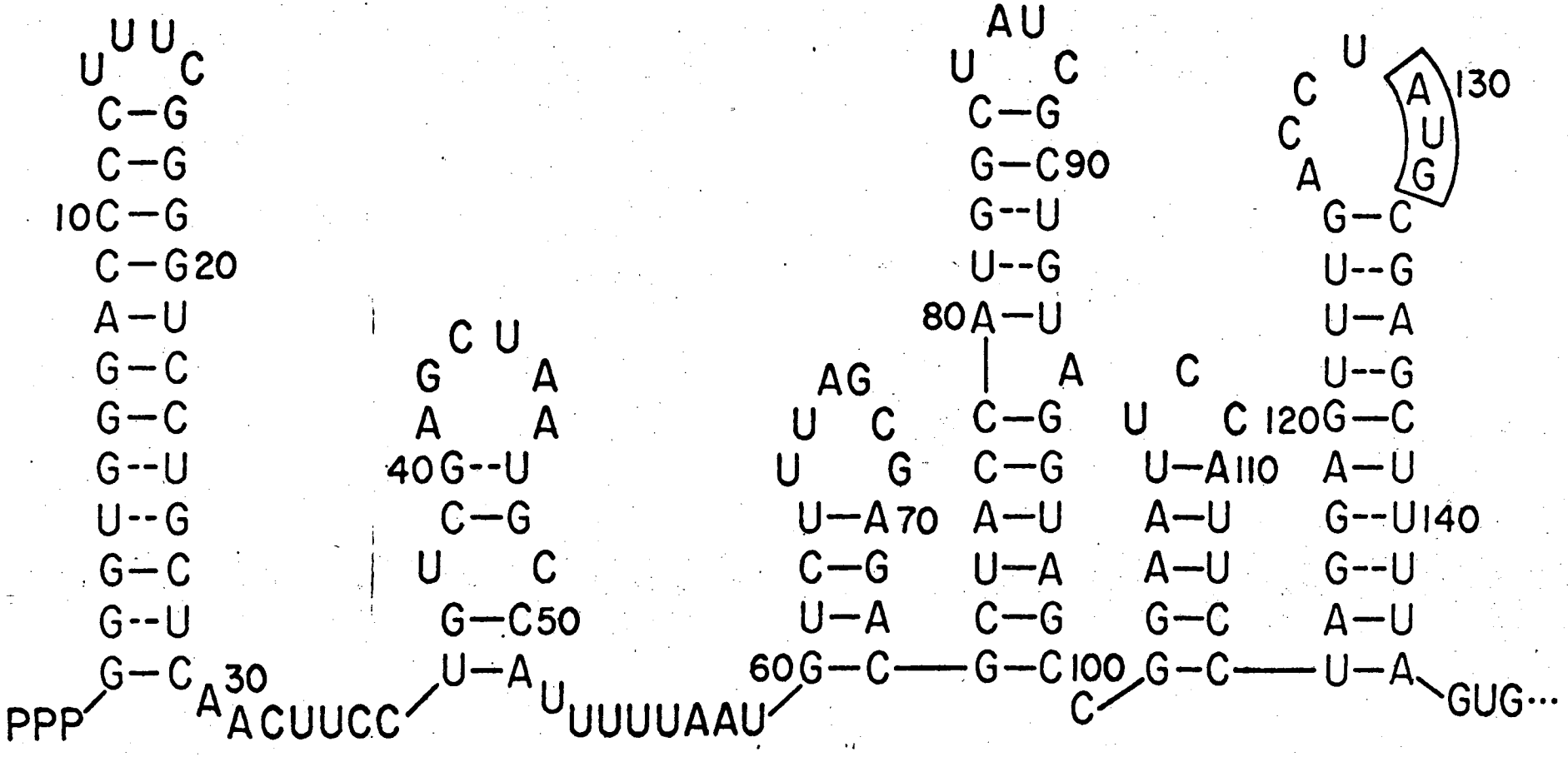
PPP
ACUUCC
UUUUAAU
GUG...
10
20
30
40
50
60
70
80
90
100
110
120
130
140

(b)

TECHNICAL INFORMATION DIVISION
LAWRENCE BERKELEY LABORATORY
UNIVERSITY OF CALIFORNIA
BERKELEY, CALIFORNIA 94720